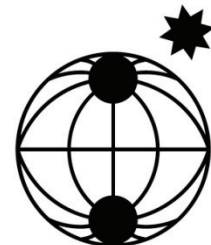


# Berichte

zur Polar-  
und Meeresforschung

631  
2011

Reports  
on Polar and Marine Research



The Expedition of the Research Vessel "Polarstern"  
to the Antarctic in 2010 (ANT-XXVI/4)

---

Edited by  
Arne Körtzinger  
with contributions of the participants

---

 HELMHOLTZ  
| GEMEINSCHAFT

ALFRED-WEGENER-INSTITUT FÜR  
POLAR- UND MEERESFORSCHUNG  
In der Helmholtz-Gemeinschaft  
D-27570 BREMERHAVEN  
Bundesrepublik Deutschland

ISSN 1866-3192

# Hinweis

Die Berichte zur Polar- und Meeresforschung werden vom Alfred-Wegener-Institut für Polar- und Meeresforschung in Bremerhaven\* in unregelmäßiger Abfolge herausgegeben.

Sie enthalten Beschreibungen und Ergebnisse der vom Institut (AWI) oder mit seiner Unterstützung durchgeführten Forschungsarbeiten in den Polargebieten und in den Meeren.

Es werden veröffentlicht:

- Expeditionsberichte (inkl. Stationslisten und Routenkarten)
- Expeditionsergebnisse (inkl. Dissertationen)
- wissenschaftliche Ergebnisse der Antarktis-Stationen und anderer Forschungs-Stationen des AWI
- Berichte wissenschaftlicher Tagungen

Die Beiträge geben nicht notwendigerweise die Auffassung des Instituts wieder.

# Notice

The Reports on Polar and Marine Research are issued by the Alfred Wegener Institute for Polar and Marine Research in Bremerhaven\*, Federal Republic of Germany. They appear in irregular intervals.

They contain descriptions and results of investigations in polar regions and in the seas either conducted by the Institute (AWI) or with its support.

The following items are published:

- expedition reports (incl. station lists and route maps)
- expedition results (incl. Ph.D. theses)
- scientific results of the Antarctic stations and of other AWI research stations
- reports on scientific meetings

The papers contained in the Reports do not necessarily reflect the opinion of the Institute.

The „Berichte zur Polar- und Meeresforschung“  
continue the former „Berichte zur Polarforschung“

## \* Anschrift / Address

Alfred-Wegener-Institut  
Für Polar- und Meeresforschung  
D-27570 Bremerhaven  
Germany  
[www.awi.de](http://www.awi.de)

Editor in charge:  
Dr. Horst Bornemann

Assistant editor:  
Birgit Chiaventone

Die "Berichte zur Polar- und Meeresforschung" (ISSN 1866-3192) werden ab 2008 ausschließlich als Open-Access-Publikation herausgegeben (URL: <http://epic.awi.de>).

Since 2008 the "Reports on Polar and Marine Research" (ISSN 1866-3192) are only available as web-based open-access publications (URL: <http://epic.awi.de>)

# **The Expedition of the Research Vessel "Polarstern" to the Antarctic in 2010 (ANT-XXVI/4)**

---

**Edited by  
Arne Körtzinger  
with contributions of the participants**

**Please cite or link this item using the identifier  
hdl:10013/epic.37888 or <http://hdl.handle.net/10013/epic.37888>  
ISSN 1866-3192**

**ANT-XXVI/4**

**7 April – 17 May 2010**

**Punta Arenas – Mindelo – Las Palmas – Bremerhaven**

**Chief Scientist  
Arne Körtzinger**

**Coordinator  
Eberhard Fahrbach**

---

## **Inhalt**

<b>1. Zusammenfassung und Fahrtverlauf</b>	<b>2</b>
<b>Summary and itinerary</b>	<b>5</b>
<b>2. Weather conditions</b>	<b>6</b>
<b>3. OCEANET PROJECTS</b>	<b>8</b>
<b>3.1 OCEANET – chemical measurements</b>	<b>9</b>
<b>3.2 OCEANET – biological measurements</b>	<b>14</b>
<b>3.3 OCEANET – bio-optical measurements</b>	<b>16</b>
<b>3.4 OCEANET – atmospheric measurements</b>	<b>22</b>
<b>4. FURTHER PROJECTS</b>	<b>30</b>
<b>4.1 Measurements of aerosol optical thickness</b>	<b>31</b>
<b>4.2 Atmospheric dust and irradiation effects on ocean surface processes – biogeochemistry in the Atlantic Ocean</b>	<b>34</b>
<b>4.3 Determination of photochemical processes during a transect through the Atlantic</b>	<b>41</b>
<b>4.4 Concentration and isotopic ratio of molecular hydrogen along a meridional Atlantic transect</b>	<b>45</b>
<b>4.6 Glider swarm experiment at Cape Verde Ocean Observatory</b>	<b>48</b>
<b>4.7 Posidonia system testing and calibration</b>	<b>50</b>
<b>4.8 Further projects and guests</b>	<b>55</b>
<b>A.1 Teilnehmende Institute / participating institutions</b>	<b>58</b>
<b>A.2 Fahrtteilnehmer / cruise participants</b>	<b>60</b>
<b>A.3 Schiffsbesatzung / ship's crew</b>	<b>61</b>
<b>A.4 Stationsliste / Station List PS 75</b>	<b>62</b>

---

# 1. ZUSAMMENFASSUNG UND FAHRTVERLAUF

Arne Körtzinger  
IFM-GEOMAR, Kiel

Die Reise ANT-XXVI/4 begann am späten Nachmittag des 7. April 2010 in Punta Arenas/Chile. Nach kurzer Fahrt durch die Magellanstraße musste zunächst die ausschließliche Wirtschaftszone von Argentinien verlassen werden, für die keine Forschungsgenehmigung beantragt worden war. Diese kurze Dampfstrecke bot allen beteiligten Arbeitsgruppen die Möglichkeit, bis zum Beginn der Stationsarbeiten sämtliche Geräte aufgebaut und in Betrieb genommen zu haben. Die Stationsarbeiten wurden dann am späten Abend des 9. April mit der ersten Station auf dem patagonischen Schelf aufgenommen. Im weiteren Verlauf der Reise wurde täglich eine Station zum Zeitpunkt des lokalen Sonnenhöchststandes durchgeführt. Die dabei standardmäßig zum Einsatz kommenden Geräte waren CTD-Kranzwasserschöpfer, GO-FLO Wasserschöpfer für kontaminationsfreie Probennahme für Spurenmetalle sowie Sensorkomplexe mit optischen Sensoren für Ozeanreflektanz, Lichtfeld, Lichtstreuung und Lichttransmission. Die Profiltiefen waren dabei üblicherweise auf die oberen 400 m der Wassersäule beschränkt. Tiefe CTD-Profile bis zum Boden wurden lediglich im Vema-Kanal im Südwestatlantik und bei der ozeanischen Langzeit-Beobachtungsstation nördlich der Kapverden (CVOO – Cape Verde Ocean Observatory) durchgeführt. Desweiteren wurden umfangreiche kontinuierliche Messungen in Oberflächenwasser und Luft sowie Aerosolbeprobungen über die gesamte Dauer der Reise durchgeführt. Auch die Messungen im OCEANET-Atmosphärencontainer erfolgten über den gesamten Zeitraum.

FS *Polarstern* stattete am 3. Mai mit dem Ankern in der Bucht von Mindelo auf São Vicente den Kapverden zum ersten Mal in seiner Geschichte einen Kurzbesuch ab (Abb. 1.2). Hier stiegen zwei weitere Kieler Wissenschaftler zu, und es wurde wissenschaftliche Ausrüstung übernommen. Außerdem wurde ein kleiner Empfang für die kapverdischen Kooperationspartner vom Instituto Nacional de Desenvolvimento das Pescas (INDP) gegeben. Nach dem Auslaufen aus der Bucht von Mindelo konnte ein Schwarm von vier Gleitern mit umfangreicher Ausstattung an physikalischen und biogeochemischen Sensoren des IFM-GEOMAR erfolgreich geborgen werden. Damit ging das erste Gleiterschwarmexperiment in Europa erfolgreich zu Ende. Ein weiterer kurzer Hafenbesuch stand mit Las Palmas de Gran Canaria auf dem Programm. Hier stieg eine Gruppe von acht weiteren Fahrtteilnehmern zu, darunter die achtjährige Katja, die die Teilnahme an der Expedition im Schülerwettbewerb „Forschungsexpedition 2009“ des BMBF gewonnen hatte.

Das wissenschaftliche Programm endete am 14. Mai im Eingang des Ärmelkanals, und FS *Polarstern* lief pünktlich am frühen Morgen des 17. Mai 2010 nach Bremerhaven ein.

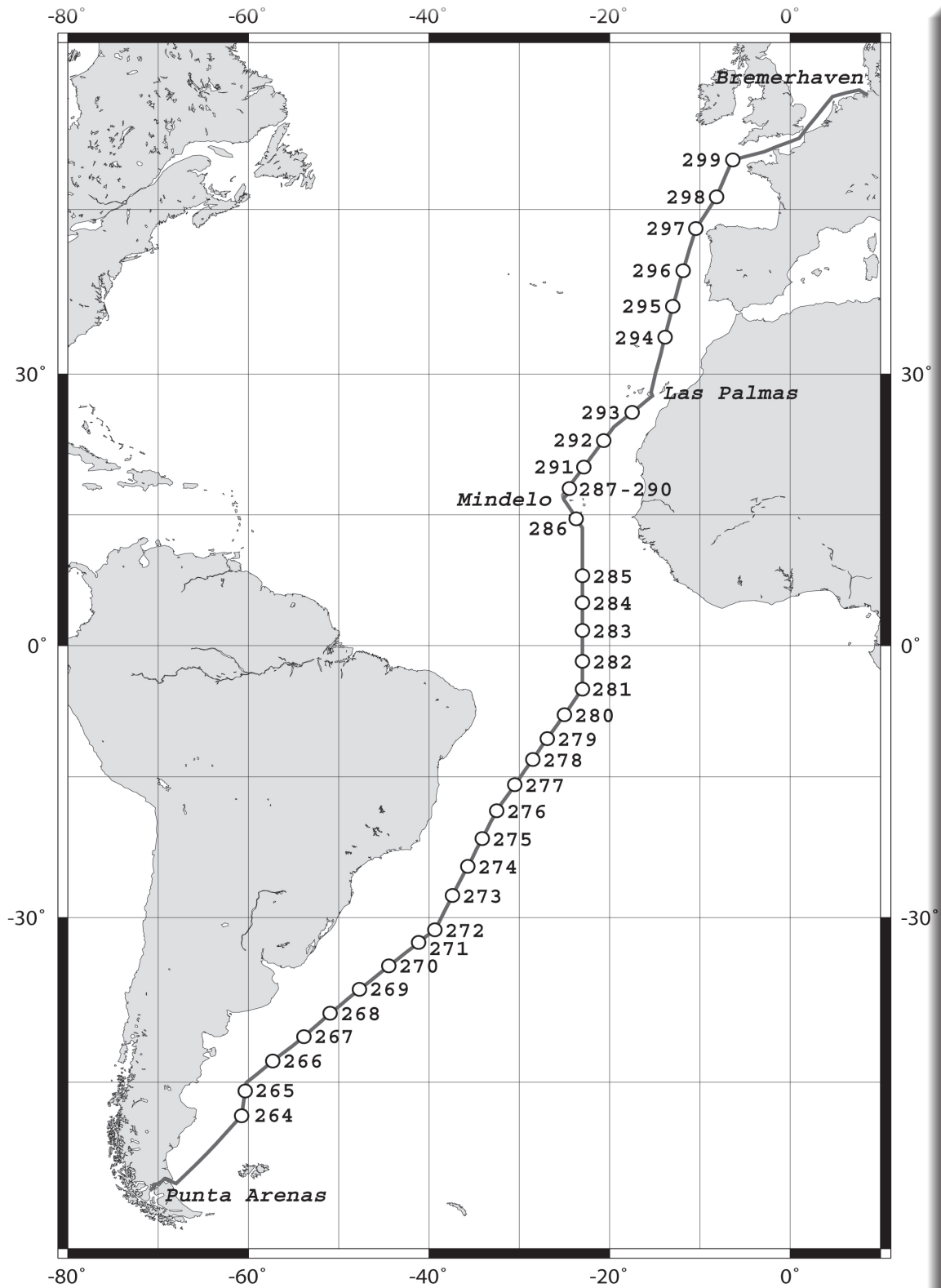


Abb. 1.1: Kurskarte der Polarstern-Reise ANT-XXVI/4  
 Fig. 1.1: Cruise track of Polarstern during the expedition ANT-XXVI/4



*Abb. 1.2: FS Polarstern auf Reede in der Bucht von Mindelo/Kap Verde auf einem Zwischenstopp der Reise ANT-XXVI/4.*

*Fig. 1.2: Polarstern in the roads in the bay of Mindelo/Cape Verde during a stopover of the expedition ANT-XXVI/4.*

---

## SUMMARY AND ITINERARY

The cruise started in the late afternoon of 7 July 2010 in Punta Arenas/Chile. After a short passage through the Strait of Magellan we had to transit the Exclusive Economic Zone of Argentina for which no research permission had been requested. This provided all groups with ample time to set up and start their various instruments prior to the onset of the regular station work. These started in the late evening of 9 April with the first station on the Patagonian shelf. Thereafter one daily station was carried out at local noon during the entire cruise. At these stations the following gear was regularly deployed: CTD-rosette, GO-FLO samplers for trace metal clean water sampling, and optical sensor packages for surface reflectance, incident light, light scattering and light transmission. Profiling depths were typically restricted to the upper 400 m of the water column. Full ocean depth CTD-rosette casts were only performed in the Vema Channel in the southwest Atlantic and at the Cape Verde Ocean Observatory (CVOO) north of the Cape Verde Islands. In addition to the station work, several continuous measurements as well as sampling of air, aerosol and surface seawater were carried out throughout the cruise. Also the OCEANET atmosphere container for remote sensing was operated during the entire cruise.

On 3 May, *Polarstern* made her first visit ever to Cape Verde with her port call to Mindelo on the islands of São Vicente for embarkation of two more scientists from Kiel and loading of scientific equipment (Fig. 1.2). The short visit was also used for a small reception for the Cape Verdean scientific partners from the local Instituto Nacional da Desenvolvimento das Pescas (INDP). After departure from Mindelo, a swarm of four gliders from the IFM-GEOMAR in Kiel equipped with a range of physical and biogeochemical sensors was successfully recovered at CVOO thereby terminating the first European glider swarm experiment. A second port call was made to Las Palmas de Gran Canaria for embarkation of a group of eight persons including an eight year-old girl who had won her participation as part of the “Research Expedition 2009”, a public activity for school kids by the German Ministry for Education and Research.

The scientific program concluded on 14 May with the final station at the entry of the English Channel and *Polarstern* reached Bremerhaven on time in the early morning of 17 May 2010.

---

## 2. WEATHER CONDITIONS

Klaus Buldt  
DWD, Hamburg

Cruise ANT-XXVI/4 started on 7 April 2010 under favorable weather conditions with a moderate breeze and calm seas due to a high pressure system off the Argentinean coast. Towards the weekend 10-11 April, a trough west of the Antarctic Peninsula had developed into a low pressure system which started to influence the weather along the cruise track with winds of up to 8 Bft. The passage of the cold front in the evening of 11 April was accompanied by distinct Mammatus clouds (Fig. 2.1).



*Fig. 2.1: Mammatus clouds during passage of a cold front on 11 April 2010.*

The following days were influenced by a stationary low off the La Plata estuary with winds of up to 6 Bft., dense cloud cover and occasional rain showers. Maximum daily temperatures reached 23°C. On Friday 16 April, the cold front of the La Plata low passed with 8 Bft. winds and strong thunderstorms. After that, high pressure conditions developed with weak to moderate south-easterly winds, low cloudiness and daytime temperatures around 24°C initially and approaching 28°C as we reached the tropics.

On 27 April the southern branch of ITCZ was reached with occasional rain showers. Under weak southeast trade winds the main ITCZ branch was passed at around 4-5°N. Highest air temperatures of 28.9°C were measured on 29 April in a region of also highest water temperatures of up to 30.3°C. After passing the ITCZ, north-easterly winds of around 4 Bft. prevailed all the way to the Cape Verde Islands. Afterwards, ever weaker trade winds of 3-4 Bft. were met on the way to Las Palmas. On the final leg, a low that moved from east of Newfoundland to Cape Finisterre influenced our weather with winds of 4-5 Bft. and rain showers. On 12 May, a nearby waterspout was observed (Fig. 2.2).



*Fig. 2.1: Waterspout observed on 10 May 2010.*

Weather conditions remained to be influenced by the frontal system of another low off the east coast of southern Greenland that moved to the Faeroe Islands before on 15 May influence from the Azores High started to dominate until Bremerhaven was reached on 17 May 2010.

During the entire cruise weather advice was provided to cruise participants. This also included calculating of passages of the TERRA and CALIPSO satellites which was necessary for comparison of aerosol optical thickness measurements (see section 4.1). Furthermore air mass back trajectories were calculated to serve as additional information for atmospheric gas measurements.

---

### 3. OCEANET PROJECTS

Arne Körtzinger  
IFM-GEOMAR, Kiel

#### Introduction

*Polarstern* Cruise ANT-XXVI/4 was primarily dedicated to the project OCEANET – Autonomous Measurement Platforms for Energy and Material Exchange between Ocean and Atmosphere – which is a joint project of IFM-GEOMAR, IfT, AWI, and GKSS. In order to provide a solid basis for the observational monitoring of energy and material exchange between ocean and atmosphere the project aims to develop an autonomous observation system for operational use onboard available cargo and research vessels. The project is based on a network of expertise from IFM-GEOMAR (CO<sub>2</sub>/O<sub>2</sub> fluxes, biological nitrogen fixation, energy budget, remote sensing), the IfT (active remote sensing), the GKSS research center (ferry box, remote sensing of marine biology with ENVISAT/MERIS) and AWI-Bremerhaven (bio-optics, remote sensing). During ANT-XXVI/4 the following observational components of OCEANET were included:

**OCEANET – chemical measurements:** Operation of autonomous systems as well as new instruments for measurement of parameters of the marine CO<sub>2</sub> system (pCO<sub>2</sub>, pH, δ<sup>13</sup>C-DIC) and ancillary parameters.

**OCEANET – biological measurements:** Phylogenetic diversity and metabolic activity of nitrogen-fixing microorganisms were determined along the meridional transects by molecular biological methods as well as with on board microcosm experiments.

**OCEANET – bio-optical measurements:** Using remote sensing data in combination with *in-situ* measurements of ocean optics, phytoplankton productivity and composition of particulate organic carbon with the aim to improve estimates of global marine primary production and the distribution of major phytoplankton functional groups and to provide the data basis for satellite groundtruthing and ocean optical modeling.

**OCEANET – atmospheric measurements:** The scientific focus of atmospheric measurements to be carried out during this cruise was placed on radiation & microwave remote sensing (multi-channel microwave radiometer) and Lidar observations (multi-channel Raman-Lidar Polly XT for aerosols).

### 3.1 OCEANET – chemical measurements

Björn Fiedler, Peer Fietzek (not on board), Arne Körtzinger  
IFM-GEOMAR, Kiel

Meike Becker, Gernot Friedrichs  
IPC CAU, Kiel

Steffen Aßmann,  
GKSS, Geesthacht

#### Objectives

The OCEANET project aims to further develop and test autonomous instrumentation for measurement of energy and matter exchange between the atmosphere and the surface ocean. At first, the instruments are tested and installed aboard *Polarstern*. Since the processes under investigation require both a rather comprehensive observational approach as well as high spatial and temporal coverage, unattended operation of the multi-parameter instrumentation aboard “Voluntary Observing Ships” is the long term goal of this initiative.

The oceanic component of this study places a strong focus on the marine carbon cycle in the surface ocean which is of high climatic relevance but at the same time susceptible to climate change. The surface ocean’s CO<sub>2</sub> source/sink function is maintained by a complex interaction of physical, chemical and biological processes. Therefore its understanding requires measurement of various different parameters.

During the fifth OCEANET cruise, the feasibility of autonomous underway measurements was assessed for a wide range of instruments for measurements of chemical parameters (CO<sub>2</sub> partial pressure, the δ<sup>13</sup>C-DIC isotope ratio, pH, alkalinity, oxygen and total gas tension).

#### Work at sea

During ANT-XXVI/4, we operated several underway instruments in the wet laboratory of *Polarstern*. The data were logged along with time and geographical position and most of the data is available in 1-min intervals. A centrepiece of the ocean component of OCEANET was the comparison of different instruments for the measurement of the CO<sub>2</sub> partial pressure (*p*CO<sub>2</sub>) in seawater and also corresponding isotopic signatures. The following four systems were operated more or less successfully throughout the cruise.

##### - General Oceanics Underway *p*CO<sub>2</sub> System (GO-LICOR)

In this commercially available system (General Oceanics, Miami/FL, USA), the gas phase is equilibrated with seawater using a spray-head equilibrator that produces a fine spray. After the equilibration process the sample gas is dried and subsequently measured via NDIR detection using a LICOR 7000 gas analyzer (LICOR Inc., Lincoln/NE, USA). The LICOR is calibrated approximately every 3.5 h with 3 standard gases ranging from 184 to 745 ppmv.

- **General Oceanics Underway  $p\text{CO}_2/\delta^{13}\text{C-CO}_2$  System (GO-CRDS)**

In this identical system, a different  $\text{CO}_2$  detector was operated. After the equilibration process, the sample gas is dried and subsequently measured via Cavity Ringdown Spectroscopy (CRDS) using an EnviroSense 2050 analyzer (Picarro Inc., Santa Clara/CA, USA). The instrument stability was checked once a day by measuring a standard gas.

- **PSI  $\text{CO}_2$  Pro Sensor**

This autonomous *in-situ* sensor (Pro Oceanus, Halifax/NS, Canada) is based on a tubular PDMS membrane across which  $\text{CO}_2$  in seawater equilibrates with the gas phase behind the membrane boundary. The  $\text{CO}_2$  in the gas phase is measured via a small NDIR cell that is calibrated every 6 h by a simple zero-point calibration.

- **CONTROS HydroC  $p\text{CO}_2$  Sensor**

This instrument (CONTROS GmbH, Kiel, Germany) is based on the same measurement principle as the PSI sensor. However, the sensor follows a different design concept for the membrane interface (planar assembly). This instrument is equipped with further peripheral internal sensors for precise assessment of measurement quality and more adequate raw data corrections during rapid changes of environmental conditions.

A second centrepiece during this cruise was the field evaluation of a newly designed underway instrument for high precision measurements for the determination of pH and alkalinity in seawater (Abmann *et al.*, 2011). The measuring principle comprises a spectrophotometric pH determination based on the absorbance spectra of a pH sensitive indicator dye. As a light source a broadband white LED is used. Entire absorption spectra (430-700 nm) are recorded and used to precisely calculate the pH. Furthermore, first experiments were conducted in order to develop a sensor for alkalinity akin to the mentioned pH measurement principle. This measurement is done by a rapid titration with a strong acid and a simultaneous determination of the pH using another indicator dye.

The setup (shown schematically in Fig. 3.1.1) featured two similar GO systems (one shipborne from AWI, one portable by IFM-GEOMAR) which were connected directly to ship's seawater supply line which drew seawater from around 11 m depth. Temperature and salinity were measured directly at the seawater intake by the shipborne thermosalinograph. Additionally, sensors for  $p\text{CO}_2$  ( $\text{CO}_2$  Pro & HydroC) and  $\text{O}_2$  (Optode Model 3830, Aanderaa, Bergen, Norway) were submerged in a thermally insulated flow-through water bath that was also connected to the seawater supply line. The container's water volume was 80 L and the water flow was maintained at approximately 10-12 L/min. In addition, we submerged a gas tension sensor (PSI HGTD, Pro Oceanus, Halifax/NS, Canada) in the flow-through container which measured the total pressure of all dissolved gases in seawater.

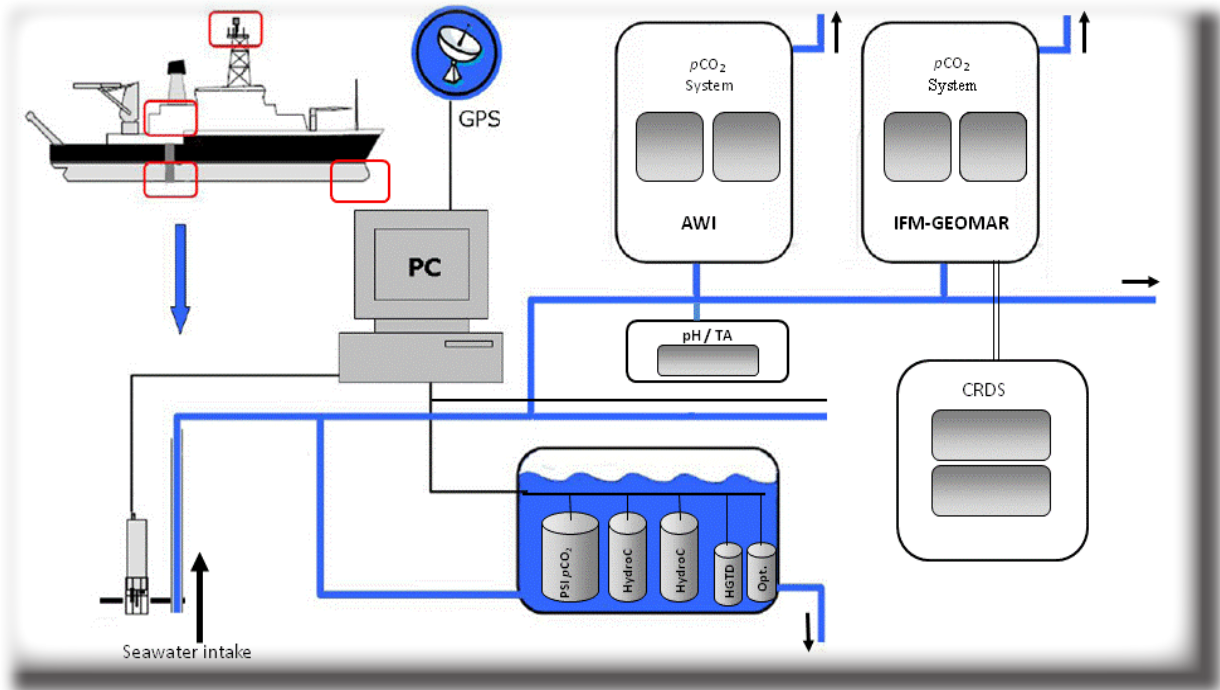


Fig. 3.1.1: Setup of underway chemical measurements during cruise ANT-XXVI/4 of Polarstern

For reference, discrete water samples for dissolved inorganic carbon (DIC) and total alkalinity (TA) were taken every 12 h for analysis at IFM-GEOMAR in Kiel. The samples were drawn into 500 mL bottles and poisoned with 100  $\mu\text{L}$  saturated mercuric chloride solution. Frozen nutrient samples for analysis at GKSS were taken twice per day. Further sampling was conducted at a time series site north of Cape Verde (CVOO, Cape Verde Ocean Observatory). Here a deep hydrocast down to 3600 dbar was performed and various samples for later shore-based analysis were collected.

Finally, intensive investigations with a second (similar) HydroC sensor for profiling applications were conducted during this cruise. Here, the instrument was mounted on the ship borne CTD and several hydrocasts down to 2000 dbar were carried out. Discrete water samples were collected simultaneously for later analysis in Kiel.

### Preliminary (expected) results

The  $\text{CO}_2$  mole fraction ( $x\text{CO}_2$ ) data as recorded by the GO systems was regularly calibrated against standard gases and together with the atmospheric pressure and the sea surface temperature the sea surface water  $p\text{CO}_2$  was calculated following the procedures described in Dickson *et al.* (2007). We used the GO system as our reference system as this is most intensively tested and internationally accepted instrument (Pierrot *et al.*, 2007).

The overall distribution of  $p\text{CO}_2$  in the surface layer (Fig. 3.1.2) during this cruise fits well into the picture which was obtained during the last four OCEANET cruises with typical supersaturation in the tropics and south Atlantic subtropics, near-equilibrium conditions in the north Atlantic subtropics and strong undersaturation in the mesotrophic

regions of the continental shelves of Europe and Patagonia. The latter regions are characterized by strong seasonality of net primary production and hence CO<sub>2</sub> source/sink function as documented in the various OCEANET cruises.

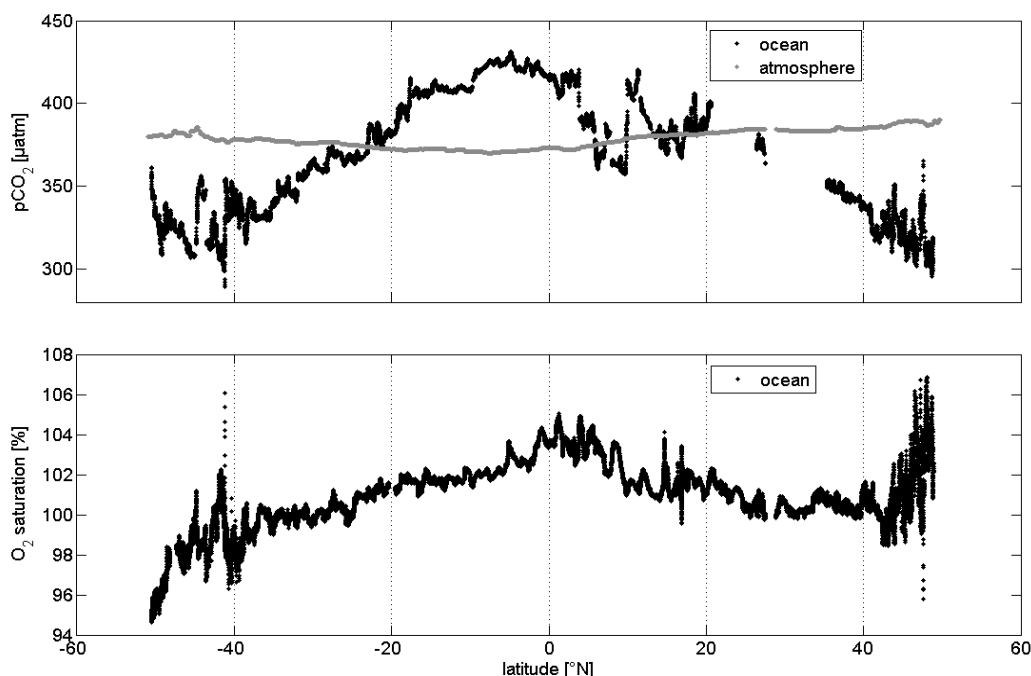


Fig. 3.1.2: Upper panel: Measurements using the GO system of the CO<sub>2</sub> partial pressure ( $p\text{CO}_2$ ) in atmosphere (gray) and surface ocean (black). Lower panel: Measurements of oxygen saturation indicating pronounced supersaturation in higher latitudes within the northern hemisphere.

The intercomparison of different types of  $p\text{CO}_2$  sensors (varying in equilibration and detection methods) was very successful. *Polarstern* served as a unique platform for this kind of investigation. Despite a few minor events, the HydroC and to a somewhat lesser degree also the CO<sub>2</sub> Pro sensors have shown a high potential for underway applications. Most promising results were obtained by the new CRDS detector in combination with a GO equilibration unit. Here both  $p\text{CO}_2$  and  $\delta^{13}\text{C}\text{-DIC}$  could be measured with good accuracy. Comparing the produced  $p\text{CO}_2$  data with the reference system shows very good agreement (Fig. 3.1.3). The offset in measurements of atmospheric  $p\text{CO}_2$  is smaller than the accuracy of the instruments. The slightly higher offset in seawater measurements is caused by the use of two independent equilibrators systems. For verifying the isotope ratio data discrete IRMS samples were taken. Between these two datasets, an offset of 0.35 ‰ was obtained (Fig. 3.1.3). Recently, the manufacturer has identified a cross-sensitivity of the  $\delta^{13}\text{C}\text{-CO}_2$  measurement to methane which appears to explain this systematic deviation. The transect in  $\delta^{13}\text{C}\text{-DIC}$  shows higher variability in mesotrophic regions (e.g., on the European shelf) compared to the subtropical gyres.

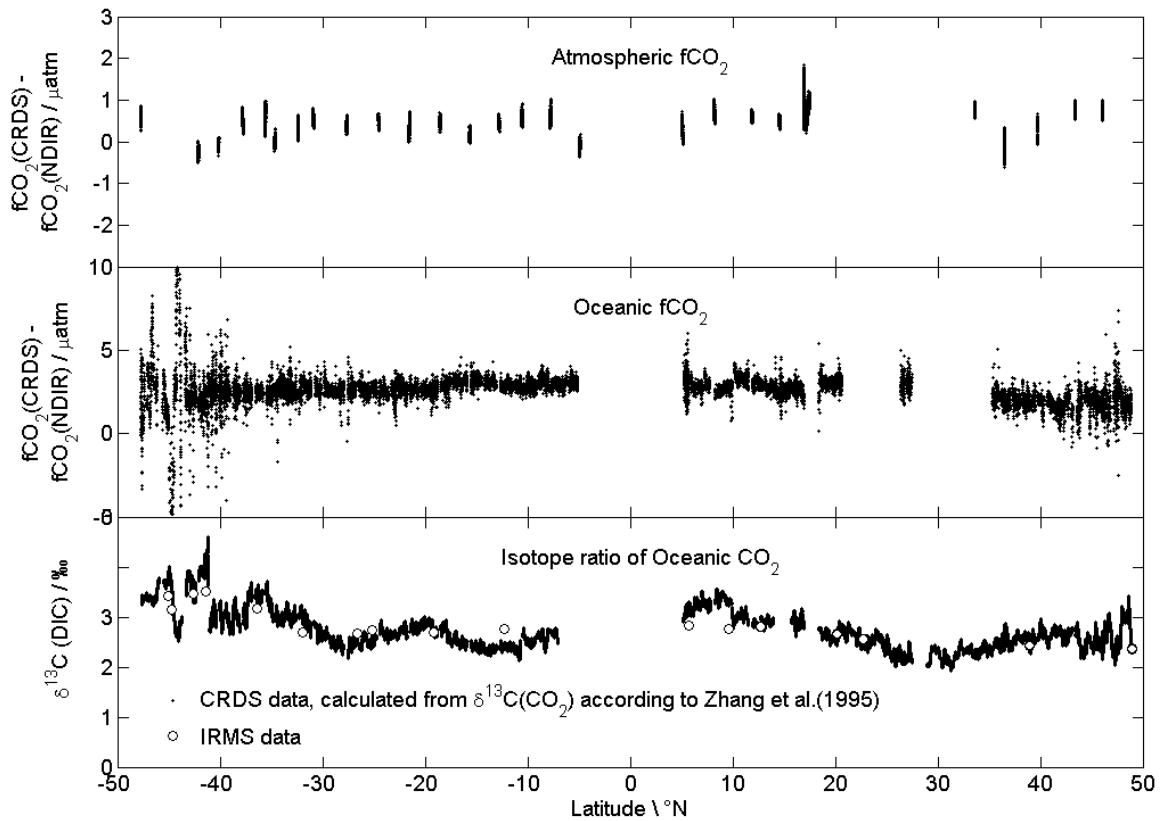


Fig. 3.1.3: Comparison of atmospheric  $p\text{CO}_2$ , surface ocean  $p\text{CO}_2$ , and  $^{13}\text{C}/^{12}\text{C}$  isotope ratio of total dissolved inorganic carbon ( $\delta^{13}\text{C}\text{-DIC}$ ) as measured by CRDS with reference methods (for  $p\text{CO}_2$ : GO system,  $\delta^{13}\text{C}\text{-DIC}$ : discrete samples measured by Leibniz Laboratory for Dating and Isotope Research, Christian Albrecht University, Kiel, Germany).

Five vertical casts with a HydroC sensor mounted on the CTD rosette were carried out during the entire cruise (Fig. 3.1.4). The sensor was being tested for measurement stability while passing rapidly steep gradients (temperature and  $p\text{CO}_2$ ). Further the effect of hydrostatic pressure on the response time of the sensor was investigated. Here a linear relationship between both was found. However, this effect was found to be small compared to other sensors.

The newly developed instrument for autonomous underway pH measurements worked very stable, when a continuous sample flow was provided. One new feature of the instrument – the temperature control of the sample flow due to Peltier elements – was proven successfully. This made a high precision of  $\pm 0.0007$  pH units possible (ABmann *et al.*, 2011). For alkalinity measurements basic experiments were conducted and further examinations are planned. The evaluation of the entire dataset is currently underway at the respective institutions.

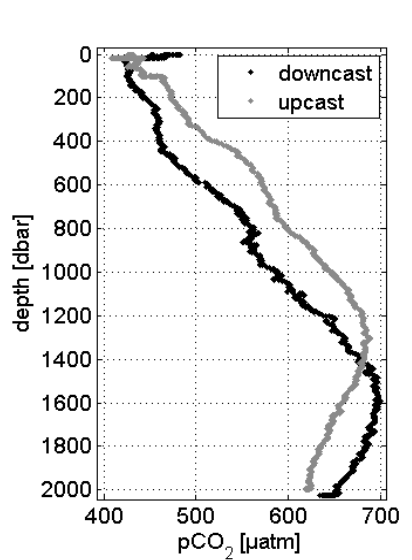


Fig. 3.1.4:  $p\text{CO}_2$  measurements obtained by the HydroC during a deep hydrocast. Data is separated into up- and downcast which show a clear sensor hysteresis.

#### References

- Aßmann S, Frank C, Körtzinger A (2011). Spectrophotometric high-precision seawater pH determination for use in underway measuring systems. *Ocean Sci. Disc.* 8, 1339-1367 doi:10.5194/osd-8-1339-2011
- Dickson AG, Christopher CL, Christian JR (eds.) (2007). Guide to best practices for Ocean  $\text{CO}_2$  measurements. PICES Special Publication 3, IOCCP Report No. 9, 175 pp.
- Pierrot D, Neill C, Sullivan K, Castle R, Wanninkhof R, Lüger H, Johannessen T, Olsen A, Feely RA, Cosca CE (2009). Recommendations for autonomous underway  $p\text{CO}_2$  measuring systems and data-reduction routines. *Deep-Sea Research II*, 56, 512–522.

### 3.2 OCEANET – biological measurements

Wiebke Mohr, Scarlett Sett, Julie LaRoche (not on board)  
IFM-GEOMAR, Kiel

#### Objectives

The main objectives of this project were to assess the abundance, activity and diversity of diazotrophic microorganisms and the determination of the rates of primary production and dinitrogen ( $\text{N}_2$ ) fixation along the meridional transect. Regular 6 h time interval samples during ship's steaming time provided a roughly  $1^\circ$  latitude horizontal resolution enabling the assignment of biogeographical regions for the different diazotrophic groups to be analyzed. The analysis of *nifH* gene expression patterns will be correlated to environmental conditions such as temperature or light. The molecular analysis of the sample seawater will be supplemented with analytical flow cytometry samples as well as the determination of rates of  $\text{N}_2$  fixation and primary production using the stable isotopes  $^{15}\text{N}_2$  and  $\text{NaH}^{13}\text{CO}_3$ , respectively. The overall data set will provide a spatial (both horizontal and vertical) and temporal distribution of the abundance and activity of diazotrophs throughout the Atlantic Ocean.

### Work at sea

The first surface seawater samples using the ship's clean seawater supply were obtained after midnight on the 10 April 2010 just outside the Argentinean EEZ. From thereon, samples were taken at regular 6 h intervals throughout the cruise until 14 May 2010 at the entrance to the Western English Channel. In summary, a total of about 130 stations were sampled for molecular analysis of the diazotrophic community during the cruise. In specific, these surface seawater samples (usually about 2 L) were filtered onto Durapore membrane filters (0.22  $\mu\text{m}$  pore size, 47 mm diameter) within 1-2 h time, shock-frozen in liquid nitrogen and stored at  $-80^{\circ}\text{C}$  until further analysis in the molecular laboratory of IFM-GEOMAR in Kiel. To supplement the molecular analysis, analytical flow cytometry (AFC) samples were taken in parallel to the seawater filtrations.

In addition to the regular 6 h interval sampling, samples for molecular analysis were taken from daily noon CTD casts including about 10 depths covering the upper 400 m of the ocean. The sampling depths were distributed throughout the water column and were adjusted according to the chlorophyll *a* fluorescence maximum, the red/blue transmission minimum or hydrographical features. A total of 32 upper ocean casts were sampled and two full ocean depth CTD casts were sampled, one at the Vema Channel in the Southern Hemisphere and the other at the CVOO station in the Northern Hemisphere including 14-18 sampling depths.

To complement the molecular and AFC analysis of the diazotrophic community, on-deck 24 h seawater incubations were performed to determine rates of  $\text{N}_2$  fixation and primary production using the stable isotopes  $^{15}\text{N}_2$  and  $\text{NaH}^{13}\text{CO}_3$ , respectively. In specific, triplicate 4 L polycarbonate bottles were filled with seawater from the clean seawater supply generally coinciding with the noon CTD cast. The stable isotopes were added to the bottles which were placed in an on-deck incubator with ambient surface seawater flow-through for about 24 h. Non-amended seawater incubations for the analysis of the natural abundance of  $^{15}\text{N}$  and  $^{13}\text{C}$  were included during each incubation. After the incubation time, the samples were filtered onto pre-combusted GF/F filters, dried at  $50^{\circ}\text{C}$  and stored at room temperature until bulk mass spectrometric analysis.

### Preliminary (expected) results

Using molecular biological techniques (quantitative PCR), we will obtain abundance estimates for at least seven different phylotypes of diazotrophs using specific probes for the *nifH* gene which encodes the iron-subunit of the nitrogenase enzyme complex. *nifH* gene expression analysis on these samples will reveal (potential) activity patterns of diazotrophs during the cruise. The combination of the 6 h regular interval sampling and the steaming of the ship will provide a horizontal and temporal distribution of the abundance and activity of diazotrophs. The daily CTD casts down to 400 m depth will provide an insight into the vertical distribution of the different diazotrophic groups. The conjunction of the horizontal and vertical distribution will reveal biogeographical information of diazotrophs throughout the Atlantic Ocean including areas of highest dust deposition, i.e. the Eastern North Atlantic. While passing this area, atmospheric dust could be observed from the ship. Dust has previously been shown to stimulate  $\text{N}_2$  fixation (Mills *et al.*, 2004) by providing iron and possibly phosphorus to the surface ocean microbial community (Baker *et al.*, 2007). Both elements are considered to be

limiting nutrients for  $N_2$  fixation. As on ANT-XXVI/1, rates of  $N_2$  fixation and primary production have been obtained through laboratory-based mass spectrometric analysis. However, ANT-XXVI/4 was conducted in the Austral Fall and Boreal Spring, vice versa from ANT-XXVI/1. The conjunction of both data sets will show whether the observed spatial and temporal patterns seasonally fluctuate or persist with certain environmental or hydrographic conditions.

#### References

- Baker AR, Weston K, Kelly SD, Voss M, Streu P, Cape JN (2007). Dry and wet deposition of nutrients from the tropical Atlantic atmosphere: Links to primary productivity and nitrogen fixation. *Deep-Sea Research I* 54, 1704-1720.
- Mills MM, Ridame C, Davey M, LaRoche J, Geider RJ (2004). Iron and phosphorus co-limit nitrogen fixation in the eastern tropical North Atlantic. *Nature*, 429, 292-294.

### 3.3 OCEANET – bio-optical measurements

Anja Feyen, Marta Kasper, Tilman Dinter (not on board), Bettina Schmitt (not on board), Anja Theis (not on board), Astrid Bracher (not on board)  
AWI, Bremerhaven

Pierre Gernez, Rick Reynolds, Dariusz Stramski (not on board), Julia Uitz (not on board)  
SIO, La Jolla/CA, USA

Julia Mroz, Rüdiger Röttgers (not on board)  
GKSS, Geesthacht

Alireza Sadeghi  
IUP-HB, Bremen

#### Objectives

Hyperspectral optical measurements represent a promising approach for discriminating and quantifying distinct phytoplankton groups in the world's oceans. A major objective towards reaching this goal is to develop algorithms for assessing the biodiversity of phytoplankton communities from hyperspectral optical sensors. Our objective for this cruise was to collect a unique set of bio-optical data encompassing a broad variety of oceanic environments. Based on the analysis of this dataset, we will determine how different phytoplankton communities, discriminated in terms of pigment-based dominant taxa and cell size, quantitatively affect the shape of hyperspectral remote-sensing reflectance,  $R_{rs}(\lambda)$ . For this purpose, we will examine relationships between hyperspectral  $R_{rs}(\lambda)$ , inherent optical properties (IOPs) such as the spectral absorption coefficient, and phytoplankton taxa-specific pigment composition. We will also examine how other inorganic and organic seawater constituents co-existing with phytoplankton communities affect  $R_{rs}(\lambda)$ . Similar analysis will be conducted at the level of IOPs, which are primary determinants of  $R_{rs}(\lambda)$ .

## Work at sea

*Discrete seawater samples* were collected from Niskin bottles triggered at several depths within the upper water column during CTD-rosette profiles at the noon stations. Sampled depths were: surface, depth of the chlorophyll *a* maximum as determined from the CTD fluorometer profile, and occasionally one or two extra depths. Additionally surface water samples were taken from the ship's moon pool between stations (see Table 1 for an overview). Analyses performed onboard and after the cruise are as follows:

- *Phytoplankton pigments*: Seawater samples were filtered through glass fiber filters (GF/F, Whatman) under low vacuum. Sample filters were stored in liquid nitrogen until subsequent analysis by high performance liquid chromatography (HPLC). Samples will be analysed at the AWI and the Laboratoire d'Océanographie de Villefranche (France) independently in order to get an error estimate of the method. An additional fluorometric analysis is performed to get an estimate of phycobilin pigments which are not detected by the HPLC analysis.
- *Spectral absorption coefficient of particles*: Particles from discrete water samples were collected on 25 mm GF/F filters (Whatman). After completion of the filtration, the filters were frozen in liquid nitrogen for transport back to the laboratory. As for HPLC samples, filters were taken for analysis at AWI and SIO, where they will be scanned in the integrating sphere of a spectrophotometer. The absorption coefficient of total particles and non-pigmented particles will be determined on filters placed inside the integrating sphere in the 250–850 nm spectral region with 1-nm resolution.
- *Total absorption and absorption of dissolved organic matter*: Particulate absorption in suspension and absorption of Gelbstoff was measured during the cruise using the point-source integrating-cavity absorption meter (PSICAM) (Röttgers *et al.*, 2007).
- *Particulate Organic Carbon and Nitrogen (POC and PON)*: Suspended particles were collected by filtration under low vacuum onto pre-combusted 25-mm GF/F filters (Whatman). After filtration, the filters were transferred to sterile glass vials, dried at 55°C in a clean oven, and stored until post cruise analysis in the laboratory. POC and PON concentration will be determined by high temperature combustion of sample filters via standard CHN analysis (Parsons *et al.*, 1994; Knap *et al.*, 1994).
- *Suspended Particulate Matter (SPM)*: Seawater samples were filtered onto pre-washed, pre-combusted (450°C for 5 h), pre-weighed 25-mm GF/F filters (Whatman). At the end of the filtration, de-ionized water was passed through the filters to wash out a residual amount of sea salt. The filters were then placed into petri dishes and dried at 55°C in a clean oven, and stored until post cruise analysis in the laboratory. The filters will be dried at 55°C and weighed to measure the mass concentration of SPM with a micrometric balance (MT5, Mettler-Toledo).
- *Particle size distribution (PSD)*: A Coulter counter Multisizer III (Beckman-Coulter) equipped with a 30- $\mu\text{m}$  and a 200- $\mu\text{m}$  aperture tubes was used for onboard particle

counting and sizing over the approximate size range of 0.8–120  $\mu\text{m}$ . Raw PSD data were processed with the Beckman-Coulter software (Coulter AccuComp version 3.01a). A FlowCAM system (Fluid Imaging) was used for individual particle imaging (for particle sizing and identification) over the approximate size range of 5–100  $\mu\text{m}$ . A comprehensive description of both instruments and methodology is provided in Reynolds *et al.* (2010).

- Flow cytometry: Seawater samples were preserved with glutaraldehyde and frozen in liquid nitrogen. After thawing, samples were analyzed with a FACSCalibur flow cytometer for cell fluorescence, cell size and cell counts of cells smaller than 10  $\mu\text{m}$ .

*In-situ measurements* of apparent optical properties (AOPs) and inherent optical properties (IOPs) were performed at the daily noon stations (see Table 3.3.1):

- *Apparent optical properties*: 10-min time series of underwater measurements of downwelling spectral irradiance and upwelling spectral irradiance and radiance were recorded with a hyperspectral radiometer system (HyperPRO, Satlantic) adapted to float at the sea surface and tethered such that the instrument operated at a distance of ~100 m from the vessel. Measurements were made over the spectral region 380–800 nm with a spectral resolution of 3.3 nm. Additionally, vertical profiles (0-150 m depth) of hyperspectral downwelling irradiance, upwelling radiance and upwelling irradiance were measured from aboard the vessel within the spectral region of 320-950 nm and a spectral resolution of 3.2 nm with a second set of radiometers (RAMSES, TriOS). The vessel was ideally oriented in a way minimizing ship shadow effects on the measurements. During the downcast several stops were performed to estimate wave induced fluctuations of the in-water light field.
- *Light-scattering properties*: Continuous vertical profiles of the volume scattering function (VSF) at discrete scattering angles were performed from 0-200 m using a submersible instrument package (denoted SIOP). Optical instrumentation consisted of two HydroScat-6 (HS-6, HOBILabs) for measuring the VSF at a backward scattering angle of about 140° for eleven discrete spectral bands (395, 420, 442, 470, 510, 532, 550, 589, 640, 730, and 852 nm), and a Laser In-Situ Scattering and Transmissiometer-100X (LISST-100X, Sequoia Scientific) for determining the near-forward VSF at 32 angles for a wavelength of 532 nm. The HydroScat measurements are used to derive the backscattering coefficient and the LISST measurements are used to derive the particle size distribution over a nominal size range of 1–200  $\mu\text{m}$ .
- *Beam attenuation coefficient*: Continuous vertical profiles (0–400 m) of the beam attenuation coefficient due to particles and dissolved substances were obtained using two single wavelength WETLabs C-Star transmissometers (488 and 660 nm) mounted on the main CTD-rosette.

*Online measurements* of Apparent Optical Properties:

- *Above-water remote sensing reflectance* was measured from onboard the ship with a set of three radiometers (RAMSES, TriOS). The hyperspectral radiometers

with a spectral range of 320-950 nm and a spectral resolution of 3.2 nm were installed close to the bow of the ship and measured downwelling irradiance, upwelling radiance with a viewing angle of 40° nadir and sky radiance with a viewing angle of 40° zenith. Above-water remote sensing reflectance is calculated from these parameters. When the weather conditions allowed it, measurements were conducted at every noon station and throughout the cruise.

**Tab. 3.3.1:** List of bio-optical measurements made *in-situ* (HyperPRO, SIOP, Ramses) and on discrete seawater samples taken at stations from Niskin bottles triggered at several depths within the upper water column during CTD-rosette profiles. Moon pool samples were taken between stations out of the ship's moon pool (11 m water depth). The type of measurement is indicated by the name of the technique, instrument, or measured parameter (see text for details).

Instrument/Parameter	Stations	Moon pool
HyperPRO (sea surface)	13	
SIOP (vertical profiles)	31	
Ramses (vertical profiles)	31	
HPLC (SIO)	31	
HPLC (AWI)	31	58
$a(\lambda)$ (SIO)	31	
$a(\lambda)$ (AWI)	31	58
POC	31	
SPM	31	
Coulter	29	
FlowCAM	21	
Fluorometry	31	58
Microscopy	31	58
Flow cytometry	31	58

### Preliminary (expected) results

Chlorophyll *a* (chl *a*) concentration ( $\text{mg}/\text{m}^3$ ) for 14-17 April 2010 in the Atlantic Ocean measured from satellites during *Polarstern* cruise ANT-XXVI/4 is shown in Fig. 3.3.1. The cruise track plotted into the image shows how *Polarstern* first crossed some high chl *a* regions near the Patagonian coast before hitting the typically oligotrophic waters of the South Atlantic Ocean.

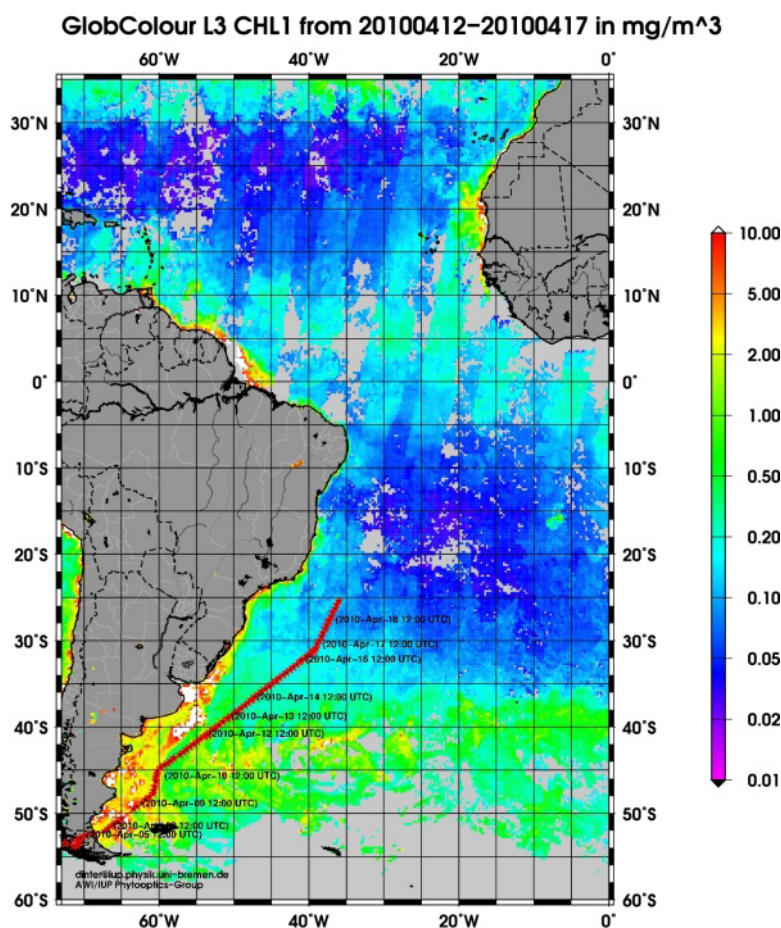


Fig. 3.3:1: Satellite chlorophyll a concentration ( $\text{mg}/\text{m}^3$ ) for 14–17 April 2010 in the Atlantic Ocean during Polarstern cruise ANT-XXVII/4. The ESA GlobColour product is a merged product of data of four different satellite instruments (MERIS, SeaWiFS, MODIS Aqua/Terra). The grid has a spatial resolution of about  $4 \times 4$  km. The cruise track for those days is also shown in the plot.

The “colour” of the ocean can be quantitatively described through the spectral remote-sensing reflectance,  $R_{rs}(\lambda)$ , which is related to the absorption,  $a(\lambda)$ , and backscattering,  $b_b(\lambda)$ , coefficients through the product  $b_b(\lambda) / a(\lambda) + b_b(\lambda)$ . Fig. 3.3.2 illustrates differences in measured ocean colour,  $R_{rs}(\lambda)$ , at two stations; this variability results from the interplay between  $a(\lambda)$  and  $b_b(\lambda)$ . At station 273, typical of oligotrophic waters encountered in the South Atlantic Ocean,  $R_{rs}(\lambda)$  peaks at blue wavebands and shows smaller values throughout the rest of the light spectrum. This is due to the increasing absorption by seawater molecules from shorter to longer wavelengths. In this environment where phytoplankton pigments and other optically significant components are present in very low concentrations, more blue light is available for backscattering by seawater molecules and particles. In contrast, the  $R_{rs}(\lambda)$  for station 265 exhibits relatively lower values at blue wavelengths and the peak is shifted towards the green. This feature is very likely related to the occurrence of large concentrations of chlorophyll and carotenoid pigments that absorb light at blue wavebands, and increased backscattering by particles. Note that for both stations, the  $R_{rs}(\lambda)$  spectra display other features (“bumps” and “shoulders”) that contain information pertaining to the composition of phytoplankton pigments, indicator of phytoplankton biodiversity. Retrieving such information is the core of our objective.

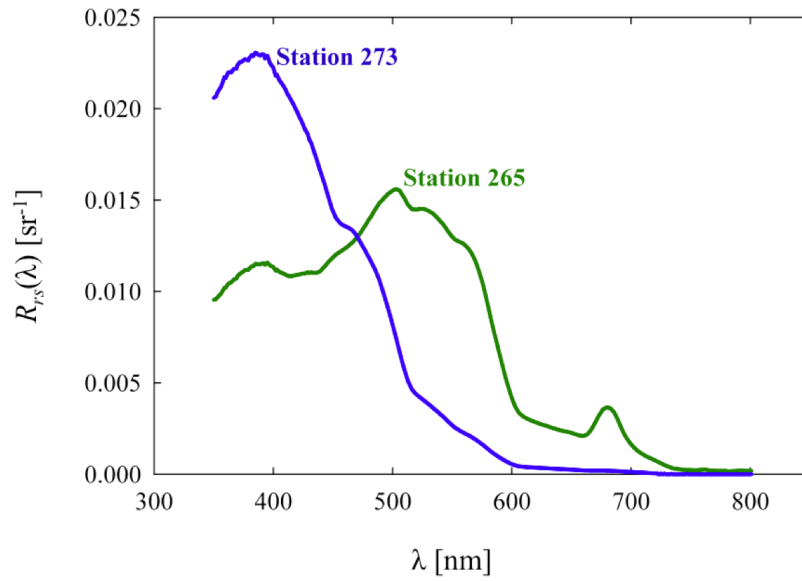


Fig. 3.3.2: Hyperspectral remote-sensing reflectance,  $R_{rs}(\lambda)$ , as a function of light wavelength,  $\lambda$ , at two contrasted stations: Station 273 sampled in the “blue” oligotrophic waters of the South Atlantic Ocean, and station 265 sampled in the “green” productive waters in the vicinity of a high-chlorophyll filament extending from the Patagonian shelf.  $R_{rs}(\lambda)$  values were derived from the HyperPRO measurements of downwelling spectral irradiance and upwelling spectral radiance.

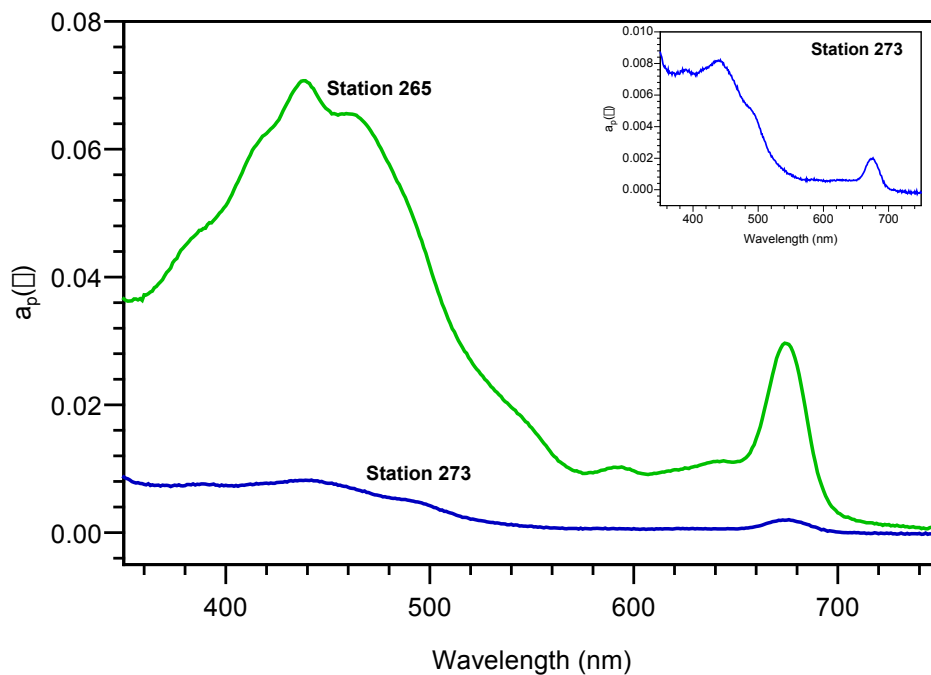


Fig. 3.3.3: Particulate absorption,  $a_p(\lambda)$ , spectra, including absorption of non-pigment particles scanned in the integrating sphere of a spectrophotometer (Varian Cary 4000) at the same stations as shown in Fig. 3.3.2: Station 273 sampled in the “blue” oligotrophic waters of the South Atlantic Ocean, and station 265 sampled in the “green” productive waters in the vicinity of a high-chlorophyll filament extending from the Patagonian shelf. The inset figure shows the rescaled station 273 spectrum.

Fig. 3.3.3 shows the particulate absorption,  $a_p(\lambda)$ , of surface water samples at the same two stations 265 and 273. As could be expected from the  $R_{rs}(\lambda)$  shown in Fig. 3.3.2, station 273 in the oligotrophic waters has little particulate absorption as phytoplankton pigments are only present in very low quantities. In contrast, station 265 on the Patagonian shelf shows high  $a_p(\lambda)$ , indicating large concentrations of chlorophyll and carotene or carotenoid pigments (main peaks around 440 and 460 nm, respectively) and possibly even some phycobilins, pigments that are characteristic of cyanobacteria (peak or "bump" around 580 nm).

#### References

- Knap A, Michaels A, Close A, Ducklow H, Dickson A (Eds.) (1994). Protocols for the Joint Global Ocean Flux Study (JGOFS) core measurements, Manuals IOC Guides 29, U. N. Educ. Sci. and Cult. Organ., Paris (Reprinted as JGOFS Rep. 19, 170 pp., 1996).
- Parsons TR, Maita Y, Lalli CM (1984). A Manual of Chemical and Biological Methods for Seawater Analysis, 173 pp., Pergamon, Oxford, UK.
- Reynolds RA, Stramski D, Wright VM, Wozniak SB (2010). Measurements and characterization of particle size distributions in coastal waters, J. Geophys. Res. 115, C08024, doi:10.1029/2009JC005930.
- Roettgers R, Haese C, Doerffer R (2007). Determination of the particulate absorption of microalgae using a point-source integrating-cavity absorption meter: verification with a photometric technique, improvements for pigment bleaching, and correction for chlorophyll fluorescence. Limnol. Oceanogr.: Methods, 5, 1-12.

### 3.4 OCEANET – atmospheric measurements

Timo Hanschmann, Thomas Kanitz, Andreas Macke (not on board), Dietrich Althausen (not on board)  
IfT, Leipzig

Yann Zoll (not on board), John Kalisch (not on board),  
IFM-GEOMAR, Kiel

Henry Kleta (not on board)  
DWD, Hamburg

#### Objectives

Clouds remain one of the biggest obstacles in our understanding of the coupled ocean-atmosphere climate system. Even under realistic forcing from observed wind, humidity and pressure fields, climate models have difficulties to reproduce the correct spatial and temporal climatology of cloud cover. Because of the strong inhomogeneity of cloud patterns on those scales that are relevant for the radiative transfer processes it is clear that subgrid-scale processes must be accounted for in radiative transfer parameterizations. Combined observations of cloud physical and radiative properties are a key to adjust or to validate such parameterizations.

The measurements are part of the Leibniz network-project OCEANET. Within the project, the OCEANET Atmosphere Observatory, a 20' sea container equipped with

*in-situ* and remote sensing instruments has been developed and is applied on the expedition ANT-XXVI for the first time (see Fig. 3.4.1). A new instrument in OCEANET Atmosphere Observatory is the Polly XT Lidar System from IfT for vertical profiling of aerosol and clouds. These measurements are accompanied by regular sun photometer observations of aerosol properties that are performed for the Marine Aeronet Network MAN operated by NASA. These measurements were operated by another group during this cruise.



Fig. 3.4.1: OCEANET Atmosphere Container during ANT-XXVI/4 (Photo by Katrin Lonitz).

### Work at sea

After lifting the OCEANET Atmosphere Container onto the Pier in Punta Arenas the Lidar was reinstalled and the container was lifted back onto compass platform above the bridge of *Polarstern*. The OCEANET Atmosphere Container comprises the following instruments:

The upward looking pyranometer Kipp & Zonen CM 21 and the pyrgeometer CG 4 operated by IFM-GEOMAR provide the broadband downwelling shortwave radiation (DSR) and the downwelling longwave radiation (DLR) every second. Every 15 s full sky images were obtained with a weather proofed digital camera system manufactured at IFM-GEOMAR. This enables a detailed analysis of the role of cloud cover and cloud type on the radiation budget at the sea surface. These images are also valuable for the aerosol remote sensing activities to identify clear sky cases.

As on the previous six OCEANET transits of *Polarstern*, a multi-channel microwave radiometer (HATPRO, Radiometer Physics) was utilized for continuous observations of atmospheric temperature and humidity profiles as well as liquid water and precipitable water path. Together with ceilometer measurements of cloud bottom height, sun photometer measurements of aerosol optical thickness (section 4.1), infrared

radiometer measurements of cloud bottom temperatures, the data from the microwave radiometer provide a unique set of information to interpret the amount of downwelling solar and thermal radiation at the sea surface. One of the seven humidity channels (the one that is most sensitive to surface-near humidity) malfunctioned at the beginning of the last cruise and could not be fixed on board. The instrument consists of 14 channels in total so that the loss of one channel was not problematic. However, the retrieval algorithm that converts microwave radiation into atmospheric properties had to be adjusted on the first transect ANT-XXIV/1 and satisfying data were still obtained on ANT-XXVI/4.

Lidar measurements were performed, whenever weather conditions were appropriate. The system was switched off during mid-day, when high sun elevations could damage the sensible optics. The employed PollyXT Lidar that had been developed at the IfT emits laser pulses at 1064 nm, 532 nm and linear polarized light at 355 nm into the atmosphere and measures the backscattered elastic light at 180° scattering angle. Additionally the Raman method is utilized by detecting molecular scattering of nitrogen at 387 and 607 nm. The opportunity of observing depolarization at 355 nm rounds up the system. The scattered light at each wavelength is measured every 30 s up to 20 km height at a range resolution of 30 m. Thus, it provides the chance of a high temporal and range resolved description of the vertical aerosol distribution. The analysis of the retrieved optical and microphysical properties allows the characterization of separated aerosol layers with high vertical resolution. In combination with a radiative transfer model the results will help to quantify the solar aerosol radiative forcing above oceans. As a byproduct, Polly XT provides cloud base and top height, the latter for clouds of optical thickness up to 2.5 only.

Within the OCEANET project, a shipborne automatic weather station has been developed. The so called SCalable Automatic Weather Station (SCAWS) is based on standard hardware (Campbell Scientific) and measures autonomously the following parameters: time, position, speed and course over ground, heading, barometric pressure, temperature, relative humidity, wind (direction and speed) and radiation (short- and longwave). During the cruise sections ANT-XXVI/1-3, SCAWS was measuring on *Polarstern* fully automatically. After the first days on the present section, a problem with the GPS-compass occurred. This led to loss of heading data and position information and resulted in a lack of true wind information. This problem could be fixed preliminarily during the cruise. Note that by using ship system data a post-computation of the true wind is still possible. The sensors are standard within the maritime network of the DWD. The system provides a complete set of data every second (proprietary NMEA 0183 protocol) and an hourly weather report (FM13 SHIP) which is transmitted ashore via the DWD-owned Data Collection Platform (DCP). In addition to these standard outputs, SCAWS monitors the power supply of the sky imager installed on top of the OCEANET Atmosphere Container. This information is included with mean values of the connected radiation sensors and transmitted ashore as well, thus allowing real-time monitoring of the radiation fluxes and the status of the sky imager. It is planned to add further instruments to SCAWS in the future.

### Preliminary (expected) results

The time series of integrated water vapour (IWV) and liquid water paths (LWP) along the cruise are shown in Fig. 3.4.2. The *in-situ* observed IWV from the radiosonde measurements is also shown, and provides a generally good agreement with the indirectly obtained microwave products. Largest water vapour paths of more than 50 kg m<sup>-2</sup> are observed at the thermal equator, where the warm conditions and strong cloud induced upwind pump most humidity from the ocean into the troposphere. The cloud LWP is given by the occasional data points above a background noise, which needs to be corrected for during later analysis. The corrections make use of the sky camera images and upward looking IR-radiometer measurements which indicate clear sky situations above the ship during day time.

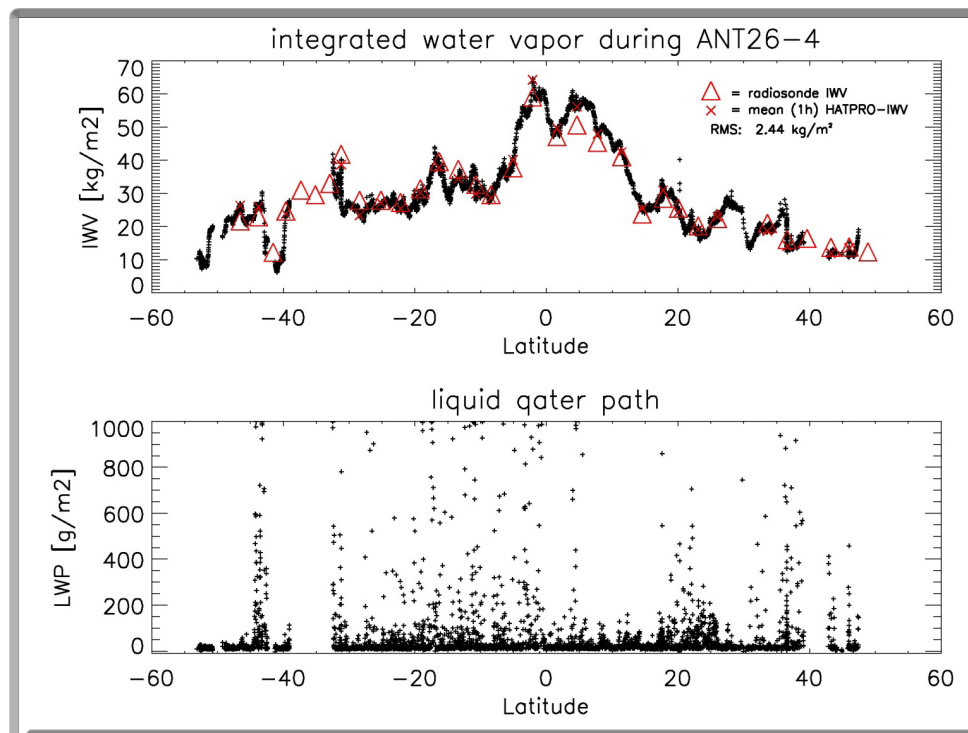


Fig. 3.4.2: Time series of water vapour path (upper panel) and liquid water path (lower panel) from HATPRO microwave radiometer. The water vapour path from the radiosonde measurements is also shown (graph by Yann Zoll).

The daily time series of the downwelling shortwave and longwave radiation along the entire *Polarstern* cruise are summarized in Figs. 3.4.3-3.4.5. For reference, the theoretical curve for clear sky radiation is also shown. Although clouds usually block the sun and reduce the downwelling solar radiation, many occasions of a radiation excess can be found, which is attributed to the increased diffuse downwelling radiation during broken cloud conditions (because of this termed as “broken cloud effect”). Further analysis will test the correlation between the observed cloud properties like cloud cover and liquid water path, and the surface radiation budget.

### 3.4 OCEANET – atmospheric measurements

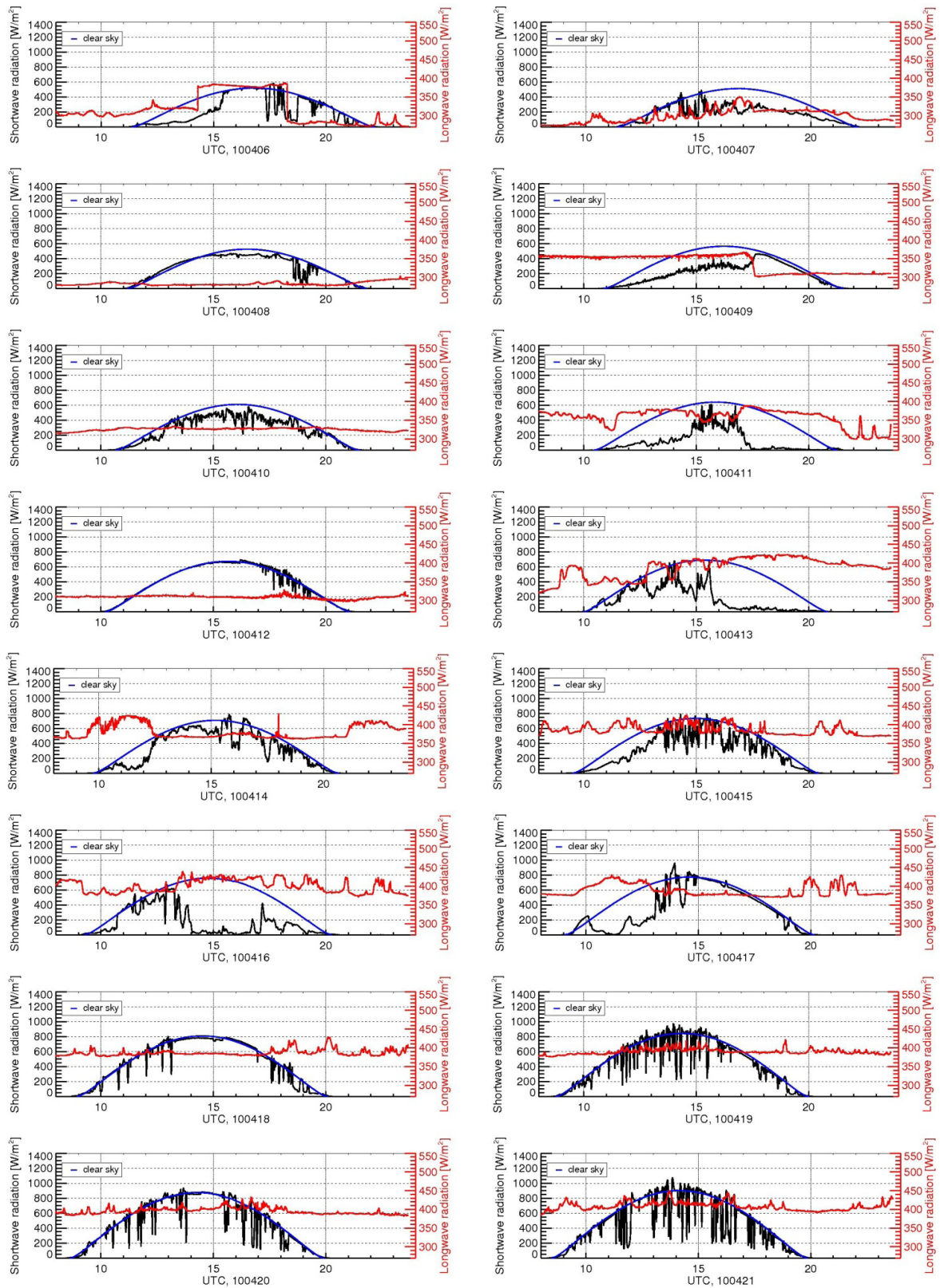


Fig. 3.4.3: Daily time series of downwelling broadband solar (black) and thermal (red) radiation from 6-21 April 2010. The reference clear sky radiation (blue) is shown for comparison (graph: John Kalisch).

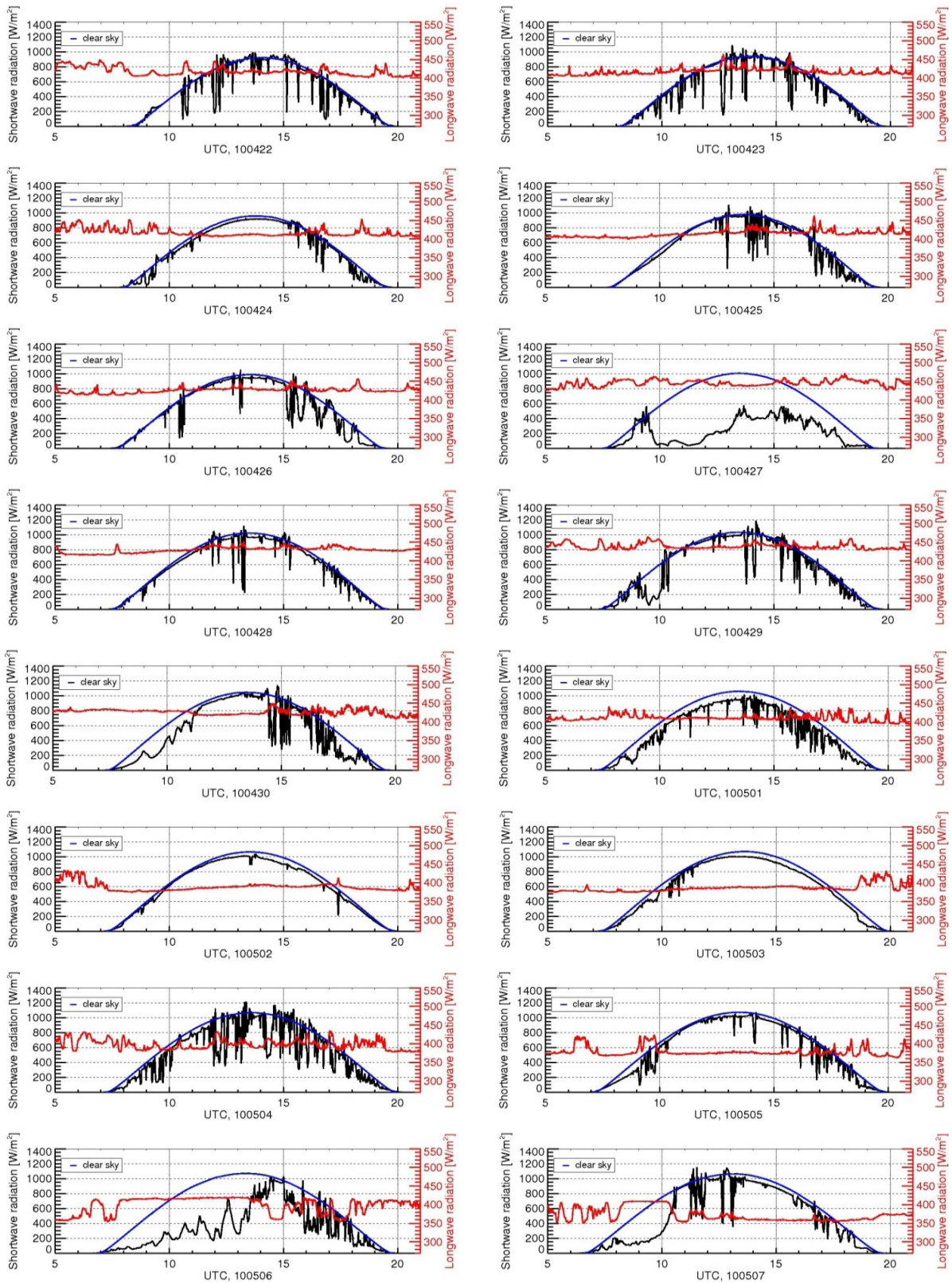


Fig. 3.4.4: Daily time series of downwelling broadband solar (black) and thermal (red) radiation from 22 April to 7 May 2010. The reference clear sky radiation (blue) is shown for comparison (graph: John Kalisch).

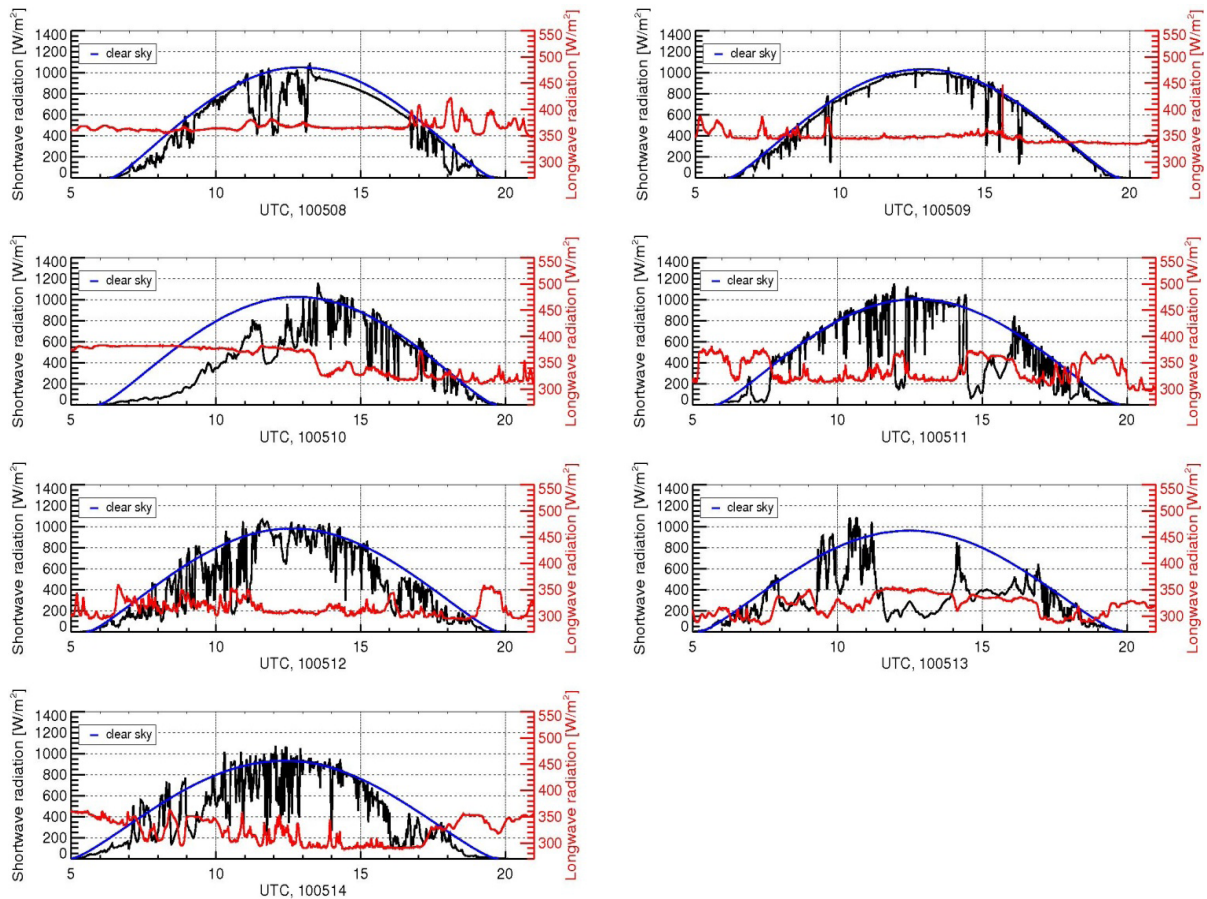


Fig. 3.4.5: Daily time series of downwelling broadband solar (black) and thermal (red) radiation from 8-14 May 2010. The reference clear sky radiation (blue) is shown for comparison (graph: John Kalisch).

After its first marine deployment during ANT-XXVI/1, the PollyXT lidar had been stored in Punta Arenas at a host institute. It was picked up again for this cruise to complete our measurements during the cruise ANT-XXVI/4.

A smoke plume was observed between 30 April and 2 May 2010 along the west coast of Africa. Fig. 3.4.6 shows the range-corrected signal at 1064 nm at a logarithmic scale with time and position as function of height. At about 04:00 UTC one lofted layer reached the *Polarstern* from about 2.2 to 3 km height and split thereafter. Thus, at about 08:00 UTC two single lofted layers were observed. Both of them and the maritime boundary layer were separated by less loaded layers. The top of the plume reached up to 4000 m height and the base was at around 1500 m altitude during the presented measurement. MODIS and HYSPLIT trajectories point at fires at the west coast of Africa to be the source of these layers which has to be confirmed by the determination of the optical properties. Unfortunately, this time series had to be terminated because of the high sun elevation at 11.23 UTC. Nevertheless this plume had been observed through the next days.

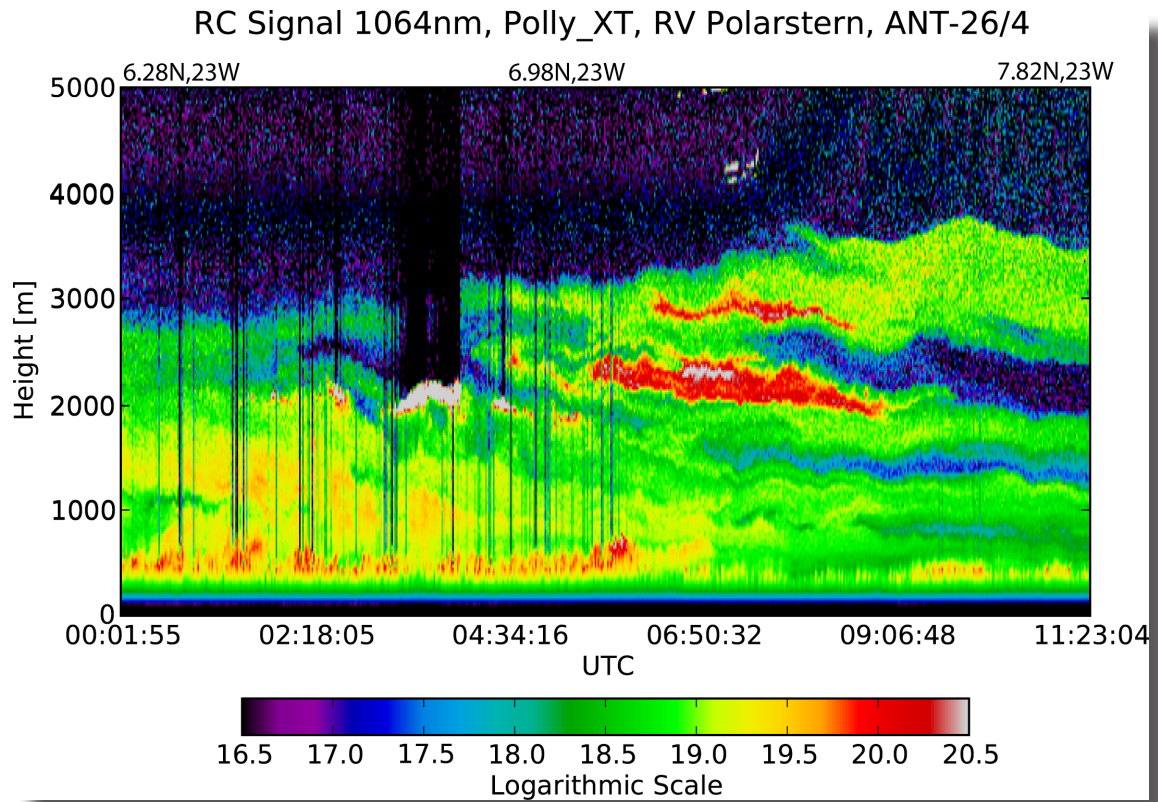


Fig. 3.4.6: Range-corrected backscattering signal of the smoke plume at 1064 nm on 30 April 2010. (graph: Thomas Kanitz).

---

## 4. FURTHER PROJECTS

In addition to the OCEANET projects, a number of further projects participated in the cruise ANT-XXVI/4. These are summarized below:

**4.1 Measurements of aerosol optical thickness:** In order to improve our knowledge about the optical properties of aerosols, regular measurements of the aerosol optical thickness were performed for the Marine Aeronet Network (MAN) operated by NASA by using a sun photometer.

**4.2 Atmospheric Dust and Irradiation effects on Ocean surface processes – Biogeochemistry in the Atlantic Ocean (ADIOS-BAO):** The aim of the project was to produce comprehensive data on crust-derived trace metals (Al, Fe and Ti) and phosphate in the surface ocean over contrasting regions of the Atlantic Ocean.

**4.3 Determination of photochemical processes during a transect through the Atlantic:** Aim of this project was to determine the distribution and properties, including reactivity with superoxide, of CDOM in the upper ocean along a meridional transect in the Atlantic Ocean. These measurements allow to examine the influence of irradiation on dust dissolution via redox processes.

**4.4 Measurement of concentration and isotopic signature of hydrogen in surface ocean and atmosphere:** This project measured the concentration and isotopic signature of hydrogen in the atmosphere and surface ocean. The ultimate goal is to quantify oceanic hydrogen emissions and their role in the global atmospheric hydrogen cycle. The latitudinal distribution of atmospheric hydrogen will be used to improve atmospheric models.

**4.5 Abyssal temperature fluctuations in the Vema Channel:** Revisit to the Vema Sill site for continuation of a time series of high precision CTD observations of the coldest AABW in the Vema channel.

**4.6 Glider swarm experiment at Cape Verde Ocean Observatory:** Recovery of four gliders from the first Kiel glider swarm experiment that was aimed at studying physical-biogeochemical submesoscale coupling in a region of high variability.

**4.7 Testing of the Posidonia system of Polarstern:** Testing and calibration of the Posidonia system with a transponder mooring after further system changes and removal of protective window.

## 4.1 Measurements of aerosol optical thickness

Katrin Lonitz, Stefan Kinne (not on board)  
MPI-MET, Hamburg

### Objectives

Aerosols in the atmosphere are known to significantly influence the Earth's radiative forcing. Estimates of the total net anthropogenic forcing are about  $1.6 \text{ W m}^{-2}$  ( $0.6 - 2.4 \text{ W m}^{-2}$ , IPCC 2007) where most of the high uncertainty of this value can be attributed to the role of aerosols. Our knowledge about the optical properties of aerosols is still incomplete, resulting in the significant uncertainty of the overall radiative forcing. One reason for this is the inhomogeneous distribution of aerosols in time and space. Therefore a big need exists for global and continuous monitoring of aerosol properties. Onboard *Polarstern*, regular sun photometer observations were performed for the Marine Aeronet Network (MAN) operated by NASA. Such measurements have been made for many years now and are the only way to measure the aerosol optical thickness (AOT) aboard a moving ship.

### Work at sea

The Microtops II sun photometer is a hand-held Volz-type device with narrow field-of-view sensors, which can be manually pointed at the sun. These photometers are in use worldwide. Measurements with the sun photometer were performed whenever possible, that is during daytime when no cloud was covering the sun. Every 2-3 min ten consecutive measurements were taken at five different wavelengths (380, 440, 675, 870 and 936 nm) to measure the water vapor and the aerosol optical thickness (AOT). Difficulties arose when the ship was seesawing due to waves or when the wind was blowing strong. Then, the direct pointing into the sun of the sun photometer was difficult. Measurements have been performed for different times during the day and when the satellites TERRA or CALIPSO were passing close to the *Polarstern* track.

### Preliminary (expected) results

Three examples of preliminary results are presented. Fig. 4.1.1 shows the aerosol optical thickness (AOT) at four wavelengths (380, 440, 675 and 870 nm) on 9 April 2010. During the whole day the AOT values remained at very low levels of about 0.1. This is typical for pristine air which is common above the open ocean. Another variable that informs about the aerosol particle size is the Ångström exponent. In Fig. 4.1.2, the Ångström exponent does not change with wavelength and shows values around 0.5 indicating that large aerosols were present, which probably originate from sea spray.

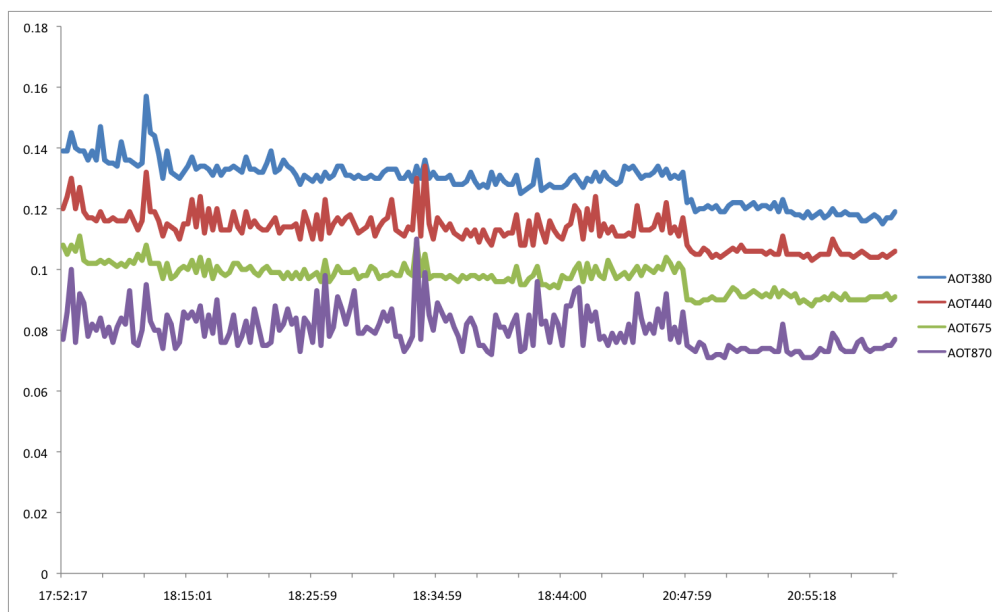


Fig. 4.1.1: AOT at four different wavelengths on 9 April 2010.

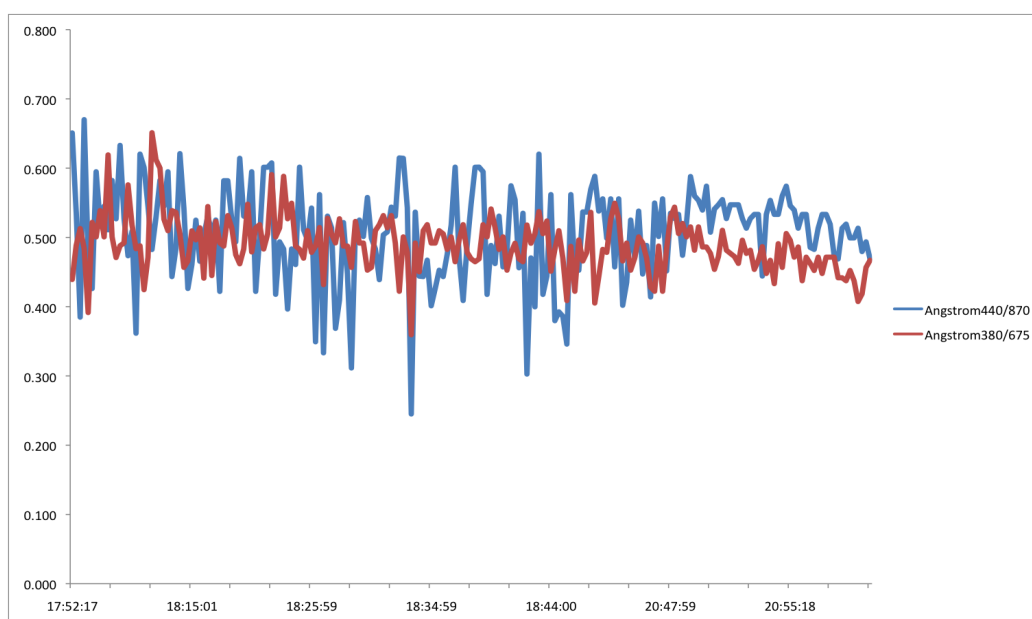


Fig. 4.1.2: Ångström exponent at two different wavelengths on 9 April 2010.

The second example shows the almost cloud free day of 18 April 2010, where only some cumulus clouds appear. On this day, the satellite TERRA, which has a Multi-angle Imaging SpectroRadiometer (MISR) aboard, crossed the *Polarstern* track at an angle of  $71^\circ$ . The measurements performed on board the *Polarstern* around 12:30 UTC fall in the swath width of MISR. Therefore, the AOT retrieved with MISR and measured with the Microtops could be compared (Fig. 4.1.3). For this day, the AOT values compare very well with each other.

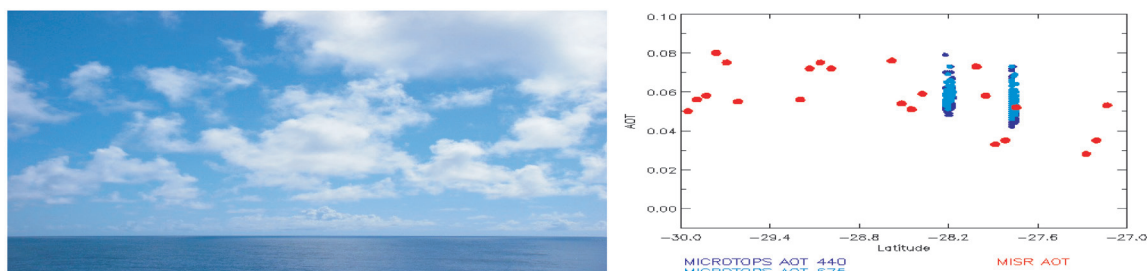


Fig. 4.1.3: Weather conditions and AOT values from CALIPSO and the Microtops sun photometer taken 18 April 2010

The third example shows a similar comparison as before with retrievals from the satellite CALIPSO. The day of 9 May 2010 was selected for this comparison, where the weather condition can be seen in Fig. 4.1.4. CALIPSO crossed the track of *Polarstern* around 14:15 UTC in an angle of  $75.8^\circ$ , which equals a distance of about 178 km. The distribution of AOT values retrieved with CALIPSO fell mostly around 0.05. An exception occurred in the latitude range of the sun photometer measurements, when suddenly the AOTs jumped to values above 0.1, which fell in the range of the Microtops AOT values. Here it was not quite clear if the CALIPSO values were in general too low or the regime in which the *Polarstern* was located had different aerosol properties as the surrounding air.

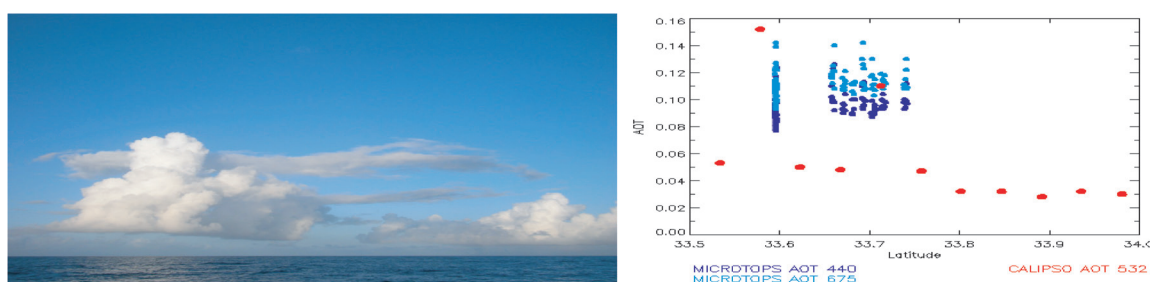


Fig. 4.1.4: Weather conditions and AOT values from MISR and the Microtops sun photometer taken on 9 May 2010

## References

IPCC, Climate Change (2007): The Physical Science Basis. Contribution of Working Group I to the Fourth Assessment Report of the Intergovernmental Panel on Climate Change, Solomon S, Qin D, Manning M, Chen Z, Marquis M, Averyt KB, Tignor M, Miller HL (eds.), Cambridge University Press, Cambridge, UK and New York, NY, USA, 996 pp.

## 4.2 Atmospheric dust and irradiation effects on ocean surface processes – biogeochemistry in the Atlantic Ocean

Thibaut Wagener, Maija Heller, Anna Dammshäuser, Peter Croot (not on board), IFM-GEOMAR, Kiel

Diego Gaiero  
UNC, Córdoba, Argentina

### Overall Objectives

While full basin scale oceanographic transects through the Atlantic Ocean are becoming more frequent now thanks to the annual repositioning cruises of *Polarstern* and the United Kingdom's AMT program (Robinson *et al.*, 2009), coverage is still relatively sparse in terms of some key processes and regions and this is especially so for atmospheric deposition to the Southern Atlantic. Trace metal measurements in surface waters have been made on some of these expeditions but the bulk of the measurements are from the NE Atlantic (Bowie *et al.*, 2002; Sarthou *et al.*, 2003; Measures *et al.*, 2008). In the NE Atlantic, these studies have revealed a close relationship between atmospheric dust fluxes and metal concentrations in surface waters along the meridional transects driven principally by the Saharan dust plume in the Tropical North Atlantic. Currently data is in particular lacking from the SW Atlantic and south of the ITCZ which would provide information on regions not impacted by the Sahara.

The supply of iron and other crustal metals to the surface ocean is predominantly from atmospheric dust deposition. The Tropical North Eastern Atlantic is the region of the world's oceans which receives the most dust deposition from the adjacent Sahara. Contrastingly the South Western Atlantic receives low dust fluxes which are far more episodic and seasonal in nature. A meridional section in the Atlantic that combines these two regions is then a natural laboratory to study the processes that occur when atmospheric dust dissolves and sinks through the water column. By performing at sea experiments with freshly collected seawater and aerosols we are able to better understand the key processes involved in the dissolution of trace elements from aerosols. This will also allow us the possibility to explore the properties of the seawater and dissolution rates of aerosols. The information gained from this work will give insights into the key biogeochemical processes such as scavenging and dissolution. This information can be used to estimate residence times and distributions for each trace element under consideration. This data is important for improving our understanding of trace metal biogeochemistry and primary productivity in the ocean and the results can also be applied to other regions where the same chemical processes are occurring.

During ANT-XXVI/4, the IFM-GEOMAR Aqueous Trace Oxidant and Metal Speciation Laboratory (ATOMSLab) had 5 main research themes funded by the DFG, BMBF and EU:

- (1) To obtain near surface distributions of the rapidly scavenged, crust-derived elements aluminium (Al), titanium (Ti) and iron (Fe) in the surface ocean along a transect from Punta Arenas to Bremerhaven in the Atlantic Ocean.

- (2) To study Fe speciation in the surface ocean along a transect from Punta Arenas to Bremerhaven in the Atlantic Ocean.
- (3) To examine the distribution of  $\text{H}_2\text{O}_2$  and Fe(II) in surface waters along a transect from Punta Arenas to Bremerhaven in the Atlantic Ocean and assess the influence of irradiation on trace metal redox cycles.
- (4) To investigate the kinetics of processes that supply P and Fe to surface seawater from aerosol deposition along a meridional transect in the Atlantic Ocean.
- (5) To determine the distribution and properties, including reactivity with superoxide, of CDOM in the upper ocean along a meridional transect in the Atlantic Ocean.

The overall aim of this work is to investigate and quantify concentrations, fluxes and rates pertaining to aerosol deposition of key trace elements to the Atlantic Ocean.

## A. Atmospheric deposition of trace metals and phosphorus

### Objectives

Atmospheric deposition of particles is a major source of chemical elements to the surface ocean. Along the ANT-XXVI/4 cruise track, the dissolution processes of four chemical elements (Fe, Al, Ti, P) in seawater have been investigated. Indeed, all these elements are transported by desert dust particles which represent the largest flux of atmospheric particles deposited on the ocean at the global scale. Along the ANT-XXVI/4 transect in the Atlantic, two potentially different plumes of lithogenic dust particles to the ocean have been crossed: South American arid areas for South Atlantic and Sahara Desert for North Atlantic.

### Methods/Work at Sea

*Water Sampling:* Seawater sampling for the study of trace metals was performed using 4 Teflon coated 8 L PVC General Oceanics (Miami/FL, USA) GO-FLO bottles. The bottles were deployed on the Kevlar line of *Polarstern*. Along the cruise transect, two types of GO-FLO stations were performed: Surface stations with one cast down to 30 meters depth and deep stations with two casts (one down to 100 m and the other a deeper cast down to 400 m). Bottles were immediately transferred into the IFM-GEOMAR clean container (Class 5 HEPA filtered air environment) after recovery, in order to avoid the contamination of the seawater samples. Seawater was filtered with a small overpressure (0.2 bar) of nitrogen on Sartobran (Sartorius, Germany) membranes ( $0.2 \mu\text{m}$ ) directly connected to the bottles.

*Aerosol sampling:* Along the cruise transect, aerosol samples for the study of trace metal deposition have been collected using a sampler developed at the Laboratoire d'Océanographie de Villefranche sur Mer (CNRS-FRANCE) allowing a confident cumulative sampling for the study of trace elements (Wagener *et al.*, 2008a). The sampler was located on the highest deck of *Polarstern*. Pumps and control devices were located above the compass platform.

*Experiments performed on board:* Two types of experiments have been done on board in order to evaluate the importance of atmospheric and marine processes on the dissolution from atmospheric particles of the studied elements:

- (1) Leaching experiments on the collected aerosol samples with Milli-Q and collected seawater in parallel were performed every two day in order to estimate the amount of dissolved Al, Fe and Ti following the leaching protocol described by Buck *et al.* (2006). Additional leaching experiments on aerosols collected close to South American source areas were performed with south Atlantic seawater from GOFLO-02 and GOFLO-11.
- (2) Batch reactor dust dissolution experiments over ten days with “end member dust particles” (soil particles that are eolisable from Sahara and Patagonia) were performed three times along the cruise transect with surface (25 m) seawater collected on GOFLO-03, GOFLO-09 and GOFLO-19 in order to determine the possible role of “the biogeochemical state” of seawater for controlling the dissolution of these elements following a protocol described in Wagener *et al.* (2008b).

*Chemical measurements performed on board:* For seawater or dust dissolution experiments, dissolved iron (dFe) was measured on filtered and acidified seawater (< pH 2) collected from the GO-FLO bottles. dFe is measured by flow injection analysis with chemiluminescence detection after preconcentration on a 8-hydroxyquinoleine column following the original method of Obata *et al.* (1993).

During ANT-XXVI/4, 5 major GO-FLO stations were performed in which samples down to 400 m were collected. A further 12 GO-FLO stations were made where only surface samples were obtained. Details of all GO-FLO stations sampled can be found in Table 4.2.1. A total of 16 aerosol samples were also collected during the course of this cruise and details on these samples can be found in Table 4.2.2.

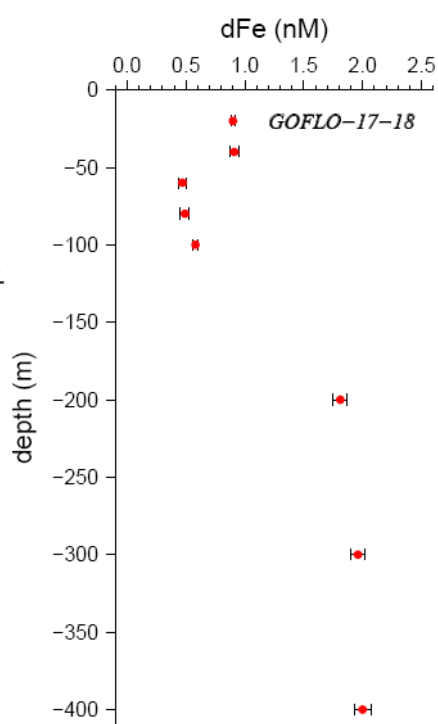
**Table 4.2.1:** GOFLO stations during ANT-XXVI/4

Date	Time UTC	Station	Latitude	Longitude	Label
2010-avr.-10	04:36:00	PS75/0264-2	-47,6602	-60,7483	GOFLO_1
2010-avr.-11	17:58:00	PS75/0266-4	-43,223	-57,2972	GOFLO_2
2010-avr.-13	15:20:00	PS75/0268-1	-39,0932	-50,9337	GOFLO_3
2010-avr.-15	15:19:00	PS75/0270-1	-34,716	-44,4405	GOFLO_4
2010-avr.-17	12:31:00	PS75/0272-2	-31,2002	-39,3422	GOFLO_5
2010-avr.-17	15:44:00	PS75/0272-4	-31,2088	-39,3677	GOFLO_6
2010-avr.-19	14:17:00	PS75/0274-1	-24,754	-35,7127	GOFLO_7
2010-avr.-21	14:14:00	PS75/0276-1	-18,7878	-32,5228	GOFLO_8
2010-avr.-23	14:22:00	PS75/0278-1	-13,0563	-28,5098	GOFLO_9
2010-avr.-24	14:13:00	PS75/0279-2	-10,7143	-26,9122	GOFLO_10
2010-avr.-24	16:16:00	PS75/0279-6	-10,7078	-26,9292	GOFLO_11
2010-avr.-26	14:17:00	PS75/0281-1	-5,1628	-23,1097	GOFLO_12
2010-avr.-28	12:34:00	PS75/0283-1	1,7765	-22,9992	GOFLO_13
2010-avr.-28	14:25:00	PS75/0283-5	1,7745	-23,0012	GOFLO_14
2010-avr.-30	13:19:01	PS75/0285-1	8,065	-22,9998	GOFLO_15
2010-mai-02	13:43:00	PS75/0286-2	14,5532	-23,683	GOFLO_16
2010-mai-04	02:59:00	PS75/0287-2	17,5828	-24,253	GOFLO_17
2010-mai-04	07:55:00	PS75/0287-4	17,589	-24,2608	GOFLO_18
2010-mai-04	13:16:00	PS75/0289-1	17,6088	-24,7505	GOFLO_19
2010-mai-06	11:32:00	PS75/0292-1	23,1225	-20,6535	GOFLO_20
2010-mai-09	11:29:00	PS75/0294-1	33,6005	-13,8562	GOFLO_21
2010-mai-09	13:23:00	PS75/0294-5	33,5943	-13,8572	GOFLO_22
2010-mai-11	11:47:00	PS75/0296-1	39,7625	-11,8458	GOFLO_23

**Table 4.2.2:** Aerosol samples collected during ANT-XXVI/4

Label	Time Start	Time End
ANT26-4_Aero_1	09.04.2010 17:01	10.04.2010 17:15
ANT26-4_Aero_2	10.04.2010 17:20	12.04.2010 17:00
ANT26-4_Aero_3	13.04.2010 11:30	14.04.2010 16:05
ANT26-4_Aero_4	14.04.2010 16:17	16.04.2010 15:52
ANT26-4_Aero_5	16.04.2010 16:00	18.04.2010 16:10
ANT26-4_Aero_6	18.04.2010 16:15	21.04.2010 10:40
ANT26-4_Aero_7	21.04.2010 11:20	23.04.2010 14:41
ANT26-4_Aero_8	23.04.2010 15:06	25.04.2010 15:03
ANT26-4_Aero_9	25.04.2010 15:12	28.04.2010 9:30
ANT26-4_Aero_10	28.04.2010 09:42	29.04.2010 15:18
ANT26-4_Aero_11	29.04.2010 15:27	01.05.2010 07:50
ANT26-4_Aero_12	01.05.2010 08:00	02.05.2010 14:40
ANT26-4_Aero_13	04.05.2010 09:40	05.05.2010 12:50
ANT26-4_Aero_14	05.05.2010 13:00	07.05.2010 11:37
ANT26-4_Aero_15	07.05.2010 11:48	09.05.2010 15:25
ANT26-4_Aero_16	09.05.2010 15:35	11.05.2010 07:30

Fig. 4.2.1: Dissolved iron concentrations measured onboard Polarstern during cruise ANT-XXVI/4 at the CVOO time series site near Cape Verde.



### Preliminary (expected) results

Sampling of aerosols and seawater was carried out successfully. Some preliminary shipboard data was obtained using the iron FIA system onboard. An example of data from this is shown in Fig. 4.2.1 where the influence of Saharan dust can be seen in the elevated iron concentrations found in near surface waters at the CVOO site. The bulk of the samples collected during ANT-XXVI/4 are being analyzed in the laboratory in Kiel.

## **B. Titanium and Aluminium along a south/north transect in the Atlantic Ocean**

### **Objectives**

As part of the ADIOS-BAO program we examined the upper ocean distribution of Al and Ti along the cruise transect. This information will allow us to better constrain the residence times of Ti and Al in the ocean and in particular to examine the processes that determine the surface concentrations of these elements.

While it is established now that Fe can be a (co)limiting nutrient for phytoplankton in High Nutrient Low Chlorophyll (HNLC) regions of the world, we still know little about the processes by which Fe is supplied to the ocean and how processes in the ocean scavenge/uptake or remineralize dissolved Fe. In many cases, examination of other elements similar in chemistry to iron reveals more information on the key processes involved – such elements include Ti(IV), Al(III) and Mn(II). By comparison of the concentrations of these strongly hydrolysed elements in the soluble, dissolved and particulate phases we hope to be able to better understand the processes affecting dust dissolution and particle scavenging in the surface ocean.

There is little information on Ti biogeochemistry in open ocean seawater with only one single deep-water profile from the Pacific (Orians and Boyle, 1993; Orians *et al.*, 1990) which showed picomolar concentrations in surface waters and increasing to ~300 pM in deep waters. Overall there is little information on the global Ti distribution in the ocean. Based on the work of Orians *et al.* (1990), Ti has a short residence time in the ocean and is enriched with depth due to remineralisation processes. In the present study, through the use of a new voltametric technique, developed at IFM-GEOMAR, that allows shipboard determination of pM levels of Ti, we are set to test this hypothesis.

By comparison of the chemistries and distributions of Ti and Al we aim to improve our knowledge of the processes effecting trace metal distributions in the ocean with emphasis on dust deposition. The work performed during ANT-XXVI/4 is also a continuation of similar earlier work performed on the *Polarstern* (ANT-XVIII/1 and ANT-XXIII/1) (Bowie *et al.*, 2002; Sarthou *et al.*, 2003) and the Meteor Cruise M55 (Croot *et al.*, 2004).

### **Methods/Work at Sea**

*Water Sampling:* In the present work we obtained vertical profiles for Ti and Al along the Atlantic meridional transect in the Atlantic Ocean at selected stations (Tables 4.2.2 and 4.2.3) using individual GO-FLO samplers and the Niskin bottles on the CTD rosette. All sample handling was performed in a Class 5 clean environment within the IFM-GEOMAR clean container located on the working deck.

*Measurement of Al and Ti:* Samples were analysed for Ti(IV) using a new voltametric method developed at IFM-GEOMARhy. Samples for Al were analysed by the fluorometric method of Hydes and Liss (1976) using a Hitachi FL 2700 Fluorescence Spectrophotometer. Volumes of 125 mL of unfiltered seawater were sampled from the CTD in LDPE bottles and acidified with 375  $\mu$ L of sub-boiled distilled HCl for

approximately 24 h before the samples were analyzed for total dissolvable Al using the reagent lumogallion.

Samples for total dissolvable Al were taken at 14 CTD stations (table 4.2.3). Suspended particulate matter (SPM) was sampled at ten GO-FLO stations (5-6, 10-11, 13-14, 17-18, 21-22) for the analysis of total particulate Al, Fe and Ti. The samples were taken on 0.2  $\mu\text{m}$  polycarbonate filters directly from the GO-FLO bottles using nitrogen overpressure and Teflon filter holders. SPM samples will be digested following the procedure described by Cullen and Sherrell (1999).

**Table 4.2.3:** CTD stations sampled for total dissolvable Al during ANT-XXVI/4

Date	Time UTC	Station	Latitude	Longitude	Label
10/04/2010	03:47:00	PS75/0264-1	47° 39.87' S	60° 44.99' W	CTD264_1
10/04/2010	17:15:00	PS75/0265-2	45° 35.39' S	60° 21.25' W	CTD265_2
13/04/2010	16:23:00	PS75/0268-3	39° 5.33' S	50° 56.40' W	CTD268_3
15/04/2010	16:24:00	PS75/0270-3	34° 43.12' S	44° 27.18' W	CTD270_3
17/04/2010	10:17:00	PS75/0272-1	31° 11.73' S	39° 20.37' W	CTD272_1
19/04/2010	15:24:00	PS75/0274-3	24° 45.12' S	35° 43.12' W	CTD274_3
21/04/2010	15:16:00	PS75/0276-3	18° 47.22' S	32° 31.57' W	CTD276_3
23/04/2010	15:22:00	PS75/0278-3	13° 3.68' S	28° 30.79' W	CTD278_3
26/04/2010	15:13:00	PS75/0281-3	5° 9.77' S	23° 6.66' W	CTD281_3
28/04/2010	13:54:00	PS75/0283-3	1° 46.52' N	23° 0.06' W	CTD283_3
30/04/2010	14:15:00	PS75/0285-3	8° 4.09' N	23° 0.21' W	CTD285_3
04/05/2010	01:00:00	PS75/0287-1	17° 35.00' N	24° 15.16' W	CTD287_1
06/05/2010	12:30:00	PS75/0292-4	23° 7.16' N	20° 39.72' W	CTD292_4
11/05/2010	12:46:00	PS75/0296-3	39° 45.84' N	11° 51.37' W	CTD296_3

### Preliminary (expected) results

Dissolved Al and Ti concentrations varied along the transect and were highest in the high dust flux regions. Dissolved concentrations of Al and Ti at the CVOO time series station in the Eastern Tropical Atlantic (Fig. 4.2.1) show elevated concentrations in near surface waters due to dust deposition and possible evidence for scavenging of Ti in the vicinity of the chlorophyll maximum (60-80 m deep).

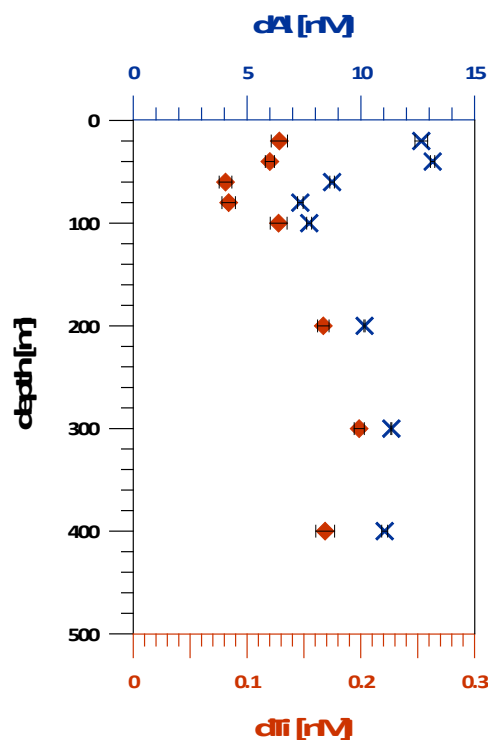


Fig. 4.2.1: Dissolved Al and Ti at the CVOO station ( $17^{\circ}35.00'N$ ,  $24^{\circ}15.16'W$ ).

## References

- Bowie AR, Whitworth DJ, Achterberg EP, Mantoura RFC, Worsfold PJ (2002). Biogeochemistry of Fe and other trace elements (Al, Co, Ni) in the upper Atlantic Ocean. *Deep-Sea Research*, 49: 605-636.
- Buck CS, Landing WM, Resing JA, Lebon GT (2006). Aerosol iron and aluminum solubility in the northwest Pacific Ocean: Results from the 2002 IOC cruise. *Geochem. Geophys. Geosyst.*, 7, Q04M07, doi:10.1029/2005GC000977.
- Croot, P.L., Streu, P. and Baker, A.R. (2004). Short residence time for iron in surface seawater impacted by atmospheric dry deposition from Saharan dust events. *Geophysical Research Letters*, 31: L23S08, doi:10.29/2004GL020153.
- Cullen and Sherell (1999), Techniques for determination of trace metals in small samples of size-fractionated particulate matter: phytoplankton metals off central California, *Mar. Chem.* 67, 233-247.
- Hydes and Liss (1976), Fluorimetric method for determination of low concentrations of dissolved aluminum in natural waters, *Analyst*, 101(1209), 922-931.
- Measures CI, Landing WM, Brown MT, Buck CS (2008). High-resolution Al and Fe data from the Atlantic Ocean CLIVAR-CO<sub>2</sub> repeat hydrography A16N transect: Extensive linkages between atmospheric dust and upper ocean geochemistry. *Global Biogeochemical Cycles*, 22(1).
- Obata H, Karatani H, Nakayama E (1993). Automated determination of iron in seawater by chelating resin concentration and chemiluminescence detection. *Analytical Chemistry*, 65(11), 1524-1528.
- Orians, K.J. and Boyle, E.A. (1993). Determination of Picomolar Concentrations of Titanium, Gallium and Indium in Sea-Water by Inductively-Coupled Plasma-Mass Spectrometry Following an 8-Hydroxyquinoline Chelating Resin Preconcentration. *Analytica Chimica Acta*, 282(1): 63-74.

- Orians, K.J., Boyle, E.A. and Bruland, K.W. (1990). Dissolved titanium in the open ocean. *Nature*, 348: 322-325.
- Robinson C, Holligan P, Jickells T, Lavender S (2009). The Atlantic Meridional Transect Programme (1995-2012) Foreword. *Deep-Sea Research Part II-Topical Studies In Oceanography*, 56(15): 895-898.
- Sarthou G et al. (2003). Atmospheric iron deposition and sea-surface dissolved iron concentrations in the East Atlantic. *Deep-Sea Research*, 50: 1339-1352.
- Wagener T, Guieu C, Losno R, Bonnet S, Mahowald N (2008). Revisiting atmospheric dust export to the Southern Hemisphere ocean: Biogeochemical implications. *Global Biogeochem. Cycles*, 22, GB2006, doi:10.1029/2007GB002984.
- Wagener T, Pulido-Villena E, Guieu C (2008). Dust iron dissolution in seawater: Results from a one-year time-series in the Mediterranean Sea. *Geophys. Res. Lett.*, 35, L16601, doi:10.1029/2008GL034581.

### 4.3 Determination of photochemical processes during a transect through the Atlantic

Thibaut Wagener, Maija Heller, Peter Croot (not on board),  
IFM-GEOMAR, Kiel

Diego Gaiero  
UNC, Córdoba, Argentina

#### A. The distribution of $H_2O_2$ and Fe(II) in the euphotic zone along a south-north transect in the Atlantic Ocean

##### Objectives

$H_2O_2$  is a short lived photochemically produced trace oxidant found throughout the water column but predominantly in sunlit surface waters. Information on  $H_2O_2$  concentrations allows us to constrain the oxidation time of reduced metal species (e.g. Cu(I), Fe(II)) in the ocean where  $H_2O_2$  can be the principal oxidant, this information is important for understanding the biogeochemical cycling of these metals. Furthermore,  $H_2O_2$  can be used as a tracer for vertical mixing in surface waters and/or a tracer of recent (last few days) rain or snow events. For ANT-XXIV/4 our objective was to make a synoptic survey of  $H_2O_2$  throughout the Atlantic sector of the Southern Ocean and examine the influence of different biogeochemical provinces on its formation and decay.

##### Methods/Work at Sea

*Simultaneous measurements of  $H_2O_2$  and Fe(II) in the water column:* For this work, we employed a new technique developed at the IFM-GEOMAR which uses an established flow injection system in which both species,  $H_2O_2$  and Fe(II), can be measured simultaneously in one sample. Samples for  $H_2O_2$  and Fe(II) analysis were drawn into 100 ml low density brown polyethylene bottles which were impervious to light. Samples were analyzed unfiltered within 1-2 h of collection where possible.

$H_2O_2$  was measured using a slight variation of an earlier flow injection chemiluminescence (FIA-CL) reagent injection method (Yuan and Shiller, 2001b). In

brief, the chemiluminescence of luminol is catalysed by the reaction of  $\text{H}_2\text{O}_2$  present in the sample with  $\text{Co}^{2+}$  at alkaline pH.  $\text{H}_2\text{O}_2$  standards were made by serial dilution from a primary stock solution (30% Fluka, Trace Select). The concentration of the primary and secondary standard was determined by direct spectrophotometry of the solution ( $\epsilon = 40.9 \text{ mol L}^{-1} \text{ cm}^{-1}$  (Hwang and Dasgupta, 1985)). Fe(II) was measured using an adaptation of a method developed early during EisenEx (Croot and Laan, 2002). The rapid reaction between Fe(II) and luminol was utilized to make rapid (90-112 s per measurement) analyses of the Fe(II) concentration in the seawater. Vertical profiles for Fe(II) and  $\text{H}_2\text{O}_2$  were also obtained to examine the influence of photochemistry. Samples were analyzed using 4 replicates: typical precision for  $\text{H}_2\text{O}_2$  was 2-3 % through the concentration range 1-100 nM, the detection limit ( $3 \sigma$ ) was typically  $0.6 \text{ nmol L}^{-1}$ . For Fe(II) the detection limit ( $3 \sigma$ ) was typically  $6 \text{ pmol L}^{-1}$ , as the Fe(II) signal is time dependent due to oxidative losses, the precision is concentration dependent. Seawater samples for  $\text{H}_2\text{O}_2$ /Fe(II) measurements were obtained using Niskin bottles on a standard CTD rosette. Samples were run as quickly as possible, normally each station was completed within 2 h.

### Preliminary (expected) results

Below(Fig. 4.3.1) is shown the example for a vertical profile of  $\text{H}_2\text{O}_2$  for the CVOO station (Stn 287) which was sampled in the very early morning (around 4 am). This station indicates that at the CVOO station, which had been sampled in the early morning, there was still some  $\text{H}_2\text{O}_2$  in the surface waters but this suddenly decreased in the top 100 m.

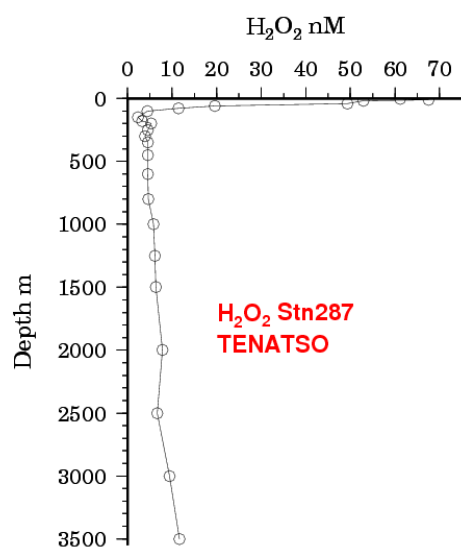


Fig. 4.3.1: Vertical profile of  $\text{H}_2\text{O}_2$  at the CVOO station ( $17^{\circ}35.00'N$ ,  $24^{\circ}15.16'W$ ).

Where a major phytoplankton bloom is occurring,  $\text{H}_2\text{O}_2$  concentrations are elevated in the surface waters which is typically found in tropical regions. The possible reasons for this include (1) release of large amounts of photolabile DOC by the phytoplankton due to senescence or (2) direct biological production of  $\text{H}_2\text{O}_2$  by phytoplankton cells. Deep water profiles often showed elevated  $\text{H}_2\text{O}_2$ , and it is thought that these may be

related to enzymatic reactions associated with the remineralization of organic matter that occurs at this depth.

## **B. CDOM properties and superoxide reactivity along a south-north transect in the Atlantic Ocean**

### **Objectives**

To determine the distribution and properties, including reactivity with superoxide, of CDOM in the upper ocean along a meridional transect in the Atlantic Ocean

### **Methods/Work at Sea**

*Coloured dissolved organic matter (CDOM)*: Samples for CDOM fluorescence and absorbance measurements were syringe filtered through 0.2  $\mu\text{m}$  filters (Sarstedt). The first 10 mL were always discarded due to contamination issues of the filters. 3D CDOM fluorescence measurements were performed with a Hitachi FL-2700 Fluorometer using a 1cm quartz cell. For this, excitation wavelengths were scanned (12000 nm/min) from 250 to 500 nm (5 nm slit width and 5 nm increments) and emission wavelengths (5 nm slit width and 5 nm increments) from 280 to 600 nm, the PMT voltage was set at 700 V and the response time 0.08 s. The resulting data matrix was subjected to parallel factor analysis (PARAFAC) to determine the relationships between the fluorescence of the sample and its components (Andersen and Bro, 2003; Fellman *et al.*, 2009; Kowalczyk *et al.*, 2010; Stedmon and Bro, 2008). Separate measurements of the humic-type fluorescence (Sierra *et al.*, 2005; Tani *et al.*, 2003) were made by analysis of samples using excitation at 320 nm and determining the emission at 420 nm (10 nm slit width). Sample fluorescence was normalized to daily measurements of standards of quinine fluorescence (QSU) (Mopper and Schultz, 1993) or to the Raman induced fluorescence of water (Determann *et al.*, 1994).

CDOM absorbance measurements were performed using a LWCC-2100 50 cm pathlength liquid waveguide cell (World Precision Instruments, Sarasota/FL, USA) and an Ocean Optics USB4000 UV-VIS spectrophotometer in conjunction with an Ocean Optics DT-MINI-2-GS light source. The absorbance was measured by direct injection into the LWCC. Absorbance measurements were made relative to MQ water and corrected for the refractive index of seawater based on the procedure outlined in Nelson *et al.* (2007). The resulting dimensionless optical density spectra were converted to absorption coefficient ( $\text{m}^{-1}$ ):  $a_{\text{CDOM}}(\lambda) = 2.303 A_{\lambda}/l$ , where 2.303 converts decadal logarithmic absorbance to base e, and  $l$  is the effective optical pathlength of the waveguide.

*Superoxide Measurement Technique and Apparatus*: For this work, we employed a chemiluminescence analysis method for superoxide utilizing MCLA using a commercially available FeLume (Waterville Analytical) system (Heller and Croot, 2010a; Heller and Croot, 2010b). The FeLume system comprises a light tight box equipped with a Plexiglas spiral flow cell mounted below a photon counter (Hamamatsu HC135-01) linked to a laptop computer via a Bluetooth connection controlled through a purpose built Labview<sup>TM</sup> (National Instruments) virtual instrument. The photon counter has a base counting period of 10 ms, for the present work we used average counts of an

integration time of 200 ms. Dark background counts for this detector were typically 60–120 counts s<sup>-1</sup>. For superoxide determination we ran the sample and the MCLA reagent directly into the flow cell using a peristaltic pump (Gilson Minipuls 3, operating at 18 rpm) with the sample line being pulled through the flow cell as this leads to the smallest amount of dead time in the system (typically 2-3 s). The overall flow rate through the cell was 8.25 mL min<sup>-1</sup>, comprising 5.0 mL min<sup>-1</sup> from the MCLA and 3.25 mL min<sup>-1</sup> from the sample. The transit time through the optical cell (300 μL) was therefore 2.18 s. For this work 2 different sources of superoxide were used (KO<sub>2</sub> and SOTS-1) in order to determine the concentration and production rate of superoxide in seawater (Heller and Croot, 2010a).

Seawater samples for CDOM measurements were obtained using Niskin bottles on a standard CTD rosette while superoxide measurements were performed with water obtained from the trace metal clean GO-FLO bottles. For this, discrete water samples from depth were for this obtained via GO-FLO samplers deployed on a Kevlar line. Dissolved samples were collected after filtration through 0.2 μm cartridge filters with slight N<sub>2</sub> overpressure. The GO-FLO sample collection was carried out in the IFM-GEOMAR Clean Air Container situated on the working deck close to the Kevlar winch.

#### **Preliminary (expected) results**

The combination of PARAFAC modelling and  $a_{\text{CDOM}}(\lambda)$  can be used to identify purely statistical fluorophore components that are responsible for specific regions. The additional humic-type fluorescence measurements could already be used to obtain a picture of the distribution of humic substances during the transect through the Atlantic which will in near future be useful to compare with the results from the PARAFAC modelling. The PARAFAC modelling has been described in detail elsewhere (Andersen and Bro, 2003; Bro, 1997; Ohno and Bro, 2006) but as it is a new approach of our working group we are still in the process of developing and validating MATLAB procedures for this analysis.

#### **References**

- Andersen, CM, Bro R (2003). Practical aspects of PARAFAC modeling of fluorescence excitation-emission data. *Journal of Chemometrics*, 17(4): 200-215.
- Bro, R (1997). PARAFAC. Tutorial and applications. *Chemometrics and Intelligent Laboratory Systems*, 38(2): 149-171.
- Croot, PL, Streu P, Peeken I, Lochte K, Baker AR (2004). Influence of the ITCZ on H<sub>2</sub>O<sub>2</sub> in near surface waters in the equatorial Atlantic Ocean. *Geophysical Research Letters*, 31: L23S04, doi:10.1029/2004GL020154.
- Croot PL, Laan P (2002). Continuous shipboard determination of Fe(II) in polar waters using flow injection analysis with chemiluminescence detection. *Analytica Chimica Acta*, 466, 261-273, DOI: 10.1016/S0003-2670(02)00596-2
- Determann S, Reuter R, Wagner P, Willkomm R (1994). Fluorescent matter in the eastern Atlantic Ocean. Part 1: method of measurement and near-surface distribution. *Deep Sea Research Part I: Oceanographic Research Papers*, 41(4): 659-675.
- Fellman, JB, Miller MP, Cory RM, D'Amore DV, White D (2009). Characterizing dissolved organic matter using PARAFAC modeling of fluorescence spectroscopy: a comparison of two models. *Environmental Science & Technology*, 43(16): 6228-6234.

- Heller, MI, Croot PL (2010a). Application of a superoxide ( $O_2^-$ ) thermal source (SOTS-1) for the determination and calibration of  $O_2$  fluxes in seawater. *Analytica Chimica Acta*, 667: 1-13.
- Heller, MI, Croot PL (2010b). Superoxide decay kinetics in the Southern Ocean. *Environmental Science & Technology*, 44(1): 191-196 DOI: 10.1021/es901766r.
- Hwang H, Dasgupta PK (1985). Flow-injection analysis of trace hydrogen-peroxide using an immobilized enzyme reactor. *Mikrochimica Acta*, 3, 77-87.
- Kowalczyk, P et al. (2010). Characterization of dissolved organic matter fluorescence in the South Atlantic Bight with use of PARAFAC model: Relationships between fluorescence and its components, absorption coefficients and organic carbon concentrations. *Marine Chemistry*, 118(1-2): 22-36.
- Mopper K, Schultz CA (1993). Fluorescence as a possible tool for studying the nature and water column distribution of DOC components. *Marine Chemistry*, 41(1-3): 229-238.
- Nelson, NB et al. (2007). Hydrography of chromophoric dissolved organic matter in the North Atlantic. *Deep Sea Research Part I: Oceanographic Research Papers*, 54(5): 710.
- Ohno T, Bro R (2006). Dissolved organic matter characterization using multiway spectral decomposition of fluorescence landscapes. *Soil Science Society of America Journal*, 70(6): 2028-2037.
- Sierra MMD, Giovanela M, Parlanti E, Soriano-Sierra EJ (2005). Fluorescence fingerprint of fulvic and humic acids from varied origins as viewed by single-scan and excitation/emission matrix techniques. *Chemosphere*, 58(6): 715-733.
- Stedmon C, Bro R (2008). Characterizing dissolved organic matter fluorescence with parallel factor analysis: a tutorial. *Limnol. Oceanogr. Methods*, 6: 572-579.
- Steinberg DK, Nelson NB, Carlson CA, Prusak AC (2004). Production of chromophoric dissolved organic matter (CDOM) in the open ocean by zooplankton and the colonial cyanobacterium *Trichodesmium* spp. *Marine Ecology-Progress Series*, 267: 45-56.
- Tani H et al. (2003). Iron(III) hydroxide solubility and humic-type fluorescent organic matter in the deep water column of the Okhotsk Sea and the northwestern North Pacific Ocean. *Deep-Sea Research*, 50: 1063-1078.
- Yuan J, Shiller AM (2001). The distribution of hydrogen peroxide in the southern and central Atlantic ocean. *Deep-Sea Research II*, 48: 2947-2970.

#### 4.4 Concentration and isotopic ratio of molecular hydrogen along a meridional Atlantic transect

Sylvia Walter  
IMAU, Utrecht, Nederlande

##### Objectives

Hydrogen is one of the most promising energy carriers of the future. Due to a lack of measurements, the global biogeochemical cycle is not well constrained and the consequences of an increased use are discussed controversially. A better understanding of the biogeochemical cycle of hydrogen in advance is indispensable before using it on a large scale.

Several sources and sinks for  $H_2$  are known, however, there exist large uncertainties regarding their strength and the contribution to the global budget. Beside soil deposition as the major sink and methane oxidation or anthropogenic production as the major sources, the oceans play a significant role as a net source of  $H_2$ . Production can take

place directly during  $N_2$  fixation or indirectly via photochemical destruction of organic compounds released to the atmosphere. Sources and sinks have characteristic isotopic signatures, which allow tracking them. Biologically produced  $H_2$  has a D/H isotopic signature with a  $dD$  of  $-700$  ‰. This value is far away from the tropospheric isotopic ratio of  $+130$  ‰ or anthropogenically produced  $H_2$  with an isotopic ratio of approximately  $-270$  ‰.

Aim of the cruise was to examine whether areas of expected hydrogen production can be identified based on the isotopic signatures, e.g. those known for the occurrence of  $N_2$  fixers like *Trichodesmium*. In the context of former measurement campaigns, which were performed in April 2008, April 2009 and October 2009, we would like to compare results regarding annual and interannual variability, and to establish a high-resolution meridional transect.

#### Work at sea

During this cruise, 119 air samples were taken regularly over the cruise track to investigate the D/H isotopic ratio of  $H_2$  and the mixing ratio of  $H_2$  and CO. The main focus is placed on differences between the hemispheres and the different oceanic regimes. Additionally a new setup to extract headspace samples from surface water for  $H_2$  isotope measurements was tested. In total 16 samples were taken. Together with the air samples they will be measured at the IMAU lab.

During the entire cruise continuous measurements of the surface water concentration and the atmospheric concentration of  $H_2$  and CO were determined with an RCP (Reducing Compound Photometer) to investigate fluxes between the ocean surface and the atmosphere.

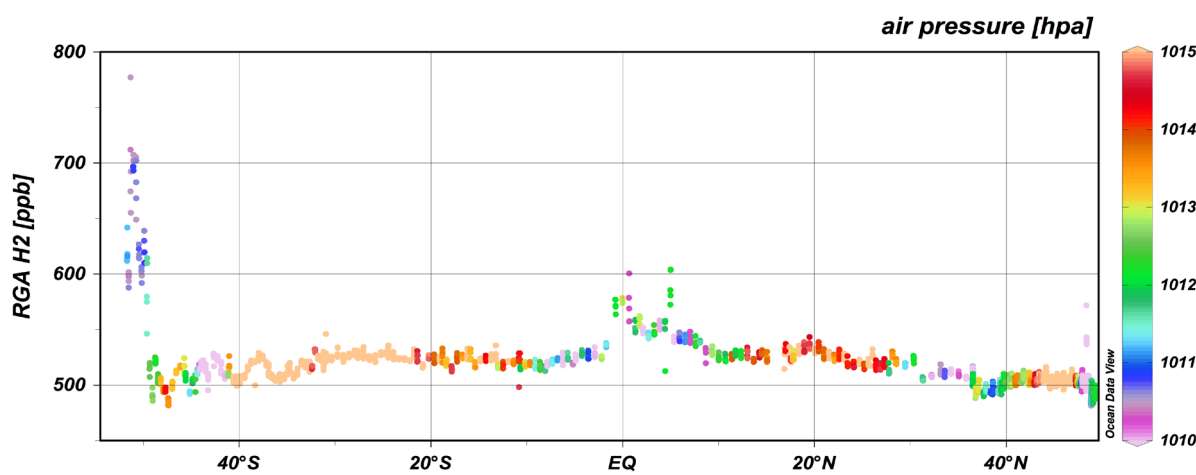


Fig. 4.4.1:  $H_2$  mixing ratio (ppb) along the latitudinal transect during ANT-XXVI/4; atmospheric pressure (hPa) is color-coded

#### Preliminary (expected) results

Preliminary results for  $H_2$  mixing ratios (in ppb) as measured continuously during the cruise are shown in Fig. 4.4.1. The atmospheric pressure (hPa) is color-coded to identify the location of the Intertropical Convergence Zone (ITCZ) which separates

southern and northern air masses. The distribution of  $H_2$  shows a clear winter signal between the hemispheres. This means that the mixing ratio of the southern and the northern hemisphere is not distinguishable with  $521 \pm 7$  ppb (SH) and  $511 \pm 14$  ppb (NH). During winter,  $H_2$  accumulates due to reduced biological activity and thus a weakened soil deposition, which is the main sink for  $H_2$ . Two areas of significantly higher  $H_2$  concentrations can be also identified. This is the shelf area near Chile and Argentina ( $645 \pm 48$  ppb) and the ITCZ ( $530 \pm 11$  ppb). The isotope measurements will give a more detailed picture about the origin of these enhanced values.

#### 4.5 Abyssal temperature fluctuations in the Vema Channel

Walter Zenk, Martin Visbeck (not on board)  
IFM-GEOMAR, Kiel

##### Objectives

The equator bound flow of Antarctic Bottom Water (AABW) represents a significant limb of the global thermal circulation. In the South Atlantic, the deep western boundary along the continental rise carries AABW northward. The advected water masses originate from the Weddell Sea, where they are formed by deep winter-time convection. At a latitude of about  $32^\circ\text{S}$ , the abyssal flow encounters a topographical constrain in the form of the zonally aligned Rio Grande Rise. This submarine mountain chain separates the Argentine Basin in the South from the Brazil Basin to the north. AABW finds its equator ward pathway through the natural impedance via a 790 km long canyon called Vema Channel (Fig. 4.5.1). This meridionally directed channel provides a choke point for observations of water mass property and transport fluctuations. Such parameters are vital components in monitoring the global climate system.

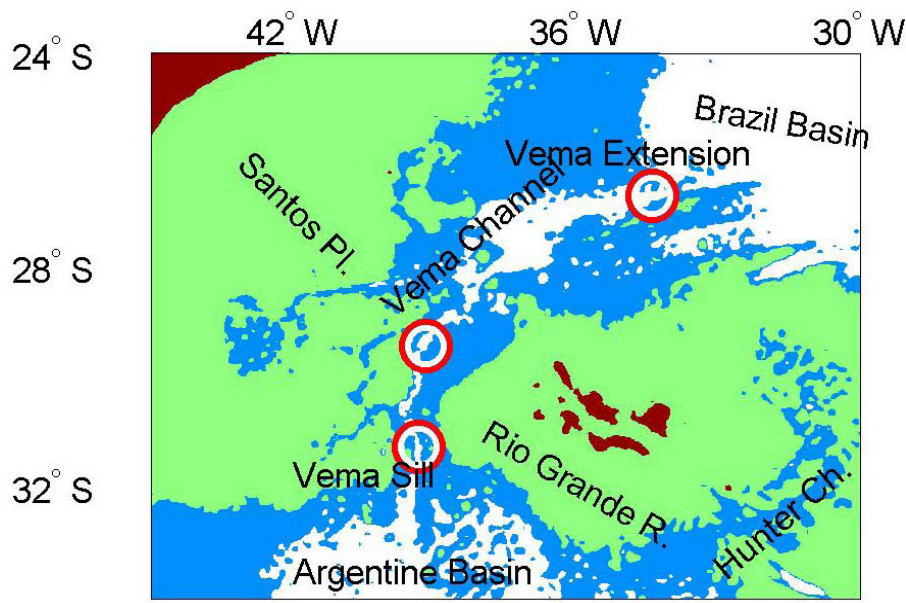


Fig. 4.5.1: Vema Channel of the South Atlantic. This canyon enables Antarctic Bottom Water to leave the Argentine Basin on its equatorbound drift towards the Brazil Basin. Depths below 4500 m are shown in white. At the Vema Sill, a full water column CTD cast was taken during Polarstern cruise ANT-XXVI/4 (Figure adopted from Zenk and Morozov (2007)).

A decade-long record from the channel entrance (31°S, 39°W) indicates a clear increase of the lowest temperatures in the bottom waters (Zenk and Morozov, 2007; Zenk, 2008). Comparable observations from the exit region of the Vema Channel (26°S, 35°W) confirm the near-bottom temperature rise since 1991. The Vema Sill station at the entrance is officially acknowledged as an “OceanSITES” observatory. “OceanSITES” is a worldwide system of long-term, deepwater reference stations measuring dozens of variables ([www.oceansites.org](http://www.oceansites.org)).

#### Work at sea

Due to tight constraints on station time only one full water depth CTD cast was carried out at the Vema Sill observatory site. The CTD probe was kindly provided by the AWI. It was equipped with two independent pairs of temperature and conductivity sensors.

#### References

- Zenk W, Morozov E (2007). Decadal warming of the coldest Antarctic Bottom Water flow through the Vema Channel. *Geophysical Research Letters*, 34, L14607, doi:10.1029/2007GL030340.
- Zenk W (2008). Temperature fluctuations and current shear in Antarctic Bottom Water at the Vema Sill. *Progress in Oceanography*, 77, 276-284, doi 10.1016/j.pocean.2006.05.006.

#### 4.6 Glider swarm experiment at Cape Verde Ocean Observatory

Mario Müller, Arne Körtzinger, Thorsten Kanzow (not on board)  
IFM-GEOMAR, Kiel

#### Objectives

For the most part, physical-biogeochemical submesoscale coupling has been studied near ocean margins and ocean frontal systems. In contrast, an open-ocean study north of Cape Verde in the vicinity of the Cape Verde Ocean Observatory (CVOO) was carried out, where both surface chlorophyll and temperature display pronounced submesoscale. Our objectives were (i) quantification of submesoscale variability of temperature, salinity, chlorophyll fluorescence, oxygen and turbidity in the surface mixed layer and the upper thermocline, and (ii) demonstration of the coupling between physical processes (lateral and vertical advection) and biogeochemical processes (phytoplankton biomass, oxygen production/consumption, fertilization by Saharan dust).

#### Work at sea

A swarm of 6 gliders of IFM-GEOMAR's had been deployed during a field campaign from 5-19 March 2010 at the Cape Verde Ocean Observatory. During this time the team was based in Mindelo, on the Island of São Vicente, Cape Verde. Initially software updates, hardware checks, and verifications of the functionality and ballasting of the gliders were performed on the premises of Instituto Nacional de Desenvolvimento das Pescas (INDP). The gliders were tested and deployed south of the São Vicente off the village of São Pedro in about 700 m water depth. The deployment location was near 16°46' N / 26°07' E. Of the 6 gliders, four completed the whole deployment period

until 5 May 2010, when they were recovered aboard *Polarstern* during cruise ANT-XXVI/4. Two gliders failed prematurely before reaching the research area. Both units were recovered successfully, however. IFM06 was recovered by the expedition team while still present. IFM03 failed after 19 March, and was thankfully recovered by our colleagues Pericles Silva and Nuno Vieira from INDP.

To achieve the research goals, the glider-based observations of the submesoscale variability focused on an area of 50 x 50 km centred around CVOO. Each of the gliders carried out roughly 8-12 vertical profiles of T, S, chlorophyll, oxygen and turbidity per day along predefined tracks with a horizontal speed of about 25 km d<sup>-1</sup> for the duration of eight weeks. Upon arrival at the site, the gliders followed butterfly-shaped tracks. The two pairs of gliders followed tracks that were rotated by 90°, assuring good coverage in both zonal and meridional domains (Fig. 4.6.1). Within each glider pair, the units followed the butterfly course in opposing directions so that the whole range of variability over spatial scales between 0 to 50 km was sampled gradually.

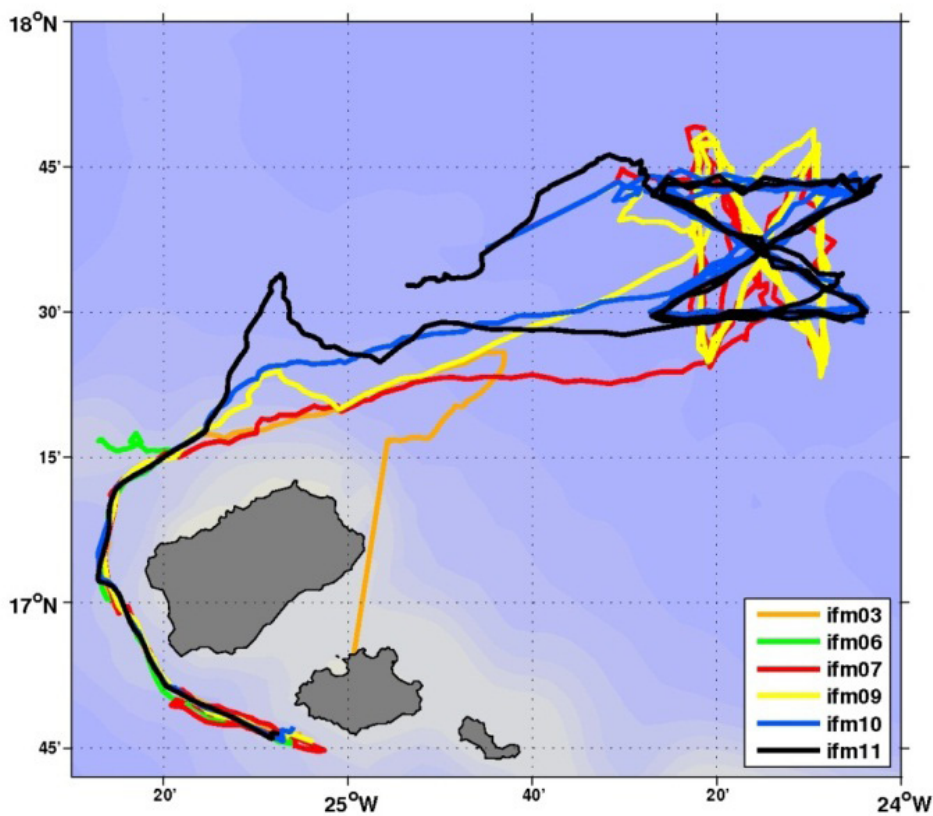


Fig. 4.6.1: Glider tracks from the spring 2010 campaign. The gliders were deployed south of São Vicente and navigated autonomously towards CVOO, where they carried out missions, following predefined, butterfly-shaped courses. Together, the gliders covered a distance of 3800 km. The devices performed 3500 dives, during which 18,000,000 measurements of salinity, temperature, pressure, chlorophyll, turbidity and oxygen were carried out.

### Preliminary (expected) results

The data acquisition phase was very successful and data processing has progressed far. We have successfully been able to demonstrate small scale physical-biogeochemical

co-variability. We have implemented the methodology to infer vertical velocities from the gliders. Since the cruise several tasks have been carried such as the finalization of oxygen calibration and the calibration of the chlorophyll and turbidity measurements. We will continue to analyze the spatial scales of physical-biochemical co-variability. We shall assess the potential of vertical velocities computed from the gliders to explain the small-scale variability of the biophysical parameters. In collaboration with Thomas Ohde (IOW) we shall intensify the work on the detectability of Sahara dust deposition. In collaboration with Johannes Karstensen (IFM-GEOMAR) we will assess the potential of remote sensing to infer vertically integrated chlorophyll contents. IFM-GEOMAR plans to carry out further glider fleet experiments. Experiences gained from this pilot study will help to conduct (and process and analyze the data from) future missions.

#### 4.7 Posidonia system testing and calibration

Saad El Naggar, Peter Gerchow, Gerd Rohardt (not on board)  
 AWI, Bremerhaven  
 Werner Dimmler  
 Fielax, Bremerhaven

##### Objectives

The underwater navigation system Posidonia had been upgraded during the shipyard visit of *Polarstern* in Bremerhaven between 20 May and 12 June 2008. Newly designed hardware and software were installed and tested in the harbour of Bremerhaven. A new acoustic array and window were installed nearby the moon pool in addition to the mobile acoustic array. A complete new electronic cabinet was installed, modified and tested.

The first operational test under real conditions at sea was carried out during the cruise ARK-XXIII/1+2. A final sea trial and calibration were planned to be carried out at water depth of more than 3000 m during the cruise ANT-XXV/1 in November 2008 on the way to Las Palmas. However, the planned calibration and sea trials could not be carried out during that cruise due to technical problems that occurred to the system. Because the system was faulty and not operational it was repaired by IXSEA in Bremerhaven during the last shipyard visit of *Polarstern* in May/June 2009, where the damaged

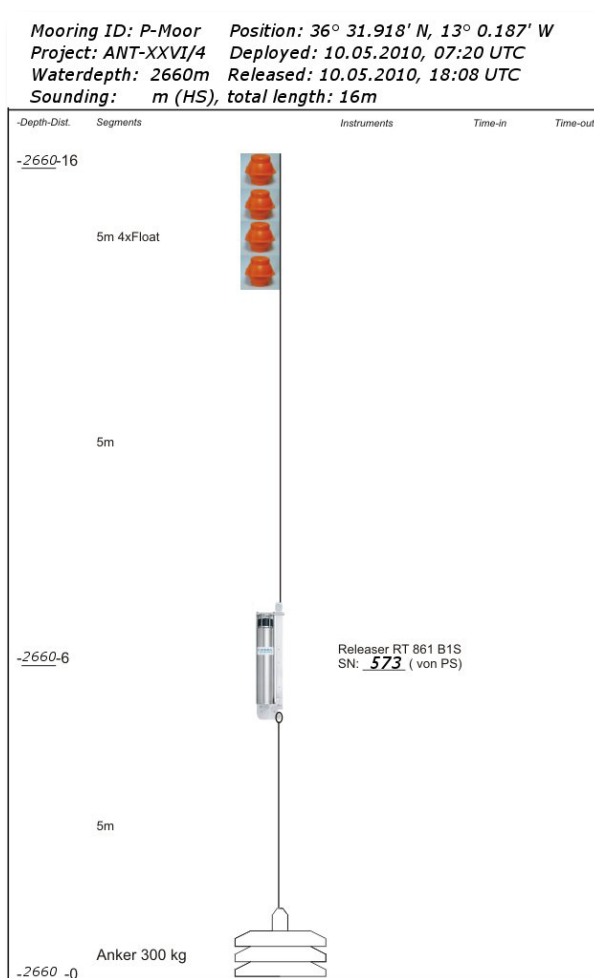


Fig. 4.7.4: Ship's tracks: Line track at distance of 1000 m parallel to first line track in Fig. 4.7.3

acoustic array and window were replaced by new components.

The Posidonia system was successfully used again during ARK-XXIV cruise, but the new acoustic array was not useable, due to the diffraction occurring at the protection window. The system was not able to locate the target correctly and within the expected error. A new sea trial and calibration were done on both Posidonia systems during ANT-XXVI/1 and on the way between Bremerhaven and Las Palmas (16-27 October 2009). The newly installed acoustic array was not fully operational, however, and it could not be calibrated due to disturbances from the protection window. Further investigations were necessary to improve the acoustical characteristic of the fixed array.

Finally, during ANT-XXVI/4 on the way from Las Palmas to Bremerhaven (8-17 May 2010) further calibration tests were carried out on the new Posidonia system after removal the protective window in Punta Arenas on April 2010. The main objectives here were to eliminate the effects of the protective window on the system, to check and to calibrate the system without the protective window.

### Work at sea

The following steps were carried out during ANT-XXVI/4:

- System operability check including transponder test
- Preparation of transponder mooring (Fig. 4.7.1)
- Sea trial and calibration (about 12 h)
- Recovery of transponder mooring
- Data analysis and validations

The general conditions during the calibration and tests are listed below:

- Date: 10 May 2010
- System used: POSIDONIA 6000; Abyss 1.49,
- Fix Flush Acoustic Array, 80 cm Ø
- Transponder used: RT 861 B1S, Ser. Nr. 573 (*Polarstern*)
- Transponder Position: 36° 3.92' N; 013° 00.19' W
- Transponder depth: 2661 m
- Water temperature: 17.3° C
- Air temperature: 15.4° C
- Sea state: 2 m swell
- Wind speed: 10 m/s
- Wind direction: 38°
- Salinity: 36.33 P
- Track circle diameter: about 1800 m
- Ship speed during measurement: 3 Knots
- All other acoustic systems: OFF
- Transponder RT 861 B1S, Ser. Nr. 573; *Polarstern*
- Start of Tests: 10 May 2010; 06:00 UTC
- End of Tests: 10 May 2010; 20:00 UTC

A corrected sound profile was obtained with temperature and salinity data from a CTD cast down to 2550 m and used for calibration. The calibration and tests were carried out according the ship's tracks presented in Figs. 4.7.2-4.7.4.

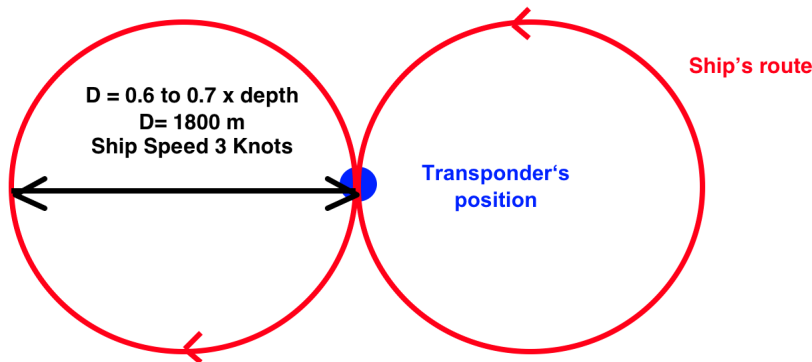


Fig. 4.7.2: Ship's tracks: loop 1 and loop 2 (8-shape)

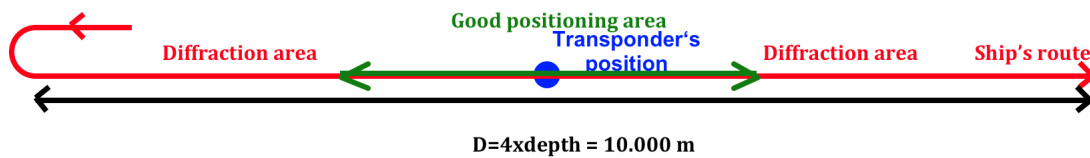


Fig. 4.7.3: Ship's Tracks: Line track over the Transponder

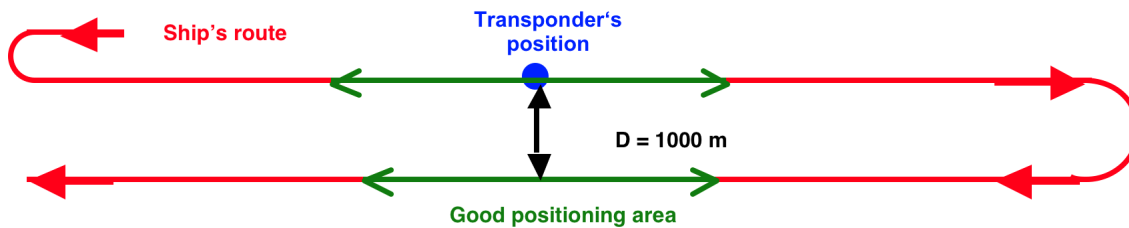


Fig. 4.7.4: Ship's tracks: Line track at distance of 1000 m parallel to first line track in Fig. 4.7.3

### Preliminary (expected) results

Data analysis from first loop (8 shape, Fig. 4.7.2) show that the non-mobile acoustic array works without window properly. Positioning data obtained here were within the specifications and good enough to carry out the calibration (Fig. 4.7.7). The calculated bias of the array's axis relative to the ship's axis was:

Heading: -0.62°  
 Pitch: -0.25°  
 Roll: -0.44°

The accuracy of the system at this depth was about  $\pm 12$  m. The signal/noise ratio was similar to the mobile array. Considering the positioning data distribution (Fig. 4.7.5) we identified a systematic error distribution surrounding the main position similar to

what was found when using the protective windows during ANT-XXVI/1, but at lower magnitude (Fig. 4.7.6).

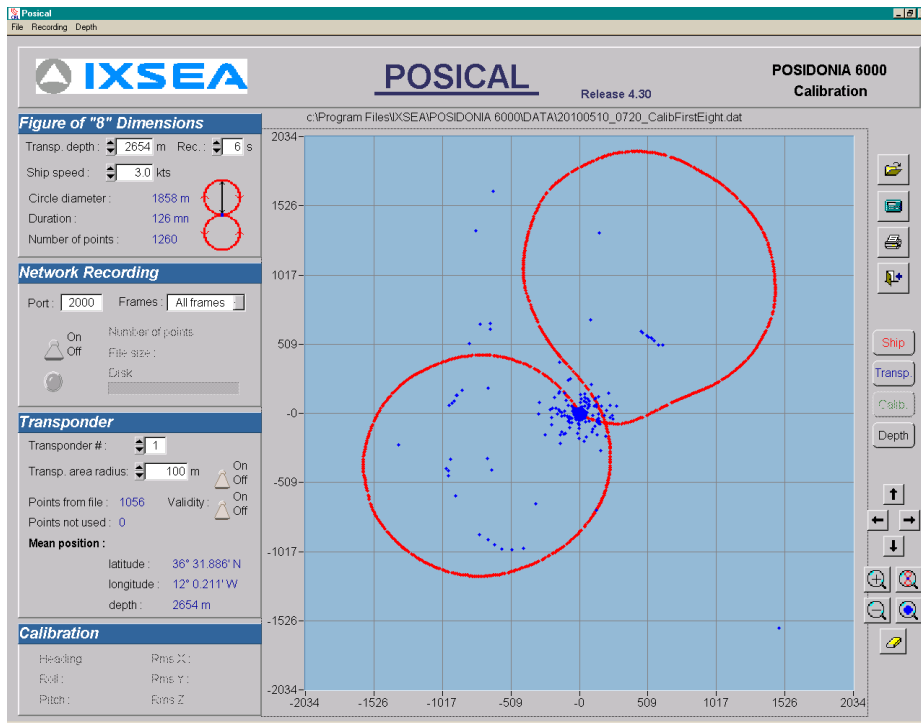


Fig. 4.7.5: Calibration of the fixed acoustic array without window; Red line = ship's track, blue dots = detected transponder positions.

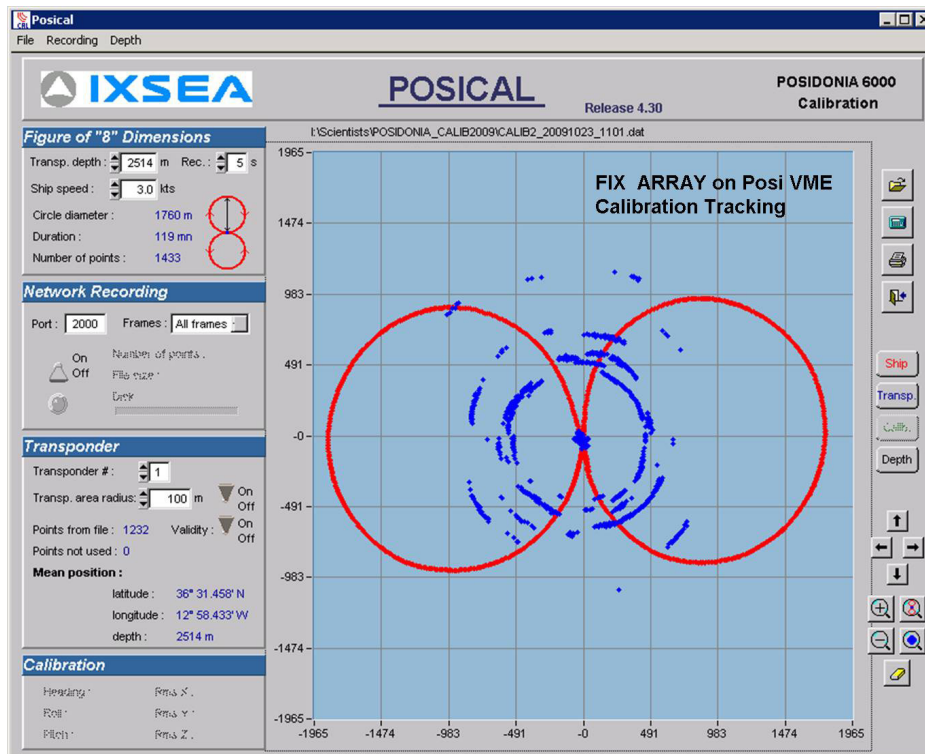


Fig. 4.7.6: Calibration of the fixed acoustic array during ANT-XXVI/1 with window. Red line = ship's track; blue dots = detected transponder positions.

## 4.7 Posidonia system testing and calibration

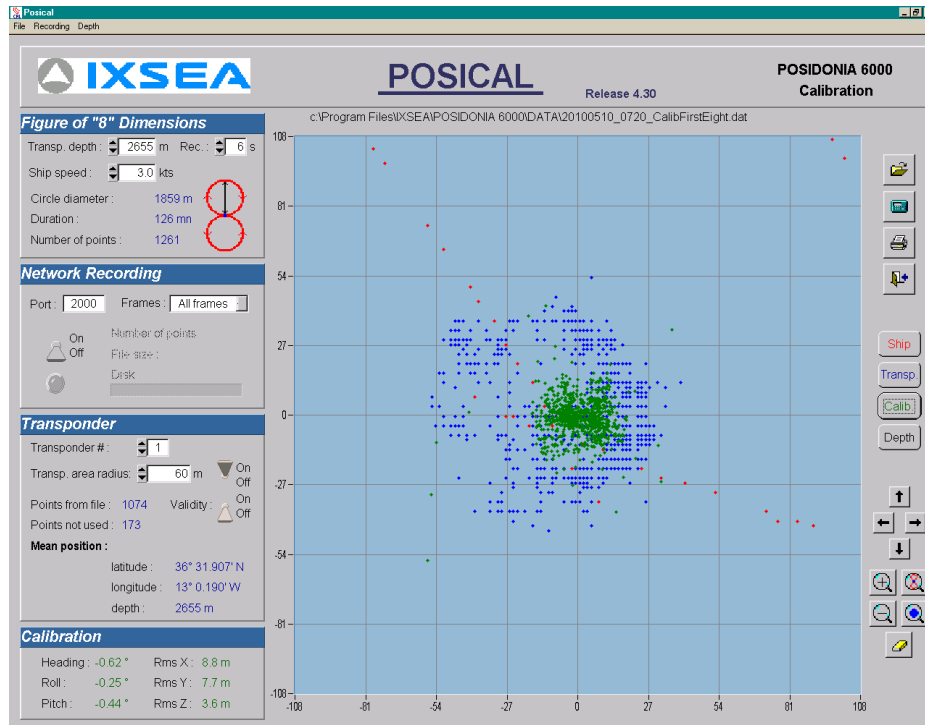


Fig. 4.7.7: Calibration of the fixed array without window, first loop (8-shape). Blue dots are positions before correction and green dots are recalculated positions after the correction. Positioning distributions were reduced from  $\pm 50$  m to  $\pm 12$  m.

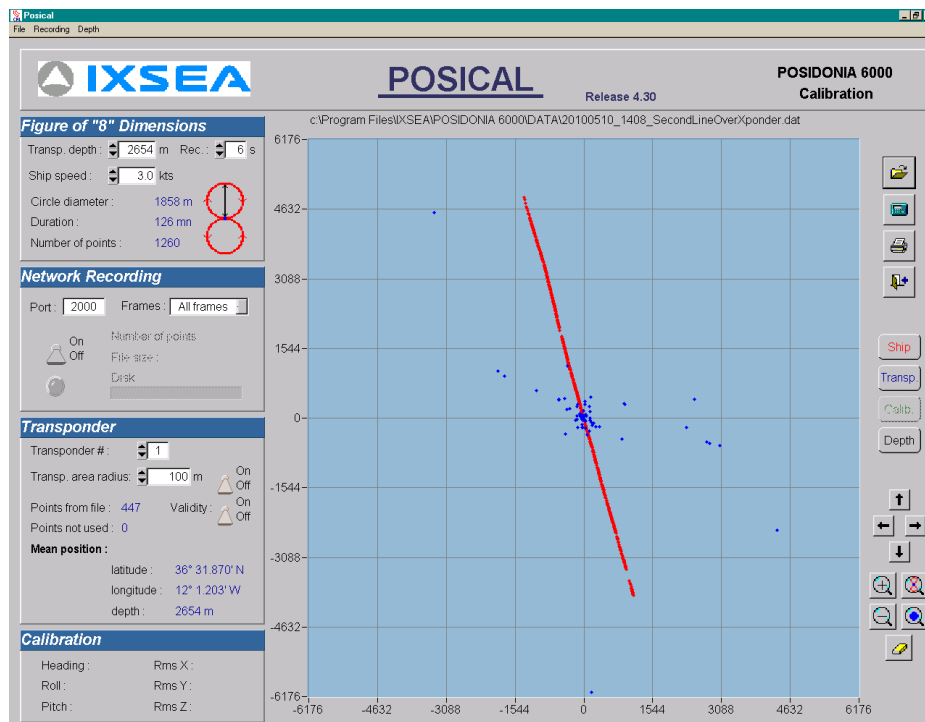


Fig. 4.7.8: Calibration of the fixed acoustic array without window. Influence of the ship's symmetry on the accuracy of the positioning. Ship's track over transponder; red line = ship's track, blue dots = detected transponder positions.

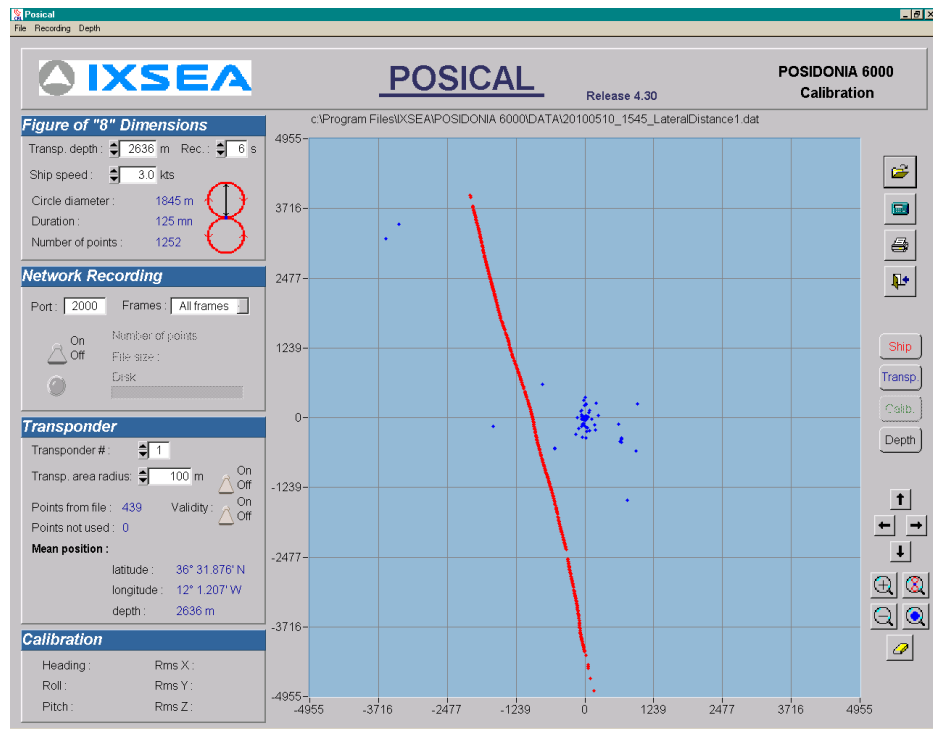


Fig. 4.7.9: Calibration of the fixed acoustic array without window. Influence of the ship's symmetry on the accuracy of the positioning. Ship's track nearby. Red line = ship's track, blue dots = detected transponder positions.

Measurements according to Figs. 4.7.3 and 4.7.4 were carried out to check the influence of the ship's symmetry on the accuracy of the positioning. Results are presented in Figs. 4.7.8 and Fig. 4.7.9. We found that best positioning can be obtained, when the ship is headed to the transponder. Starboard side is more disturbed than port side.

According to the test performed it can be concluded that the installation ambient of the fixed installed array has minor disturbances on the functionality of the Posidonia system. The reason is not known. The protective window disturbs and attenuates the signals in addition, so that the ambient effects became stronger. Those lead to disturbance in the complete system. The protective window is still the main reason for the system faulty. Further investigations at installation ambient and at the window are necessary to make the system fully usable.

#### 4.8 Further projects and guests

Sabrina Niebling  
IUP-HD, Heidelberg

**Multi-Axis Differential Optical Absorption Spectroscopy (MAX-DOAS) of trace gases in the troposphere and stratosphere:** This is a long-term project which focuses primarily on the meridional transits of *Polarstern*. MAX-DOAS measurements enable the retrieval of the partial columns (in the troposphere and stratosphere) of many trace gases. Information on their appearance and quantity can be derived. The major objectives are to identify possible trends of  $\text{NO}_2$  and  $\text{HCHO}$  in the troposphere

and shed light on the important role that halogen oxides (BrO, IO) appear to play in atmospheric chemistry.

The measurements are usually carried out unattended but during ANT-XXVI/4 maintenance work on the MAX-DOAS system had to be carried out during the final leg of ANT-XXVI/4 from Las Palmas to Bremerhaven.

Gerlind Rüge  
Wissenschaftsrat, Köln  
Rainer Knust  
AWI, Bremerhaven

**German Council of Science and Humanities:** Gerlind Rüge from the German Council of Science and Humanities (Wissenschaftsrat) in Cologne, who had accepted an invitation from Professor Karin Lochte, Director of the Alfred-Wegener-Institute, joined cruise ANT-XXVI/4 for the final leg from Las Palmas to Bremerhaven. For 10 days she took every opportunity to learn about the scientific facets of our current cruise and gained insight into logistical and organizational aspects of ship-based marine research in Germany.

Katja Heldmann, Frau Ute Lange  
Claudia Klages  
AWI, Bremerhaven

**“Research Expedition 2009”:** Eight year-old Katja Heldmann, who had won her participation in ANT-XXVI/4 as part of the “Research Expedition 2009”, a public activity for school kids by the German Ministry for Education and Research, is perhaps the youngest cruise participant ever on *Polarstern*. During the 10-days leg from Las Palmas to Bremerhaven, Katja – who was accompanied by her mother and Claudia Klages as her personal guide from the AWI – had ample time to explore the ship and hear about some exciting aspects of marine research.



Fig. 4.8.1: Katja says Goodbye to Captain Uwe Pahl after an exciting and enjoyable adventure during *Polarstern* Cruise ANT-XXVI/4 (from Katja's cruise diary).

---

## **APPENDIX**

**A.1 PARTICIPATING INSTITUTIONS**

**A.2 CRUISE PARTICIPANTS**

**A.3 SHIP'S CREW**

**A.4 STATION LIST**

---

## A.1 TEILNEHMENDE INSTITUTE / PARTICIPATING INSTITUTIONS

---

	<b>Address</b>
AWI	Stiftung Alfred-Wegener-Institut für Polar- und Meeresforschung in der Helmholtz-Gemeinschaft Postfach 120161 27515 Bremerhaven Germany
DWD	Deutscher Wetterdienst Geschäftsbereich Wettervorhersage Seeschiffahrtsberatung Bernhard-Nocht-Str. 76 20359 Hamburg Germany
GKSS	Forschungszentrum Geesthacht Institut für Küstenforschung Max-Planck-Straße 1 21502 Geesthacht Germany
IFM-GEOMAR	Leibniz-Institut für Meeresforschung an der Universität Kiel Wischhofstraße 1-3 24149 Kiel Germany
IfT	Institut für Troposphärenforschung Permoserstrasse 15 04318 Leipzig Germany
IMAU	Institute for Marine and Atmospheric Research (IMAU) Utrecht University Princetonplein 5 3584 CC Utrecht Niederlande
IPC-CAU	Institut für Physikalische Chemie Christian-Albrechts-Universität zu Kiel Olshausenstr. 40 24098 Kiel Germany
IUP-HB	Institut für Umweltphysik Universität Bremen Otto-Hahn-Allee 1 28359 Bremen Germany

---

	<b>Address</b>
IUP-HD	Institut für Umweltphysik Universität Heidelberg Im Neuenheimer Feld 229 69120 Heidelberg Germany
MPI-MET	Max-Planck-Institut für Meteorologie Bundesstr. 53 20146 Hamburg Germany
SIO	Scripps Institution of Oceanography Marine Physical Laboratory 8622 Discovery Way La Jolla, CA 92037 U.S.A.
UNC	Universidad Nacional de Córdoba Facultad de Ciencias Exactas, Físicas y Naturales Avenida Velez Sarsfield 1611 Córdoba - X5016GCA Argentina
WR	Wissenschaftsrat Brohler Straße 11 50968 Köln Germany

## A.2 FAHRTTEILNEHMER / CRUISE PARTICIPANTS

<b>Name/ Last name</b>	<b>Vorname/ First name</b>	<b>Institut/ Institute</b>	<b>Beruf/ Profession</b>
Aßmann	Steffen	GKSS	PhD student, chemistry
Becker	Meike	CAU	Student, chemistry
Dammshäuser	Anna	IFM-GEOMAR	PhD student, chemistry
El Naggari	Saad, Dr.	AWI	Physicist, logistics specialist
Feyen	Anja	IUP-HB	Biologist
Fiedler	Björn	IFM-GEOMAR	PhD student, chemistry
Friedrichs	Gernot, Prof. Dr.	IPC-CAU	Professor, chemistry
Gaiero	Diego, Dr.	IPC-CAU	Chemist
Gerchow <sup>1</sup>	Peter	AWI	IT specialist
Gernez	Pierre, Dr.	SIO	Biologist
Hanschmann	Timo	IfT	PhD student, meteorology
Heldmann <sup>1</sup>	Katja	Private	Pupil
Heller	Maija	IFM-GEOMAR	PhD student, chemistry
Kanitz	Thomas	IfT	PhD student, meteorology
Klages <sup>1</sup>	Claudia	AWI	Technology Transfer
Knust	Rainer, Dr.	AWI	Scientific Coordinator
Körtzinger	Arne, Prof. Dr.	IFM-GEOMAR	Chief Scientist, chemist
Lange <sup>1</sup>	Ute	private	Mother of pupil
Lonitz	Katrin	MPI-MET	Student, meteorology
Mohr	Wiebke	IFM-GEOMAR	PhD student, biology
Mroz	Julia	IUP-HB	Student, biology
Müller <sup>2</sup>	Mario	IFM-GEOMAR	Technician
Niebling <sup>1</sup>	Sabrina	IUP-UH	Student, physics
Reynolds	Rick, Dr.	SIO	Biologist
Rüve <sup>1</sup>	Gerlind, Dr.	WR	Chemist
Sadeghi	Alireza	IUP-UB	Biologist
Sett	Scarlett	IFM-GEOMAR	Student, biology
Wagener	Thibaud, Dr.	IFM-GEOMAR	Chemist
Walter	Sylvia, Dr.	IMAU	Biologist

---

### A.3 SCHIFFSBESATZUNG / SHIP'S CREW

<b>Name</b>	<b>Rank</b>
Pahl, Uwe	Master
Grundmann, Uwe	1. Offc.
Ziemann, Olaf	Ch. Eng.
Hering, Igor	2. Offc.
Janik,, Michael	3. Offc.
Erich, Matthias	Doctor
Koch, Georg	R. Offc.
Kotnik, Herbert	2. Eng.
Schnürch, Helmut	2. Eng.
Westphal, Helmut	2. Eng.
Holtz, Hartmut	Elec. Eng.
Dimmler, Werner	ELO
Feiertag, Thomas	ELO
Nasis, Ilias	ELO
Clasen, Burkhard	Boatsw.
Brickmann, Peter	A.B.
Burzan, Gerd-Ekkeh.	A.B.
Hartwig-Lab, Andreas	A.B.
Kreis, Reinhard	A.B.
Kratschmar, Uwe	A.B.
Moser, Siegfried	A.B.
Schröder, Norbert	A.B.
Schultz, Ottomar	A.B.
Beth, Detlef	Storek.
Dinse, Horst	Mot-man
Fritz, Günter	Mot-man
Kliero, Peter	Mot-man
Krösche, Eckard	Mot-man
Watzel, Bernhard	Mot-man
Fischer, Matthias	Cook
Tupy, Mario	Cooksmate
Völske, Thomas	Cooksmate
Dinse, Petra	1. Stwdess
Hennig, Christina	Stwdess/N.
Hischka, Peggy	2. Stwdess
Hu, Gun Yong	2. Steward
Streit, Christina	2. Stwdess
Sun, Yong Shang	2. Steward
Wartenberg, Irina	2. Stwdess
Ruan, Hui Guang	Laundrym.

## A.4 STATIONSLISTE / STATION LIST PS 75

Station	Date	Time	Gear Abbrev.	Latitude	Longitude	Water depth [m]	Action	Comment
PS75/264-1	2010-04-10	03:47	CTD/RO	47° 39.87' S	60° 44.99' W	396,2	on ground/ max depth	SE 32.1 357m
PS75/264-2	2010-04-10	04:34	GO-FLO	47° 39.62' S	60° 44.91' W	391	on ground/ max depth	100 m, SE 32.2
PS75/264-2	2010-04-10	04:36	GO-FLO	47° 39.61' S	60° 44.90' W	392	on ground/ max depth	40 m
PS75/265-1	2010-04-10	16:47	SIOP	45° 35.52' S	60° 21.22' W	125,5	profile start	100 m, se 32.2
PS75/265-1	2010-04-10	16:48	SIOP	45° 35.52' S	60° 21.22' W	125	profile end	
PS75/265-2	2010-04-10	17:05	CTD/RO	45° 35.45' S	60° 21.24' W	125,2	on ground/ max depth	
PS75/265-2	2010-04-10	17:15	CTD/RO	45° 35.39' S	60° 21.25' W	125	on ground/ max depth	117 m, SE 32.1
PS75/265-3	2010-04-10	17:07	HPRO	45° 35.44' S	60° 21.24' W	125	profile start	
PS75/265-3	2010-04-10	17:29	HPRO	45° 35.32' S	60° 21.31' W	124,7	profile end	
PS75/265-4	2010-04-10	17:36	PAR	45° 35.30' S	60° 21.32' W	124,7	on ground/ max depth	100 m
PS75/265-4	2010-04-10	18:06	PAR	45° 35.20' S	60° 21.44' W	126,2	profile end	
PS75/266-1	2010-04-11	16:38	SIOP	43° 13.56' S	57° 17.93' W	3262,2	profile start	
PS75/266-1	2010-04-11	17:00	SIOP	43° 13.58' S	57° 17.95' W	3260,2	profile end	
PS75/266-2	2010-04-11	17:25	CTD/RO	43° 13.52' S	57° 17.92' W	3313	on ground/ max depth	406 m, SE 32.1
PS75/266-3	2010-04-11	17:13	HPRO	43° 13.54' S	57° 17.94' W	3316,2	profile start	
PS75/266-3	2010-04-11	17:29	HPRO	43° 13.49' S	57° 17.91' W	3302,5	profile end	
PS75/266-4	2010-04-11	17:58	GO-FLO	43° 13.38' S	57° 17.83' W	3284,5	on ground/ max depth	30 m, SE 32.2
PS75/267-1	2010-04-12	16:34	SIOP	41° 06.47' S	53° 53.07' W	5148	profile start	
PS75/267-1	2010-04-12	16:45	SIOP	41° 07.06' S	53° 52.96' W	5129,5	profile end	
PS75/267-2	2010-04-12	17:09	CTD/RO	41° 08.44' S	53° 52.67' W	5127,2	on ground/ max depth	416 m, SE 32.1
PS75/267-3	2010-04-12	17:00	HPRO	41° 07.91' S	53° 52.78' W	5124	profile start	
PS75/267-3	2010-04-12	17:19	HPRO	41° 08.99' S	53° 52.60' W	5129	profile end	
PS75/267-4	2010-04-12	18:12	PAR	41° 11.95' S	53° 52.00' W	5152,7	on ground/ max depth	100 m
PS75/267-4	2010-04-12	18:20	PAR	41° 12.42' S	53° 51.93' W	5154,2	profile end	
PS75/268-1	2010-04-13	15:20	GO-FLO	39° 05.59' S	50° 56.02' W	5218,7	on ground/ max depth	40 m, SE 32.2
PS75/268-2	2010-04-13	15:47	SIOP	39° 05.46' S	50° 56.18' W	5211,2	profile start	
PS75/268-2	2010-04-13	15:58	SIOP	39° 05.41' S	50° 56.23' W	5208,2	profile end	
PS75/268-3	2010-04-13	16:23	CTD/RO	39° 05.33' S	50° 56.40' W	5205	on ground/ max depth	408 m, SE 32.1
PS75/268-4	2010-04-13	16:50	PAR	39° 05.26' S	50° 56.63' W	5205,5	on ground/ max depth	100 m
PS75/268-4	2010-04-13	16:57	PAR	39° 05.24' S	50° 56.71' W	5203,7	profile end	
PS75/268-5	2010-04-13	16:15	HPRO	39° 05.35' S	50° 56.37' W	5205	profile start	
PS75/268-5	2010-04-13	16:34	HPRO	39° 05.30' S	50° 56.47' W	5203,7	profile end	
PS75/269-1	2010-04-14	15:47	SIOP	36° 54.55' S	47° 42.30' W	5025,5	profile start	

Station	Date	Time	Gear Abbrev.	Latitude	Longitude	Water depth [m]	Action	Comment
PS75/269-1	2010-04-14	15:59	SIOP	36° 54.79' S	47° 42.61' W	5025,7	profile end	
PS75/269-2	2010-04-14	16:22	CTD/RO	36° 55.19' S	47° 43.19' W	5027,5	on ground/ max depth	406 m, SE 32.1
PS75/269-3	2010-04-14	16:11	HPRO	36° 55.03' S	47° 42.91' W	5026,7	profile start	
PS75/269-3	2010-04-14	16:33	HPRO	36° 55.40' S	47° 43.49' W	5028,2	profile end	
PS75/270-1	2010-04-15	15:19	GO-FLO	34° 42.96' S	44° 26.43' W	4779	on ground/ max depth	30 m, SE 32.2
PS75/270-2	2010-04-15	15:47	SIOP	34° 43.11' S	44° 26.85' W	4780,2	profile start	
PS75/270-2	2010-04-15	15:59	SIOP	34° 43.06' S	44° 26.92' W	4779,5	profile end	
PS75/270-3	2010-04-15	16:24	CTD/RO	34° 43.12' S	44° 27.18' W	4778,5	on ground/ max depth	409 m, SE 32.1
PS75/270-4	2010-04-15	16:43	PAR	34° 43.24' S	44° 27.36' W	4778,5	on ground/ max depth	100 m
PS75/270-4	2010-04-15	16:59	PAR	34° 43.33' S	44° 27.57' W	4780,2	profile end	
PS75/270-5	2010-04-15	16:12	HPRO	34° 43.05' S	44° 27.09' W	4779,7	profile start	
PS75/270-5	2010-04-15	16:33	HPRO	34° 43.18' S	44° 27.26' W	4779,7	profile end	
PS75/271-1	2010-04-16	15:47	SIOP	32° 27.73' S	41° 08.58' W	4394,7	profile start	
PS75/271-1	2010-04-16	15:57	SIOP	32° 27.73' S	41° 08.52' W	4395,5	profile end	
PS75/271-2	2010-04-16	16:19	CTD/RO	32° 27.86' S	41° 08.64' W	4397,5	on ground/ max depth	407 m. SE 32.1
PS75/271-3	2010-04-16	16:30	PAR	32° 27.94' S	41° 08.71' W	4396,2	on ground/ max depth	100 m
PS75/271-3	2010-04-16	16:40	PAR	32° 28.02' S	41° 08.79' W	4394,7	profile end	
PS75/271-4	2010-04-16	16:11	HPRO	32° 27.78' S	41° 08.59' W	4395,5	profile start	
PS75/271-4	2010-04-16	16:29	HPRO	32° 27.94' S	41° 08.70' W	4396,2	profile end	
PS75/272-1	2010-04-17	10:17	CTD/RO	31° 11.73' S	39° 20.37' W	4509	on ground/ max depth	winde 32,1 4611m
PS75/272-2	2010-04-17	12:31	GO-FLO	31° 12.01' S	39° 20.53' W	4530	on ground/ max depth	SE 32.2 410m
PS75/272-3	2010-04-17	14:05	CTD/RO	31° 12.09' S	39° 21.08' W	4570	on ground/ max depth	SE 32.1 2042m
PS75/272-4	2010-04-17	15:44	GO-FLO	31° 12.53' S	39° 22.06' W	4520,7	on ground/ max depth	90 m, SE 32.2
PS75/273-1	2010-04-18	15:46	SIOP	27° 46.14' S	37° 22.95' W	4618	profile start	
PS75/273-1	2010-04-18	15:56	SIOP	27° 46.14' S	37° 23.00' W	4617,7	profile end	
PS75/273-2	2010-04-18	16:19	CTD/RO	27° 46.17' S	37° 23.18' W	4620	on ground/ max depth	406 m, SE 32.1
PS75/273-3	2010-04-18	16:45	PAR	27° 46.19' S	37° 23.31' W	4618,5	on ground/ max depth	100 m
PS75/273-3	2010-04-18	16:51	PAR	27° 46.18' S	37° 23.33' W	4618	profile end	
PS75/273-4	2010-04-18	16:09	HPRO	27° 46.17' S	37° 23.12' W	4618,7	profile start	
PS75/273-4	2010-04-18	16:29	HPRO	27° 46.17' S	37° 23.22' W	4620,5	profile end	
PS75/274-1	2010-04-19	14:17	GO-FLO	24° 45.24' S	35° 42.76' W	4112	on ground/ max depth	36 m, SE 32.2
PS75/274-2	2010-04-19	14:42	SIOP	24° 45.19' S	35° 42.90' W	4117,5	profile start	
PS75/274-2	2010-04-19	14:55	SIOP	24° 45.16' S	35° 42.98' W	4122,3	profile end	
PS75/274-3	2010-04-19	15:24	CTD/RO	24° 45.12' S	35° 43.12' W	4120,5	on ground/ max depth	407 m, se 32.1
PS75/274-4	2010-04-19	15:30	PAR	24° 45.10' S	35° 43.15' W	4118,9	on ground/ max depth	100 m
PS75/274-4	2010-04-19	15:48	PAR	24° 45.08' S	35° 43.23' W	4107,2	profile end	

Station	Date	Time	Gear Abbrev.	Latitude	Longitude	Water depth [m]	Action	Comment
PS75/274-5	2010-04-19	15:04	HPRO	24° 45.15' S	35° 43.03' W	4124,5	profile start	
PS75/274-5	2010-04-19	15:26	HPRO	24° 45.11' S	35° 43.13' W	4117,5	profile end	
PS75/275-1	2010-04-20	14:45	SIOP	21° 45.97' S	34° 06.12' W	4482,2	profile start	
PS75/275-1	2010-04-20	14:57	SIOP	21° 45.99' S	34° 06.18' W	4482,2	profile end	
PS75/275-2	2010-04-20	15:23	CTD/RO	21° 46.03' S	34° 06.34' W	4482	on ground/ max depth	408 m, SE 32.1
PS75/275-3	2010-04-20	15:40	PAR	21° 46.06' S	34° 06.44' W	4481,5	on ground/ max depth	100 m
PS75/275-3	2010-04-20	15:53	PAR	21° 46.08' S	34° 06.50' W	4482,2	profile end	
PS75/275-4	2010-04-20	15:09	HPRO	21° 46.01' S	34° 06.24' W	4481,5	profile start	
PS75/275-4	2010-04-20	15:24	HPRO	21° 46.04' S	34° 06.35' W	4481,7	profile end	
PS75/276-1	2010-04-21	14:14	GO-FLO	18° 47.27' S	32° 31.37' W	4212,2	on ground/ max depth	40 m, SE 32.2
PS75/276-2	2010-04-21	14:39	SIOP	18° 47.22' S	32° 31.56' W	4218,2	profile start	
PS75/276-2	2010-04-21	14:51	SIOP	18° 47.20' S	32° 31.56' W	4217,2	profile end	
PS75/276-3	2010-04-21	15:16	CTD/RO	18° 47.22' S	32° 31.57' W	4219	on ground/ max depth	405 m, SE 32.1
PS75/276-4	2010-04-21	15:04	HPRO	18° 47.18' S	32° 31.55' W	4216,7	profile start	
PS75/276-4	2010-04-21	15:22	HPRO	18° 47.22' S	32° 31.59' W	4218,5	profile end	
PS75/277-1	2010-04-22	14:45	SIOP	15° 54.24' S	30° 29.45' W	4872,5	profile start	
PS75/277-1	2010-04-22	14:56	SIOP	15° 54.29' S	30° 29.48' W	4872,2	profile end	
PS75/277-2	2010-04-22	15:23	CTD/RO	15° 54.34' S	30° 29.41' W	4872,5	on ground/ max depth	408 m, SE 32.1
PS75/277-3	2010-04-22	15:20	PAR	15° 54.33' S	30° 29.42' W	4872,7	on ground/ max depth	100 m
PS75/277-3	2010-04-22	15:27	PAR	15° 54.35' S	30° 29.41' W	4872,5	profile end	
PS75/277-4	2010-04-22	15:05	HPRO	15° 54.31' S	30° 29.47' W	4872,5	profile start	
PS75/277-4	2010-04-22	15:29	HPRO	15° 54.35' S	30° 29.40' W	4872,5	profile end	
PS75/278-1	2010-04-23	14:22	GO-FLO	13° 03.38' S	28° 30.59' W	5511,5	on ground/ max depth	50 m, SE 32.2
PS75/278-2	2010-04-23	14:48	SIOP	13° 03.49' S	28° 30.67' W	5510,2	profile start	
PS75/278-2	2010-04-23	15:00	SIOP	13° 03.54' S	28° 30.70' W	5512	profile end	
PS75/278-3	2010-04-23	15:22	CTD/RO	13° 03.68' S	28° 30.79' W	5510,7	on ground/ max depth	407 m, SE 32.1
PS75/278-4	2010-04-23	15:30	PAR	13° 03.74' S	28° 30.88' W	5510,5	on ground/ max depth	100 m
PS75/278-4	2010-04-23	15:39	PAR	13° 03.79' S	28° 30.96' W	5509,5	profile end	
PS75/278-5	2010-04-23	15:11	HPRO	13° 03.60' S	28° 30.73' W	5510,5	profile start	
PS75/278-5	2010-04-23	15:20	HPRO	13° 03.67' S	28° 30.77' W	5510	profile end	abgerissen
PS75/279-1	2010-04-24	10:50	CTD/RO	10° 43.59' S	26° 54.36' W	5559,2	on ground/ max depth	SE32.1 2018m
PS75/279-2	2010-04-24	14:13	GO-FLO	10° 42.86' S	26° 54.73' W	5568	on ground/ max depth	415 m, SE 32.2
PS75/279-3	2010-04-24	15:03	SIOP	10° 42.65' S	26° 54.82' W	5568,5	profile start	
PS75/279-3	2010-04-24	15:13	SIOP	10° 42.64' S	26° 54.81' W	5567	profile end	
PS75/279-4	2010-04-24	15:35	CTD/RO	10° 42.64' S	26° 55.07' W	5569,2	on ground/ max depth	406 m, SE 32.1
PS75/279-5	2010-04-24	15:48	PAR	10° 42.55' S	26° 55.27' W	5568,5	on ground/ max depth	100 m
PS75/279-5	2010-04-24	15:52	PAR	10° 42.51' S	26° 55.36' W	5568	profile end	

Station	Date	Time	Gear Abbrev.	Latitude	Longitude	Water depth [m]	Action	Comment
PS75/279-6	2010-04-24	16:16	GO-FLO	10° 42.47' S	26° 55.75' W	5564,7	on ground/ max depth	115 m, SE 32.2
PS75/280-1	2010-04-25	14:45	SIOP	07° 58.32' S	25° 01.11' W	5690,7	profile start	
PS75/280-1	2010-04-25	14:56	SIOP	07° 58.31' S	25° 01.15' W	5691,2	profile end	
PS75/280-2	2010-04-25	15:25	CTD/RO	07° 58.38' S	25° 01.09' W	5691,5	on ground/ max depth	406 m, SE 32.1
PS75/280-3	2010-04-25	16:12	PAR	07° 58.49' S	25° 01.12' W	5691,5	on ground/ max depth	100 m
PS75/280-3	2010-04-25	16:26	PAR	07° 58.49' S	25° 01.10' W	5692	profile end	
PS75/281-1	2010-04-26	14:17	GO-FLO	05° 09.77' S	23° 06.58' W	5252,7	on ground/ max depth	40 m, SE 32.2
PS75/281-2	2010-04-26	14:40	SIOP	05° 09.80' S	23° 06.60' W	5248,2	profile start	
PS75/281-2	2010-04-26	14:52	SIOP	05° 09.79' S	23° 06.64' W	5244,2	profile end	
PS75/281-3	2010-04-26	15:13	CTD/RO	05° 09.77' S	23° 06.66' W	5253,2	on ground/ max depth	407 m, SE 32.1
PS75/281-4	2010-04-26	15:59	PAR	05° 09.80' S	23° 06.85' W	5252	on ground/ max depth	100 m
PS75/281-4	2010-04-26	16:04	PAR	05° 09.79' S	23° 06.89' W	5178,3	profile end	
PS75/281-5	2010-04-26	16:12	ARGOS	05° 09.64' S	23° 06.73' W	5261,2	on ground/ max depth	
PS75/282-1	2010-04-27	13:44	SIOP	01° 42.77' S	22° 59.92' W	4971,5	profile start	
PS75/282-1	2010-04-27	13:57	SIOP	01° 42.80' S	22° 59.87' W	4978	profile end	
PS75/282-2	2010-04-27	14:17	CTD/RO	01° 42.83' S	22° 59.82' W	4980,7	on ground/ max depth	406 m, SE 32.1
PS75/282-3	2010-04-27	14:30	PAR	01° 42.83' S	22° 59.77' W	4984,5	on ground/ max depth	100 m
PS75/282-3	2010-04-27	14:38	PAR	01° 42.82' S	22° 59.74' W	4985	profile end	
PS75/283-1	2010-04-28	12:34	GO-FLO	01° 46.59' N	22° 59.95' W	3925	on ground/ max depth	SE32.2 415m
PS75/283-2	2010-04-28	13:20	SIOP	01° 46.56' N	23° 00.13' W	3926,7	profile start	
PS75/283-2	2010-04-28	13:31	SIOP	01° 46.55' N	23° 00.11' W	3928,5	profile end	
PS75/283-3	2010-04-28	13:54	CTD/RO	01° 46.52' N	23° 00.06' W	3922	on ground/ max depth	406 m, SE 32.1
PS75/283-4	2010-04-28	14:33	PAR	01° 46.46' N	23° 00.06' W	3917,2	on ground/ max depth	100 m
PS75/283-4	2010-04-28	14:38	PAR	01° 46.47' N	23° 00.09' W	3921,3	profile end	
PS75/283-5	2010-04-28	14:25	GO-FLO	01° 46.47' N	23° 00.07' W	3919	on ground/ max depth	95 m, SE 32.2
PS75/283-6	2010-04-28	14:45	ARGOS	01° 46.65' N	23° 00.05' W	3934	on ground/ max depth	
PS75/284-1	2010-04-29	13:46	SIOP	04° 59.58' N	22° 59.76' W	4193,5	profile start	
PS75/284-1	2010-04-29	13:58	SIOP	04° 59.61' N	22° 59.68' W	4193,2	profile end	
PS75/284-2	2010-04-29	14:20	CTD/RO	04° 59.68' N	22° 59.51' W	4193,7	on ground/ max depth	400 m, SE 32.1
PS75/284-3	2010-04-29	14:38	PAR	04° 59.73' N	22° 59.40' W	4195,7	on ground/ max depth	100 m
PS75/284-3	2010-04-29	14:41	PAR	04° 59.74' N	22° 59.39' W	4195,5	profile end	
PS75/284-4	2010-04-29	14:47	ARGOS	04° 59.90' N	22° 59.42' W	4197,5	on ground/ max depth	
PS75/285-1	2010-04-30	13:19	GO-FLO	08° 03.90' N	22° 59.99' W	4499,7	on ground/ max depth	40 m, SE 32.2

Station	Date	Time	Gear Abbrev.	Latitude	Longitude	Water depth [m]	Action	Comment
PS75/285-1	2010-04-30	13:19	GO-FLO	08° 03.90' N	22° 59.99' W	4499,7	on ground/ max depth	
PS75/285-2	2010-04-30	13:42	SIOP	08° 03.95' N	23° 00.08' W	4500,2	profile start	
PS75/285-2	2010-04-30	13:54	SIOP	08° 04.04' N	23° 00.12' W	4506,7	profile end	
PS75/285-3	2010-04-30	14:15	CTD/RO	08° 04.09' N	23° 00.21' W	4516,7	on ground/ max depth	407 m, SE 32.1
PS75/285-4	2010-04-30	14:30	PAR	08° 04.12' N	23° 00.27' W	4514,5	on ground/ max depth	100 m
PS75/285-4	2010-04-30	14:34	PAR	08° 04.13' N	23° 00.27' W	4516	profile end	
PS75/285-5	2010-04-30	14:39	ARGOS	08° 04.27' N	23° 00.24' W	4519	on ground/ max depth	
PS75/286-1	2010-05-02	11:53	CTD/RO	14° 33.02' N	23° 40.96' W	3937,5	on ground/ max depth	SE 32.1 2014m
PS75/286-2	2010-05-02	13:43	GO-FLO	14° 33.19' N	23° 40.98' W	3933,5	on ground/ max depth	40 m, SE 32.2
PS75/286-3	2010-05-02	14:06	SIOP	14° 33.21' N	23° 40.97' W	3933	profile start	
PS75/286-3	2010-05-02	14:18	SIOP	14° 33.22' N	23° 40.94' W	3933,3	profile end	
PS75/286-4	2010-05-02	14:39	CTD/RO	14° 33.24' N	23° 40.91' W	3934,3	on ground/ max depth	406 m, SE 32.1
PS75/286-5	2010-05-02	14:43	PAR	14° 33.24' N	23° 40.90' W	3933,8	on ground/ max depth	defekt
PS75/286-5	2010-05-02	14:43	PAR	14° 33.24' N	23° 40.90' W	3933,8	profile end	defekt
PS75/286-6	2010-05-02	15:20	SIOP	14° 33.41' N	23° 40.76' W	3935,3	profile start	
PS75/286-6	2010-05-02	15:31	SIOP	14° 33.48' N	23° 40.73' W	3937	profile end	
PS75/287-1	2010-05-04	01:00	CTD/RO	17° 35.00' N	24° 15.16' W	3595,8	on ground/ max depth	3566 m, SE 32.1
PS75/287-1	2010-05-04	01:00	CTD/RO	17° 35.00' N	24° 15.16' W	3595,8	on ground/ max depth	3566 m, SE 32.1
PS75/287-2	2010-05-04	02:59	GO-FLO	17° 34.97' N	24° 15.18' W	3596	on ground/ max depth	415 m, SE 32.2
PS75/287-3	2010-05-04	04:46	CTD/RO	17° 35.02' N	24° 15.39' W	3597,2	on ground/ max depth	911m, SE 32.1
PS75/287-4	2010-05-04	07:55	GO-FLO	17° 35.34' N	24° 15.65' W	3597,2	on ground/ max depth	Winde 32.2 95m
PS75/287-5	2010-05-04	08:25	CTD/RO	17° 35.37' N	24° 15.68' W	3597,5	on ground/ max depth	Winde 32,1 408m
PS75/288-1	2010-05-04	10:41	GLD	17° 44.74' N	24° 30.23' W	3658,7	on ground/ max depth	fake
PS75/288-2	2010-05-04	11:09	GLD	17° 43.13' N	24° 30.67' W	3652,8	on ground/ max depth	fake
PS75/288-3	2010-05-04	11:34	GLD	17° 43.38' N	24° 30.86' W	3653,8	on ground/ max depth	fake
PS75/289-1	2010-05-04	13:16	GO-FLO	17° 36.53' N	24° 45.03' W	3565	on ground/ max depth	40 m, SE 32.2
PS75/289-2	2010-05-04	13:38	CTD/RO	17° 36.57' N	24° 45.02' W	3565,3	on ground/ max depth	204 m, SE 32.1
PS75/289-3	2010-05-04	14:12	SIOP	17° 36.63' N	24° 44.99' W	3565,8	profile start	
PS75/289-3	2010-05-04	14:24	SIOP	17° 36.67' N	24° 45.02' W	3567,2	profile end	
PS75/289-4	2010-05-04	14:58	PAR	17° 36.67' N	24° 45.04' W	3568	on ground/ max depth	100 m
PS75/289-4	2010-05-04	15:03	PAR	17° 36.68' N	24° 45.05' W	3568,2	profile end	

Station	Date	Time	Gear Abbrev.	Latitude	Longitude	Water depth [m]	Action	Comment
PS75/289-5	2010-05-04	14:48	CTD/RO	17° 36.68' N	24° 45.05' W	3568,2	on ground/ max depth	407 m, SE 32.1
PS75/290-1	2010-05-04	16:23	GLD	17° 32.75' N	24° 53.75' W	3395,2	on ground/ max depth	Glider im Boot
PS75/291-1	2010-05-05	12:46	SIOP	20° 15.30' N	22° 51.31' W	4277	profile start	
PS75/291-1	2010-05-05	12:58	SIOP	20° 15.36' N	22° 51.32' W	4277,3	profile end	
PS75/291-2	2010-05-05	13:22	CTD/RO	20° 15.42' N	22° 51.36' W	4277,5	on ground/ max depth	407 m, SE 32.1
PS75/291-3	2010-05-05	13:28	PAR	20° 15.42' N	22° 51.39' W	4277,7	on ground/ max depth	defekt
PS75/291-3	2010-05-05	13:31	PAR	20° 15.43' N	22° 51.41' W	4277,5	profile end	
PS75/292-1	2010-05-06	11:32	GO-FLO	23° 07.35' N	20° 39.21' W	4189,7	on ground/ max depth	40 m, SE 32.2
PS75/292-2	2010-05-06	11:56	SIOP	23° 07.34' N	20° 39.41' W	4191	profile start	
PS75/292-2	2010-05-06	12:07	SIOP	23° 07.28' N	20° 39.52' W	4191,7	profile end	
PS75/292-3	2010-05-06	12:46	PAR	23° 07.10' N	20° 39.86' W	4194,2	on ground/ max depth	100 m
PS75/292-3	2010-05-06	12:51	PAR	23° 07.06' N	20° 39.92' W	4194,5	profile end	
PS75/292-4	2010-05-06	12:30	CTD/RO	23° 07.16' N	20° 39.72' W	4193,5	on ground/ max depth	407 m, SE 32.1
PS75/293-1	2010-05-07	11:46	SIOP	26° 04.35' N	17° 29.66' W	3509,2	profile start	
PS75/293-1	2010-05-07	11:57	SIOP	26° 04.36' N	17° 29.68' W	3509,5	profile end	
PS75/293-2	2010-05-07	12:19	CTD/RO	26° 04.39' N	17° 29.71' W	3509	on ground/ max depth	407 m, SE 32.1
PS75/293-3	2010-05-07	12:40	PAR	26° 04.42' N	17° 29.74' W	3509,7	on ground/ max depth	100 m,
PS75/293-3	2010-05-07	12:45	PAR	26° 04.43' N	17° 29.74' W	3510	profile end	
PS75/294-1	2010-05-09	11:29	GO-FLO	33° 36.03' N	13° 51.37' W	4419,7	on ground/ max depth	415 m, Se 32.2
PS75/294-2	2010-05-09	12:17	SIOP	33° 35.84' N	13° 51.35' W	4420	profile start	
PS75/294-2	2010-05-09	12:28	SIOP	33° 35.80' N	13° 51.38' W	4420,2	profile end	
PS75/294-3	2010-05-09	12:50	CTD/RO	33° 35.74' N	13° 51.40' W	4419,5	on ground/ max depth	407 m, SE 32.1
PS75/294-4	2010-05-09	13:10	PAR	33° 35.69' N	13° 51.43' W	4420	on ground/ max depth	100 m
PS75/294-4	2010-05-09	13:17	PAR	33° 35.67' N	13° 51.42' W	4419,2	profile end	
PS75/294-5	2010-05-09	13:23	GO-FLO	33° 35.66' N	13° 51.43' W	4419	on ground/ max depth	95 m, SE 32.2
PS75/295-1	2010-05-10	05:50	CTD/RO	36° 31.84' N	13° 00.41' W	2654	on ground/ max depth	winde 321 2702m
PS75/295-2	2010-05-10	12:00	MOORST	36° 31.90' N	13° 00.22' W	2653,2	on ground/ max depth	pass mooring
PS75/295-3	2010-05-10	12:24	SIOP	36° 31.94' N	13° 00.15' W	2653	profile start	
PS75/295-3	2010-05-10	12:35	SIOP	36° 31.99' N	13° 00.21' W	2653,5	profile end	
PS75/295-4	2010-05-10	12:56	CTD/RO	36° 32.13' N	13° 00.31' W	2662	on ground/ max depth	405 m, SE 32.1
PS75/295-5	2010-05-10	13:12	PAR	36° 32.25' N	13° 00.33' W	2676	on ground/ max depth	100 m
PS75/295-5	2010-05-10	13:17	PAR	36° 32.29' N	13° 00.33' W	2680,5	profile end	
PS75/295-6	2010-05-10	18:57	MOR	36° 32.31' N	12° 60.00' W	2654,2	on ground/ max depth	fake

Station	Date	Time	Gear Abbrev.	Latitude	Longitude	Water depth [m]	Action	Comment
PS75/296-1	2010-05-11	11:47	GO-FLO	39° 45.75' N	11° 50.75' W	4944,2	on ground/ max depth	40 m, Se 32.2
PS75/296-2	2010-05-11	12:12	SIOP	39° 45.73' N	11° 51.09' W	4944,7	profile start	
PS75/296-2	2010-05-11	12:24	SIOP	39° 45.75' N	11° 51.19' W	4879,2	profile end	
PS75/296-3	2010-05-11	12:46	CTD/RO	39° 45.84' N	11° 51.37' W	4939,5	on ground/ max depth	407 m, SE 32.1
PS75/296-4	2010-05-11	13:16	PAR	39° 46.08' N	11° 51.85' W	5130,2	on ground/ max depth	100 m
PS75/296-4	2010-05-11	13:22	PAR	39° 46.14' N	11° 51.94' W	5131,2	profile end	
PS75/297-1	2010-05-12	12:19	SIOP	43° 23.88' N	10° 26.45' W	3663,5	profile start	
PS75/297-1	2010-05-12	12:31	SIOP	43° 23.89' N	10° 26.43' W	3659,5	profile end	
PS75/297-2	2010-05-12	12:53	CTD/RO	43° 23.88' N	10° 26.43' W	3661,7	on ground/ max depth	407 m, SE 32.1
PS75/297-3	2010-05-12	13:08	PAR	43° 23.89' N	10° 26.41' W	3659,7	on ground/ max depth	100 m
PS75/297-3	2010-05-12	13:13	PAR	43° 23.89' N	10° 26.41' W	3657,2	profile end	
PS75/298-1	2010-05-13	09:22	CTD/RO	46° 00.40' N	08° 08.89' W	4789	on ground/ max depth	steadiger wechsel zwischen 200m und 20m Tiefe
PS75/298-2	2010-05-13	10:55	SIOP	46° 00.36' N	08° 09.16' W	4790,7	profile start	
PS75/298-2	2010-05-13	11:09	SIOP	46° 00.35' N	08° 09.17' W	4791,2	profile end	
PS75/298-3	2010-05-13	11:30	CTD/RO	46° 00.34' N	08° 09.23' W	4791	on ground/ max depth	407 m, SE 32.1
PS75/298-4	2010-05-13	11:39	PAR	46° 00.32' N	08° 09.25' W	4791,7	on ground/ max depth	80 m
PS75/298-4	2010-05-13	11:43	PAR	46° 00.31' N	08° 09.26' W	4790,5	profile end	
PS75/299-1	2010-05-14	10:42	SIOP	48° 51.72' N	06° 21.88' W	130	profile start	
PS75/299-1	2010-05-14	10:49	SIOP	48° 51.71' N	06° 22.01' W	131,2	profile end	
PS75/299-2	2010-05-14	11:04	CTD/RO	48° 51.66' N	06° 22.36' W	129,2	on ground/ max depth	120 m, SE 32.1
PS75/299-3	2010-05-14	11:20	PAR	48° 51.60' N	06° 22.70' W	131	on ground/ max depth	80 m
PS75/299-3	2010-05-14	11:23	PAR	48° 51.58' N	06° 22.76' W	129,5	profile end	

#### Abbreviations:

AFLOAT	Profiling ARGO float
CTD/RO	Conductivity-temperature-depth probe installed in rosette water sampler
GLIDER	Autonomous profiling ocean glider
GO-FLO	“Close-open-close” water sampler
HPRO	“Hyper Pro” surface drifter with optical sensor package
MOORING	Transponder mooring for Posidonia testing
PAR	Optical sensor package for profiling applications
SIOP	„Scripps Institution Optical Profiler“

**Die "Berichte zur Polar- und Meeresforschung"** (ISSN 1866-3192) werden beginnend mit dem Heft Nr. 569 (2008) ausschließlich elektronisch als Open-Access-Publikation herausgegeben. Ein Verzeichnis aller Hefte einschließlich der Druckausgaben (Heft 377-568) sowie der früheren "**Berichte zur Polarforschung**" (Heft 1-376, von 1982 bis 2000) befindet sich im Internet in der Ablage des electronic Information Center des AWI (**ePIC**) unter der URL <http://epic.awi.de>. Durch Auswahl "Reports on Polar- and Marine Research" auf der rechten Seite des Fensters wird eine Liste der Publikationen in alphabetischer Reihenfolge (nach Autoren) innerhalb der absteigenden chronologischen Reihenfolge der Jahrgänge erzeugt.

*To generate a list of all Reports past issues, use the following URL: <http://epic.awi.de> and select the right frame to browse "Reports on Polar and Marine Research". A chronological list in declining order, author names alphabetical, will be produced, and pdf-icons shown for open access download.*

#### **Verzeichnis der zuletzt erschienenen Hefte:**

**Heft-Nr. 619/2010** — "Acoustic ecology of marine mammals in polar oceans", by Ilse Van Opzeeland

**Heft-Nr. 620/2010** — "Cool Libraries in a Melting World - Proceedings of the 23<sup>rd</sup> Polar Libraries Colloquy 2010, June 13-18, 2010, Bremerhaven, Germany", edited by Marcel Brannemann and Daria O. Carle

**Heft-Nr. 621/2010** — "The Expedition of the Research Vessel 'Polarstern' to the Arctic in 2010 (ARK-XXV/3)", edited by Volkmar Damm

**Heft-Nr. 622/2010** — "Environmentally induced responses of *Donax obesulus* and *Mesodesma donacium* (Bivalvia) inhabiting the Humboldt Current System", by Daniel Carstensen

**Heft-Nr. 623/2010** — "Research in the Laptev Sea region - Proceedings of the joint Russian-German workshop, November 8-11, 2010, St. Petersburg, Russia", edited by Sebastian Wetterich, Paul Pier Overduin and Irina Fedorova

**Heft-Nr. 624/2010** — "The Expedition of the Research Vessel 'Polarstern' to the Arctic in 2010 (ARK-XXV/2)", edited by Thomas Soltwedel

**Heft-Nr. 625/2011** — "The Expedition of the Research Vessel 'Polarstern' to the Arctic in 2010 (ARK-XXV/1)", edited by Gereon Budéus

**Heft-Nr. 626/2011** — "Towards data assimilation in ice-dynamic models: the (geo)physical basis", by Olaf Eisen

**Heft-Nr. 627/2011** — "The Expedition of the Research Vessel 'Polarstern' to the Arctic in 2007 (ARK-XXII/1a-c)", edited by Michael Klages & Jörn Thiede

**Heft-Nr. 628/2011** — "The Expedition of the Research Vessel 'Polarstern' to the Antarctic in 2010 (ANT-XXVII/1)", edited by Karl Bumke

**Heft-Nr. 629/2011** — "Russian-German Cooperation SYSTEM LAPTEV SEA: The expedition Eastern Laptev Sea - Buor Khaya Peninsula 2010" edited by Sebastian Wetterich, Pier Paul Overduin and Mikhail Grigoriev

**Heft-Nr. 630/2011** — "Comparative aerosol studies based on multi-wavelength Raman LIDAR at Ny-Ålesund, Spitsbergen", by Anne Hoffmann

**Heft-Nr. 631/2011** — "The Expedition of the Research Vessel 'Polarstern' to the Antarctic in 2010 (ANT-XXVI/4)", edited by Arne Körtzinger